

CRANFIELD UNIVERSITY

SAAD ABDULAZIZ ALHWAIMEL

FUSION OF MULTI SOIL DATA FOR THE DELINEATION OF
MANAGEMENT ZONES FOR VARIABLE RATE IRRIGATION

SCHOOL OF APPLIED SCIENCES
AGRICULTURAL AND ENVIRONMENTAL ENGINEERING

MSc

Academic Year: 2012 - 2013

Supervisor: Dr. Abdul Mounem Mouazen

Co-supervisor: Dr. Toby Waine

February 2013

CRANFIELD UNIVERSITY

SCHOOL OF APPLIED SCIENCES
AGRICULTURAL AND ENVIRONMENTAL ENGINEERING

MSc

Academic Year 2012 - 2013

SAAD ABDULAZIZ ALHWAIMEL

Fusion of multi soil data for the delineation of management zones for
variable rate irrigation

Supervisor: Dr. Abdul Mounem Mouazen

Co-supervisor: Dr. Toby Waine

February 2013

This thesis is submitted in partial fulfilment of the requirements for
the degree of MSc

© Cranfield University 2013. All rights reserved. No part of this
publication may be reproduced without the written permission of the
copyright owner.

ABSTRACT

Up until now, there have been no multi-sensor approaches used to estimate available water content (AWC) in order to determine variable rate irrigation. This has been a major problem for growers adopting precision farming technologies. The aim of this project is to implement an on-line multi-sensor platform and data fusion approach for the delineation of management zones for site specific irrigation in vegetable crop production systems. This is performed by simultaneous measurement of soil moisture content (MC), organic carbon (OC), clay content (CC), plasticity index (PI) and bulk density (BD) with an on-line visible and near infrared (vis-NIR) spectroscopy sensor and a load cell attached to a subsoiler and frame, which was linked to a three-point linkage of a tractor. The soil apparent Electrical Conductivity (ECa) was separately measured with an Electromagnetic Induction (EMI) device. Measurements were carried out in three fields in Lincolnshire and one in Cambridgeshire. Vis-NIR calibration models of soil properties were developed using partial least squares (PLS) regression. A multiple linear regression analysis (MLR) and an Artificial Neural Network (ANN) was used to derive zones of water holding capacity (WHC), based on correlation between on-line measured OC, CC, PI, BD and ECa with MC. The AWC was calculated with empirical equations, as a function of clay and sand fractions.

Result showed that the on-line measurement accuracy for OC and MC were good to excellent ($R^2=0.71-0.83$ and $R^2=0.75-0.85$, $RPD=2.00-2.57$ and $RPD=1.94-2.10$ for OC and MC, respectively). For CC and PI, the measurement accuracy ($R^2=0.64-0.69$ and $RPD=0.55-0.66$ for clay content and PI) was evaluated as moderate. It was observed in the study fields, that the ECa results had a minor response to MC distribution.

Furthermore, the fusion of multi-soil data to derive a WHC index with MLR and ANN resulted in successful delineation of homogeneous zones. These were divided into four different normalisation categories of low (0 – 0.25), medium (0.25 – 0.5), high (0.5 – 0.75) and very high (0.75 – 1) of WHC. Spatial similarity

between WHC maps with those of CC, IP and MC was documented, and found to be in line with the literature. AWC maps calculated as a function of soil texture classes, showed spatial similarity with WHC maps. Low values of AWC were observed at zones with low WHC index and vice versa. This supports the final conclusion of this work that multi-sensor and data fusion is a useful approach to guide positions of moisture sensor and optimise the amount of water used for irrigation.

Keywords:

Visible- and Near-Infrared Spectroscopy, Electromagnetic Induction, Soil Mapping, Multi-sensor, Data Fusion, Water Holding Capacity, Site Specific Irrigation, Available Water Content, Apparent Electrical Conductivity

ACKNOWLEDGEMENTS

First of all, I thank Allah who helped me achieve and complete my thesis. This thesis could not have been completed without the help of many people, I wish to thank them all.

I must proffer my very strong thanks to my Supervisor, Dr Abdul Mounem Mouazen, who gave me assistance all times and advised me on information I needed. He stood by me at all times. I would also like to thank Dr Toby Waine, who was my co-supervisor who helped me with my thesis.

I have to thank Dr Boyan Kuang who helped me with his experience in NIR and field measurement and I also have to thank Mr Zaka Quraishi who gave me the information on software. I thank Mr Graham Halcro and Mr Read Al-Asadi. I must thank my colleague Mohammed Al Dhumayri who advised me to study at Cranfield University.

I thank everyone who worked in the soil laboratory for helping me complete all the laboratory analysis in four months and I thank everyone who worked with me in the field and carry all the tools for the on-line NIR system.

I must thank Emma Garrod from Produce World Ltd. for identifying my study fields in Peterborough. I also thank Soyl Company for supplying the measurements of the ECa by EMI in the study fields.

I must thank Mr Ian Truckell who helped me with ArcGIS software. I acknowledge the kind assistance of Miss Rebecca Roy and Zoe Payne for helping me with academic services when I needed them. I offer my thanks to all the staff in the library and registry section.

I extend special thanks for the Agricultural Development Found in Saudi Arabia for giving me this opportunity to study for my MSc at Cranfield University.

Finally, I must express all my love to my father and my mother and thanks to my brothers and my sisters who live in Saudi Arabia. I also must express all my

love to my wife and my daughters Ghadi and Gheda, who live with me in the UK for being very patient and understanding in my studies.

Kind regards to everyone who will read and use my thesis in the future.

TABLE OF CONTENTS

ABSTRACT	i
ACKNOWLEDGEMENTS.....	iii
LIST OF FIGURES.....	viii
LIST OF TABLES	x
LIST OF EQUATIONS.....	xii
LIST OF ABBREVIATIONS	xiii
1 INTRODUCTION AND LITERATURE REVIEW	1
1.1 Introduction	1
1.2 Measurement of Soil Moisture Content (MC)	3
1.3 Irrigation systems.....	4
i. Flood irrigation	4
ii. Sprinkler irrigation.....	4
iii. Drip irrigation	5
1.4 Irrigation scheduling and moisture sensors.....	6
1.5 Key factors affecting water holding capacity and available water in the soil	8
1.6 Visible and near infrared spectroscopy(Vis-NIR) for the analysis of soil properties.....	10
1.7 Electrical conductivity methods (EC).....	12
2 RESEARCH AIM AND OBJECTIVES	16
2.1 Research gap	16
2.1 Research aim.....	16
2.1 Research objectives.....	17
3 MATERIAL AND METHODS	18
3.1 Experimental fields and collection soil samples	18
3.1.1 Collection of soil samples.....	18
3.1.2 Online vis-NIR DRS and BD measurement.....	19
3.1.3 EMI instruments for measuring the electrical measurement.....	23
3.1.4 Moisture content measurement.....	23
3.2 Laboratory Experiments.....	24
3.2.1 Moisture content analysis.....	24
3.2.2 Organic carbon analysis.....	24
3.2.3 Soil texture analysis	25
3.2.4 Plasticity index analysis.....	28
3.2.5 Optical measurement	30
3.2.6 Pre-treatment of vis-NIR spectra	30
3.2.7 Development of calibration models	31
3.2.8 Statistical evaluation of PLS model performance	33
3.2.9 Derivation of Water Holding Capacity index (WHC)	35

3.2.9.1 Multiple linear regression analysis.....	35
3.2.9.2 Artificial neural network	35
3.2.10 Calculation of available water content (AWC)	37
3.2.11 Development of maps.....	38
4 RESULTS AND DISCUSSION	39
4.1 Laboratory results	39
4.1.1 Soil Particle size distribution (PSD)	39
4.1.2 Organic carbon (OC), moisture content (MC) and plasticity index (PI) results	42
4.2 Soil volumetric moisture content measured by Theta probe	43
4.3 Soil apparent electrical conductivity (ECa).....	44
4.4 Online measurement.....	47
4.4.1 Bulk density measurement (BD).....	47
4.4.2 On-line soil Spectra	50
4.4.3 Accuracy of on-line vis-NIR measurement of soil properties.....	50
4.4.4 Mapping	54
4.4.4.1 Comparison maps	54
4.4.4.2 Full points maps	58
4.4.5 Water-holding capacity (WHC) index	64
4.4.6 The available water content (AWC).....	71
5 CONCLUSIONS	75
Future Work.....	76
REFERENCES.....	77
APPENDIX	91

LIST OF FIGURES

Figure 1-1 Shows a moisture sensor installed in field with dripping irrigation system with vegetable crop	7
Figure 1-2 Shows the transmitter and receiver dipole orientations of DUALEM-1S uses a vertical –vertical (V-V) and a vertical-horizontal (V-H) mode for the dipoles in DUALEM-1S (Abdu et al., 2007)	13
Figure 3-1 Shows the location of the four fields in England which were used in the study	19
Figure 3-2 Shows the on-line measurement lines (black) and sampling points (red), shown for Vicarage Farm as an example	21
Figure 3-3 Illustrates the multi-sensor platform for on-line measurement (Mouazen, 2006)	22
Figure 3-4 Shows the Dualem 1S sensor with a quad bike, during field measurement	23
Figure 3-5 Shows the Theta Probe ML2X for the measurement of the moisture content sensor.....	24
Figure 3-6 The United Kingdom soil classification scheme	27
Figure 3-7 Shows the penetrometer and cone used to determine the liquid limit	29
Figure 3-8 Four layer artificial neural network (ANN) used model the WHC prediction.....	36
Figure 4-1 Texture of all samples collected from (a) Vicarage field, (b) Marshalls field, (c) Wypemere field and (d) Thetford field; The soil classification is set according to the UK soil classification scheme.....	41
Figure 4-2 Spatial variation of apparent electrical conductivity (ECa) at two different depths: shallow (0 cm to 40 cm, left) and deep (0 cm to 120 cm, right) at Vicarage field	45
Figure 4-3 Spatial variation of apparent electrical conductivity (ECa) at two different depths: shallow (0 cm to 40 cm, left) and deep (0 cm to 120 cm, right) at Marshalls field	46
Figure 4-4 Spatial variation of apparent electrical conductivity (ECa) at two different depths: shallow (0 cm to 40 cm, left) and deep (0 cm to 120 cm, right) at Wypemere field	46
Figure 4-5 Full-points bulk density (BD) maps developed based on an exponential variogram shown for Marshalls field (top), Wypemere field (middle) and Thetford field (bottom)	49

Figure 4-6 On-line soil spectra collected at Wypemere field	50
Figure 4-7 Schematic illustration of different steps towards on-line measurement and mapping of soil properties	51
Figure 4-8: Comparison maps between laboratory (left) and on-line predicted (right) measured soil moisture content (MC), in Vicarage (top), Wypemere (middle) and Thetford (bottom)	55
Figure 4-9: Comparison maps between laboratory (left) and on-line predicted (right) measured soil organic carbon (OC), in Vicarage (top), Wypemere (middle) and Thetford (bottom)	56
Figure 4-10: Comparison maps between laboratory (left) and on-line predicted (right) measured soil clay content (CC), in Vicarage (top), Wypemere (middle) and Thetford (bottom)	57
Figure 4-11: Comparison maps between laboratory (left) and on-line predicted (right) measured soil plasticity index (PI), in Vicarage (top), Wypemere (middle) and Thetford (bottom)	58
Figure 4-12: Full-points maps of moisture content (MC) of Vicarage (top), Wypemere (middle) and Thetford (bottom) based on an exponential variogram of all on-line measured points	60
Figure 4-13: Full-points maps of organic carbon (OC) of Vicarage (top), Wypemere (middle) and Thetford (bottom) based on an exponential variogram of all on-line measured points	61
Figure 4-14: Full-points maps of clay content (CC) of Vicarage (top), Wypemere (middle) and Thetford (bottom) based on an exponential variogram of all on-line measured points	62
Figure 4-15: full-points maps of plasticity index (PI) of Vicarage (top), Wypemere (middle) and Thetford (bottom) based on an exponential variogram of all on-line measured points	63
Figure 4-16: Water holding capacity (WHC) maps with four classes low, medium, high and very high WHC calculated based on constants of multiple linear regressions (MLR) of individual field data (left) and all three fields data (right)	68
Figure 4-17: Water holding capacity (WHC) maps with four classes low, medium, high and very high WHC calculated based on constants of artificial neural network (ANN) of individual field data (left) and all three fields data (right)	70
Figure 4-18: Available water content (AWC) in Vicarage (top), Wypemere (middle) and Thetford (bottom), calculated as a function of on-line measured CC measured and laboratory measured sand content.....	73

Figure _Apx-1: Shows the online measurement lines (black) and sampling points (red), shown in Wypemere field (a) and Thetford field (b)..... 92

Figure_Apx-2: Scatter plots of the on-line predicted versus laboratory measured moisture content (MC) (a), organic carbon (OC) (b), clay content CC (c) and plasticity index (d) at Vicarage Farm (top), Wypemere Farm (middle) and Thetford Farm (bottom) 94

LIST OF TABLES

Table 3-1: The study fields, the on-line vis-NIR and EMI measurements took place	21
Table 3-2: Comparison of sample statistics between the calibration set and laboratory validation groups at all study fields	32
Table 4-1: Average soil texture at the four study fields.....	39
Table 4-2: Analyses of organic carbon OC, moisture content MC and plasticity index PI for the four study sites	42
Table 4-3: Theta Probe measurement of volumetric moisture content MC m ³ /m ³ from the four study sites	43
Table 4-4: Average ECa measured at two different depths (shallow and deep) in three fields.....	44
Table 4-5: On-line measured bulk density (BD) in the three study sites.....	48
Table 4-6: Summary of semi-variance properties of bulk density (BD) full points maps in the three fields	48
Table 4-7: Summary of the on-line vis-NIR measurement accuracy of organic carbon (OC), moisture content (MC), clay content (CC) and plasticity index (PI) in three fields in Vicarage, Wypemere and Thetford	53
Table 4-8: Summary of semi-variance data of OC, MC, CC and PI in all sites with exponential model variograms	59
Table 4-9: Constant values of multiple linear regression (MLR) analysis in the three fields.....	66
Table 4-10: Average water holding capacity (WHC) calculated for the three study fields using the artificial neural network (ANN) and multiple linear regressions (MLR) analysis	69
Table 4-11: Average AWC of the study fields calculated based on on-line measured clay content (CC) and laboratory measured sand content.	72
Table_APX-1: Comparison between the available water content (AWC) calculated by Eqn. (3-8) using on-line predicted clay content (CC) and laboratory measured sand content with corresponding AWC values calculated based on average laboratory measured CC and sand content of water holding capacity (WHC) zones.	95
Table_APX-2: Accuracy of the vis-NIR prediction of AWC with Eqn (3-8) as compared to laboratory measured AWC based on WHC-category average clay content (CC) and sand content measured with PSD test. Comparison	

is made for AWC calculated with artificial neural network and multiple linear regression. (MLR) analysis 96

LIST OF EQUATIONS

(1-1).....	13
(3-1).....	20
(3-2).....	26
(3-3).....	26
(3-4).....	26
(3-5).....	26
(3-6).....	26
(3-7).....	29
(3-8).....	29
(3-9).....	33
(3-10).....	37
(3-11).....	37
(3-12).....	37
(3-14).....	38

LIST OF ABBREVIATIONS

ANN	Artificial neural network
AWC	Available water content
BD	Bulk density
BSI	British Standard institute
CC	Clay content
ECa	Apparent electrical conductivity
EMI	Electromagnetic induction
MC	Moisture content
MLR	Multiple linear regression
OC	Organic carbon
PI	Plasticity index
PLSR	Partial least squares regression
PSD	Partial size distribution
R ²	Coefficient of determination
RMSEP	Root mean square error of prediction
RPD	Residual prediction deviation
SD	Standard deviation
USDA	United Stated Department of Agriculture
Vis-NIR	Visible and near infrared
WHC	Water holding capacity

1. INTRODUCTION AND LITERATURE REVIEW

1.1 Introduction

The amount of available water for irrigation is declining (Parsons and Bandaranayake, 2009), which necessitates the cautious use of water in agriculture. Estimating the amount of available water is essential to maintain yield all year round because the AWC in any field has a profound influence on crop growth and yield (Forbes & Watson, 1992; Braun et al., 1999; James et al., 2000). Irrigation systems are chosen according to the amount and the quality of water in addition to the cultural practices of the farmers. When farmers have information about the amount of water available, they can determine which crop to grow and evaluate irrigation methods; however, it is difficult to control water and yield maximisation can result in wasteful consumption. Accordingly, irrigation is often considered to be redundant, costly or entirely harmful. However, this can be put down to a bad choice or poor design of the proposed irrigation system, which leads undoubtedly to lowered efficiency and misuse of irrigation water. Effective irrigation methods depend largely on the nature of the field, soil type and spatial distribution, soil properties and efficiency of the water source. They are also affected by the type of crop as well as the prevailing climate.

Agriculture has been the main source of food and an important source of income for humans since ancient times. Land management systems in agriculture have been developed to increase the efficiency of crop production, improve product quality and protect the environment by the sustainable use of our natural resources. Information about soil properties is a vital activity in achieving these goals. With climate change, water becomes a very valuable natural resource; variable rate irrigation is one method to intelligently reduce water consumption for irrigation. As global climate change became an indisputable fact, the availability of water for agricultural resources reached maximum importance.. Its impact has meant the need to improve the capability

of agricultural irrigation water systems in order to enable agriculture to adapt to regional climate change (LU Ming-Xiang et al., 2010).

Researchers and producers are working to improve crop performance in order to generate more income through increased productivity (Fambro et al., 2003). To maximize the efficiency of crop production it is necessary to determine soil properties, such as soil fertility and the chemical and physical properties of soil. In the past, farmers lacked knowledge about soil properties, so optimal crops and cultivation of land were not possible. Today, most of the methods used to measure soil properties are based on traditional laboratory analyses and are expensive, time consuming and require an expert operator. Advanced sensing technologies including electromagnetic induction (EMI), optical, mechanical, acoustic and electrochemical techniques have become available recently either for direct use by farmers, with others still in development. These may provide fast, cost effective measurements while do not need expert operators.

The most important soil properties affecting the water holding capacity (WHC) are moisture content (MC), organic carbon (OC), soil texture, plasticity index (PI) and bulk density (BD) (Kvaerner et al., 2007; Waiser et al., 2007). Various methods are used for measuring these soil properties including advanced methods such as geophysical methods (e.g. EMI, electrical resistivity, etc.) and visible and near infrared (vis-NIR) spectroscopy in addition to the traditional laboratory methods.

In a comprehensive literature review on proximal soil sensors, Kuang et al. (2011) concluded that EMI and other geophysical measurement methods are limited technologies for extended quantitative evaluation of soil properties. Mapping the spatial variation of MC, CC, OC and BD using these geophysical methods is not feasible. Therefore, researchers focused on the use of multi-sensor concept. For example, data obtained with EMI and vis-NIR (non-mobile) sensors was fused to delineate management zones with variable-rate irrigation for vegetable crop production systems (Hedley et al., 2010). The incorporation of EMI and vis-NIR spectroscopy data enabled the determination of positions for

placing soil moisture sensors in the field, thereby reducing the requirement for large-scale scouting during field scanning (Aldhumayri, 2012). However, this author did not account for BD, although this parameter is important in determining the volume of soil water by controlling the pore space and retains the available water. Furthermore, soil BD differs with soil texture type. For example, zones in the field with high available water capacity will tend to have low soil BD (USDA, 1998). Similarly, heavy soil textures (e.g. clay soils) exhibit small BD ranges as compared to light sandy soils (Abramson et al., 2002). Therefore, BD needs to be considered for the derivation of WHC index, in addition to CC, OC, PI and MC.

One of the most important problems with agricultural systems is ensuring the best type of variable rate irrigation system for different crops. These problems can be resolved by using soil moisture sensors. These sensors determine the irrigation rate necessary for different agricultural products. This is especially important as over irrigation of agricultural crops can be just as damaging as under irrigation. Positioning of these sensors requires advanced knowledge about soil variability, particularly those affecting WHC of the soil. It is thought that the fusion of high resolution on-line collected data for key parameters of soil properties (OC, CC, PI, BD and MC) will assist not only in optimising the performance of these sensors, but also enabling the calculation of AWC for variable rate irrigation.

1.2 Measurement of Soil Moisture Content (MC)

The traditional gravimetric method is a direct measurement and it is the most important and most accurate way of measuring soil MC. It requires drying a soil sample in an oven for 24 hours at 105°C (British Standard BS 7755, 1994). A major advantage for this method is that it is easy and affordable; however, it is difficult to utilise in the field and it needs a considerable amount of time. Other methods used to measure soil moisture content include indirect methods, which require numerous efforts to calibrate. The differences between these sensors include calibration requirements, operation method, price, maintenance and

accuracy (Balendonck and Hilhorst, 2001). Among these are the Theta Probe ML2x (Delta Devices, Cambridge, UK) and Tensiometer mechanism, which is based on the measurement of the dielectric constant of the soil. These sensors are characterised by their ability to facilitate fast track decision-making, which enables swift management of the irrigation system. These sensors are installed at certain points throughout the site, based on experience or EMI measurement of the spatial variability in the field (Pardossi et al., 2009). However, soils are naturally heterogeneous, which necessitates the need for a method to quantify soil properties affecting the soil WHC.

1.3 Irrigation systems

These systems are defined by the way in which water is added to the surface of the soil or flows over it. They are considered the most common methods in arid and semi-arid areas. However, these methods are often used without adopting sensing technology to measure the amount of water needed by particular crops or any deficiency in the soil. There are many traditional methods of irrigation and among the most prominent of these are:

- i. **Flood irrigation:** This irrigation method is the simplest method of surface irrigation. It involves dividing a field into small units, and filling each and allowing water to seep through the surface horizontally. It works because the land comprises a basin surrounded by raised areas. However, these basins occupy a large area and it has been noted that this method does not provide the desired homogeneity of water as it is often filtered from neighbouring basins. By adopting this method of flood irrigation, including flow irrigation and irrigation lines, forms may vary because of cultivation of different crops (Phene, 2010). The most common problems in flood irrigation include the high percentage of water loss through evaporation as well as by leakage into the ground, ultimately resulting in higher consumption of water.
- ii. **Sprinkler irrigation:** This method is one of the newer methods and its deployment is increasing due to the availability and efficiency of sprays,

pumps and pipes. These are lightweight and made of aluminium. This method of irrigation for many different crops planted on lands of mixed topography is becoming commonplace. Adding water through the use of above ground sprays slightly resembles rainfall. Releasing pressurized water from narrow nozzle sprays means the spray can be configured and water is often pumped in order to obtain the necessary pressure. Sprinkler irrigation is suitable in many circumstances for irrigating almost all crops except rice. Thus, there are many advantages, including homogeneity in the distribution of moisture through sprinkler irrigation systems. However, adoption of this method rests largely on the properties of the ground water and local topography (Han et al., 2005). There are many types of sprinkler systems, including the Fixed System and Moving System-these often vary by location and crop. Most sprinklers feature the capacity to reduce water loss, they can irrigate uneven ground surfaces and they can be used easily and efficiently as items of agricultural machinery. Sprinklers can also control distribution of irrigation water, ensuring a homogeneous distribution in the soil, irrespective of soil properties. Under cold conditions, sprinklers can reduce the severity of any frost effects. However, there are some disadvantages, particularly the costly initial outlay and some degree of technical knowledge is required to deal with issues, such as clogged nozzles resulting from salt water deposits and so forth.

- iii. **Drip irrigation:** the drip irrigation method requires a dense network of pipes which go directly to the root zone in the form surface to soil flows to maintain an optimal level of soil moisture. This enables irrigation water to be fed to the plant continuously. It is also possible to add nutrients, unlike in other irrigation systems (Sammis et al., 2012). The adoption of this method involves the distribution of irrigation water throughout the season, depending on the changing water needs of the plant at various stages of growth. This water system allows for optimal distribution of moisture within the effective depth of the soil, leading to increased crop

yields (Hussain et al., 2010). However, the most basic advantage of drip irrigation is the significant saving in irrigation water. In addition, there are benefits in being able to provide fertilizers and pesticides at the same time with irrigation water. Furthermore, it is possible to use this method with moisture sensors to adjust nutrients and water automatically. However, the drawbacks of drip irrigation include clogging of the drippers caused by the constituents of irrigation water, in terms of fertilizer and salts, but also from irregularity in the irrigation water drippers due to differences in distribution of pressure.

1.4 Irrigation scheduling and moisture sensors

Sprinkler and drip irrigation are considered advanced irrigation methods. The increasing growth of the sprinkler irrigation pivot method in many areas of agricultural production has resulted in the drainage of a great deal of water from underground reserves. This is especially so in the absence of good management. It must follow that the best modern methods and the development of advanced technology to exploit it must be combined with the rational use of water, and irrigation scheduling mechanisms. These modern methods can be applied to provide the required amount of moisture to the root area of the plants with high efficiency. Irrigation scheduling is the process of making appropriate decisions. The primary goal of scheduling is to codify and rationalize the use of water for irrigation to ensure that losses are reduced to a minimum. At the same time, efficiency needs to be increased to the maximum to get the highest return from production. Scheduling mechanisms represents one of the most important choices in achieving this requirement, particularly the development of control systems with closed circuits using humidity sensors (Cardenas-Lailhacar and Dukes, 2010).

The basis of using scheduling mechanisms in this way is to measure the tensile soil moisture or actual MC within the root zone. In pursuance of this aim, soil sensors including Tensiometer mechanism and Theta Probes are installed in the field for measurement at different depths from the soil surface (30 and 60

cm) (Zhen et al., 2011). Each pair of sensors is connected so they can send and receive for the entire field. However, the major drawback of this method is the problem of how to determine the position of moisture sensors in order to optimise irrigation process. This is done by using an EMI instrument, which cannot quantify the values of soil properties affecting the WHC and AWC. Figure 1-1 shows a moisture sensor installed in a field with dripping irrigation system under vegetable crop production system.



Figure 1-1: Shows a moisture sensor installed in field with dripping irrigation system with vegetable crop

In order to determine the optimum position and the required number of MC sensors needed to provide input data for variable rate irrigation, it is necessary to take multiple soil samples from a site, to characterise the spatial variation in the key soil factors affecting WHC and AWC. This is an essential requirement due to the inherent heterogeneity existing in the majority of the agricultural soils. Manual collection of soil samples followed by traditional laboratory analysis is costly, time consuming and requires an expert operator. The use of multi-sensor and data fusion approach will enable optimising the number and positions of soil moisture sensor in the field, based on the existing and inherited spatial variation

in key soil properties (e.g. MC, OC, CC, PI, BD) affecting WHC and AWC. This will be possible to achieve by the delineation of homogeneous management zones based on advanced geostatistics and data fusion algorithms.

1.5 Key factors affecting water holding capacity (WHC) and available water content (AWC) in the soil

Water holding capacity is defined as the difference of water content between that at wilting point and that at the field capacity. In the current thesis, WHC was proposed to be equal to gravimetric moisture content, whose quantity is affected and derived as a function of BD, OC, CC, ECa and PI of the soil. While, depends on the quantity of salts in the solution and the amount of rock fragments (USDA, 1998). The water retention of soil depends on several physical and chemical properties that affect the amount of water available to plants as follows:

- a. **Rock fragments:** This reduces the AWC with indirect proportion to their volume unless the rocks are porous (USDA, 1998).
- b. **Organic matter:** the presence of organic matter content in soil helps to increase the amount of water absorbed, and thus increases the available water capacity of the soil. A 1% organic matter in the soil provides about 1.5% of available water holding capacity (USDA, 1998). It is believed that by applying the mixture of organic matter to the upper few inches of soil will increase the available water fraction near the surface (USDA, 1998).
- c. **Bulk density:** bulk density has an important role in controlling pore space and the available water capacity. Available water capacity in the soil is reduced at high bulk density soil (USDA, 1998).
- d. **Osmotic pressure:** This can increase the capacity in the soil solution by about 0.3 – 0.4 times with electrical conductivity. This is important given the reduction in available water capacity at electrical conductivity of more than 8 mmhos/cm (USDA, 1998).
- e. **Soil texture:** USDA studies in 1998 showed that, assuming the same BD and rock fragments (for instance in clay and silty clay), the available

water capacity was about 0.10 - 0.20. In silt, silt loam and silt clay loam soil types, the available water capacity was about 0.15 - 0.25. In addition, the available water retention capacity depends on the root depth of the type of plant.

- f. **Soil quality:** This factor is defined as the ability of a particular type of soil (within its natural limits, or within its externally improved limits) to enhance the productivity of plants. It is an integral property of soil. It is indirectly linked with AWC and WHC. According to USDA studies in 1998, for comparison between two kinds of soil with different properties and climates, it is important to select a crop that will elicit water from a depth of about 60 inches without a surface root barrier. Therefore, soil quality and water retention capacity are at their best in soil with good internal properties and a lower evapotranspiration deficit. Therefore, the soil's physical, chemical and biological make-up affects the available water and the reduction of plant growth (Ding et al., 2012).

Some other factors that will improve the availability of useable water include maintaining salts below the root zone, reducing the rate of tillage, trying to avoid mixing the layers of the soil and increasing plant yields by sowing more seeds (USDA, 1998). However, by adopting proper management strategies the WHC can be a dynamic characteristic to modify and improve.

In conclusion, based on the previous key factors, which affect the AWC and WHC, the spatial distribution of MC is a complex process. Ideally, it would be useful to measure all these key factors to characterise the spatial variation in WHC and AWC. However, this is technically impossible, as technology is not so advanced to enable realistic quantifications of all these factors quickly and in a cost effective manner. But, a selection of the most important factors e.g. OC, BD, CC and PI (CC and PI can be both under soil texture) must be made, so that they can be measured with the multi-sensor platform of Cranfield University (Mouazen, 2006). This is expected to be an essential requirement for guiding

site specific irrigation systems and positioning of moisture sensors to optimize the variable rate irrigation strategy.

1.6 Visible and near infrared Spectroscopy (vis-NIR) for the analysis of soil properties

When a soil sample is subjected to a light source, chemical bonds (such as C-H, N-H, S-H and O-H molecular bonds) start to vibrate, which leads to energy absorbance at particular wavebands. Although, the fundamental vibrations of molecules occur in the mid infrared (MID) range, these are transformed into overtones and combinations in the NIR range (Kuang et al., 2012). Although these overtones and combination bands are broad, they are important feature of NIR Spectroscopy (750-2500 nm) and enable qualitative and quantitative analyses of soil characteristics. The spectral features of ascription or particular wavelengths are the main features that enable quantitative and qualitative analyses using chemometrics. The advantages of the vis-NIR spectroscopy when used for soil analysis are that the analysis of soil properties can be undertaken simply and very quickly (Ben-Dor and Banin, 1995; Reeves et al., 1999; Stenberg et al., 2002; Chang et al., 2005). Recently, the vis-NIR spectroscopy was adopted for on-line measurement protocols (Mouazen et al., 2005).

The diffuse-reflectance measurement is the most frequently used measurement modes in NIR spectroscopy application for soil analyses. It is dependent on the highly variable physical properties of soil samples with age-long miscibility between chemometrics and NIR spectroscopy (Okparanma and Mouazen, 2011). Thus, the changes in the resulting spectrum result from variable physical and chemical parameters of soils. During the qualitative and quantitative analyses, relevant information is extracted from the spectra by means of both linear and non-linear multivariate analyses (MVA). Linear tools include multiple linear regression (MLR), principal component regression (PCR), partial least squares (PLS) regression and penalized spline. The non-linear modelling tools enable solving of problems with non-linear behaviour. These include artificial

neural network (ANN), support vector machine (SVM), boosted regression trees (BRT), random forest (RF) and wavelet. However, studies showed that PLS regression is sufficient to provide the best calibration results for soil spectroscopic analysis (Ben-Dor and Banin, 1995; Chang et al., 2001; Bogrekci and Lee, 2004; Mouazen et al., 2006a). Others proved the ANN to provide the best prediction performance in comparison with PLS or PCR (Mouazen et al., 2012; Viscarra Rossel, et al., 2010). In conclusion, the selection of a chemometrics tool for running analysis will depend on the behaviour to be linear or non-linear.

One of the most important features for the vis-NIR spectroscopy is that it is a non-destructive, rapid and cost-effective technology, which enables simultaneous estimation of a variety of soil properties including (among others) OC, CC, pH, organic matter, MC total carbon, and inorganic carbon, total nitrogen (TN), plant-available phosphorus (P) and soil type (Mouazen et al., 2005, 2006a, b, 2007, 2009, 2010; Viscarra-Rossel et al., 2006a, b, 2009; Maleki et al., 2007; Gomez et al., 2008; Viscarra-Rossel and Behrens, 2010; Canasveras et al., 2010; Wetterlind et al., 2010). However, previous research illustrates the effect of factors on performance and accuracy including moisture content (Mouazen et al., 2006b), soil texture (Mouazen et al., 2005; Cozzolino and Moron, 2006; Bathes et al., 2008), soil colour (Mouazen et al., 2007a), number of samples (Kuang et al., 2012), soil samples pre-treatment (Therhoeven-Urselmans et al., 2008; Yang et al., 2011a), methods used to develop calibration models (Mouazen et al., 2010; Viscarra Rossel and Behrens, 2010; Vohland et al., 2011), standard deviation and the range of samples concentration (Kuang and Mouazen, 2011a), spectral data pre-processing (Maleki et al., 2007; Yang et al., 2011b) and soil heterogeneity (Brunet et al., 2007). The application of vis-NIR spectroscopy for soil analysis was evaluated under three measurement scenarios, namely, laboratory, in situ (non-mobile) and on-line (mobile) measurement modes (Kuang et al., 2012). It has been shown that, under laboratory analysis, dry and processed soil samples provide the best performance in terms of accuracy compared with

other measurement methods (Kuang et al., 2011). Some of the soil properties including total C, soil OC, inorganic C, total N, cation exchange capacity, pH, texture, moisture content and mineralizable N, are slightly more accurately measured by the NIR for air dried soil than for wet soil samples (Chang et al., 2005). In the case of fresh soil, both non-mobile and on-line measurement modes resulted in decreased measurement performance due to the influence of MC. For on-line measurement conditions, in addition to MC, other parameters affect measurement accuracy, which include ambient light, machine vibration, plant root depth, debris and variation of soil-to-sensor distance (Mouazen et al., 2007; Stenberg et al., 2010).

The most important advantages associated with the on-line data collection are the high sampling and real-time measurement. Sudduth and Hummel (1993) were the first researchers to develop an on-line sensor for soil properties. They found a standard error of 5% for the prediction of organic matter. Shibusawa et al. (2000) reported on the development of soil maps of MC using the best prediction model (Shibusawa et al., 2000). Mouazen reported a new on-line NIR sensor for the measurement of soil MC (Mouazen et al., 2005), which was expanded to the measurement of other soil properties including TN, OC, P and pH (Mouazen et al., 2007 & 2009). Aldhumayri (2012) concluded that the vis-NIR sensor designed by Mouazen (2006) provided valuable data on OC, TN and MC that can guide positioning and density of MC sensors for site specific irrigation. However this author did not attempt to measure other soil properties affecting the WHC and AWC (e.g. PI, CC and BD).

1.7 Electrical Conductivity Methods (EC)

Electromagnetic induction (EMI) is used for mobile and on-line measurement of soil apparent electrical conductivity (ECa). EMI scanning is a proximate, fast and non-invasive method for obtaining information about soil properties. The simplest version consists of transmitter coil and a receiver coil with a fixed distance (fig 1-3). The transmitter coil is energised with alternating current with

high-frequency (>1 kHz) creating a magnetic field that causes a small secondary current in the soil, while the soil matrix produces a weak secondary magnetic field. The receiver coil measures the amplitude and phase of the secondary magnetic field (Abdu et al., 2007). The magnitude of eddy current loop is directly proportional to the electrical conductivity of soil

$$ECa = \frac{4}{\omega\mu_0s^2} \left(\frac{H_s}{H_p} \right)$$

H_s is secondary magnetic field (Hm^{-1}), H_p is primary magnetic field at transmitter coil (Hm^{-1}), $\omega = 2\pi f$, f = frequency (Hz), μ_0 = permeability of free space, and s = inter-coil spacing (m) (McNeill, 1980).

Recently, there is a new version of EMI known as Dualem 1S (D-1S; Dualem Inc., Milton, ON, Canada), as shown in Figure 3-4.

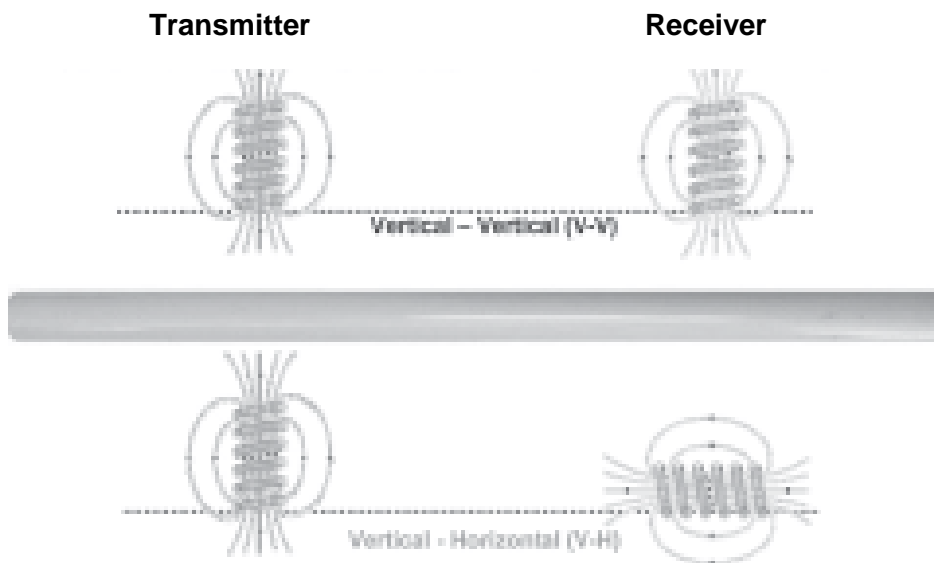


Figure 1-2: Shows the transmitter and receiver dipole orientations of DUALEM-1S using a vertical-vertical (V-V) and a vertical-horizonal (V-H) mode for the dipoles in DUALEM-1S (Abdu et al., 2007)

Dualem sensors measure ECa and susceptibility as two distinct factors of specified depths. They also enable the estimation of ECa, susceptibility and thickness in layered earth. The sensor records electromagnetic responses internally, positioning coordinates and values for time, pitch, roll, voltage and temperature. Because this instrument is operated by electromagnetic induction, there is no need to have contact with the soil's surface. Therefore, it enables surveying at moderate speed over rough, dry or non-conductive terrain. The sensors can be portable or drawn by a vehicle. The Dualem contains a 1m separation between the transmitter coil and dual receiver coils, so it can more measurements of depths from 0.5 m to 1.5 m (www.dualem.com). It consists of three coils: one vertical transmitter coil and two receiver coils. The vertical coil (coplanar, 1m apart from the transmitter) and horizontal coil (perpendicular, 1.1m apart from the transmitter) provide two simultaneous ECa readings (V-V and V-H, respectively) (Urdanoz & Aragues, 2012). However, this sensor is most sensitive at the surface and the sensitivity decreases rapidly with depth (Abdu et al., 2007). Data reading using these instruments is undertaken every second at two depth levels (30 cm and 120 cm), with the waves falling vertically on the surface.

Researchers have showed that EMI can be either directly or indirectly used to determine soil properties (Sudduth et al., 2005). This method has proved to provide successful measurement of few soil properties in few cases while failing to do so in many other cases, which may be attributed to the multiple effects of several factors on EMI signal including MC, texture, OC, salinity and soil compaction (McNeill, 1980; Friedman, 2005; Padhi and Misra, 2011; Kuang et al., 2012). However, in salt affected areas, strength of the solution is the main contributor to ECa (Williams and Hoey, 1987). In some countries with temperate climates, salt is not a problem, where organic matter content, mineralogy, bulk density and soil MC are factors affecting ECa measurement (Brevik and Fenton, 1987). The EMI soil sensing and yield map sequence analysis methods provide information for the determining soil texture boundaries and crop management zones. However, an EMI-determined ECa map cannot always determine the

optimum management zones without physical soil examination in the field to confirm specific soil properties (King et al., 2005). Another disadvantage of EMI is the need to maintain the zero measurement and the calibration of the instrument. There can also be errors in accuracy, which can become significant in areas of low conductivity. Measurement accuracy is +/-5% at 30 mS/m (Geonics Ltd., TN6). Aldhumayri (2011) wrote about ECa measured by an EMI sensor to provide a minor response with MC distribution in the field with a small contribution to the data fusion algorithms used to delineate homogeneous management zones. Despite these disadvantages (among others) EMI remains a widely adopted method for positioning soil moisture sensors for variable rate irrigation systems.

ECa measurements with the EMI technique have received great attention within precision farming community (Corwin and Lesch, 2005; Padhi and Misra, 2011). Waive et al., (2000) reported that soil MC and soil type can be measured by EMI. EMI surveys may be used for improving traditional soil sampling survey. It has also shown to be useful for improving soil mapping of agricultural landscapes, particularly in terms of continuous monitoring where there is a large number of fallows and cropped sites (Zhu et al., 2010; Padhi and Misra, 2011). EMI techniques have also been used for the determination of soil texture boundaries (James et al., 2000; 2003), to map soil topography and weed status (Godwin and Miller, 2003) and to map soil water status in irrigated maize fields (Hedley et al., 2010).

2 RESEARCH AIM AND OBJECTIVES

2.1 Research gap

Following on from the previous literature review, there are gaps in this research area. Although a previous study by Aldhumayri (2011) combined EMI and vis-NIR data using a simple data fusion approach, for CC, PI and BD measured with the vis-NIR sensor were not included in the analysis. Furthermore, only a linear regression analysis was used to quantify correlations between OC, TN, ECa with MC based on correlation coefficient values established between each pair of properties. Therefore, there is a need to account for the most important factors of influencing soil WHC, and to explore their measurement with the on-line multi-sensor platform based on vis-NIR spectroscopy and EMI sensors. These include CC, PI and BD (in addition to ECa, OC and MC). Also, there are other methods e.g. clustering analysis, more advanced data analysis methods including the multiple linear regression analysis (MLR) and artificial neural network (ANN) will be used to derive the WHC as an important index to assist optimising the position and number of soil moisture sensors. The WHC will also assist the calculation of AWC and enable variable rate irrigation. So far, no previous reports on the use of on-line vis-NIR sensor to measure soil PI can be found in the open literature.

2.2 Research aim

The aim of this project is to implement a multi-sensor platform and data fusion approach for the delineation of management zones for site specific irrigation. This will aim at simultaneous measurement of MC, OC, PI, CC, BD and ECa which enables deriving WHC index and calculate AWC. The delineation of homogeneous zones of WHC and AWC will be a useful approach to optimise the position and the number of soil moisture sensors in addition to providing input data for variable rate irrigation. In order to achieve this aim the following objectives were assigned.

2.3 Research objectives

The research has the following objectives:

1. To collect data on soil measured by the on-line vis-NIR and EMI sensors from selected fields with different textures. In this context, fields with vegetable crop production systems are selected. Soil properties, such as OC, CC, BD, MC, PI and ECa are measured.
2. To develop calibration models for CC and PI for the vis-NIR spectroscopy. These models should be validated for the measured fields under non-mobile and mobile measurement conditions.
3. To fuse soil data, using mathematical and statistical methods to derive water holding capacity index.
4. To implement and validate empirical models available in the literature to calculate AWC
5. To delineate management zones for optimising the number and position of the moisture sensors and guiding the variable rate irrigation based on the derived WHC and AWC.

3 MATERIAL AND METHODS

3.1 Experimental field and collection of soil samples

In collaboration with the grower Produce World, four test fields were identified. Soil samples were collected before on-line measurement was carried out for the development of the calibration model for the vis-NIR spectrophotometer. Further soil samples were collected during the on-line measurements to validate measurement accuracy.

3.1.1 Collection of soil samples

Four fields were identified in England with different soil textures. The fields in question are located at Thetford, Vicarage and Marshall's in Lincolnshire and Wypemere in Cambridgeshire. These fields are intended for growing different vegetable crops. Approximately 60 samples were collected; before on-line measurement, with 14 samples each from three of the fields and 18 samples from Marshall's field. The samples were taken from the bottom of the trenches at about 15 cm depth, to conduct the physical and chemical analysis with traditional laboratory methods for MC, OC, CC and PI. Afterwards, the points were chosen for taking samples from each field; the coordinates of these points were recorded using a hand-held GPS device. Figure 3-1 shows the locations of these fields in England. Another 81 soil samples were collected during the on-line measurement; of which 21 samples each were collected from three fields and 18 samples from Vicarage field. The positioning of these soil samples was carefully recorded using a DGPS (EZ-Guide 250, Trimble, USA). Table 3-1 contains detailed information about the locations of the study fields. Between one and three samples were collected from each of the on-line, vis-NIR measurement line. Figure 3-2 shows an example of on-line measurement lines from Vicarage Farm. All of these soil samples were employed to develop new vis-NIR DRS calibration models of plasticity index; also they were used to upgrade the soil models for OC, CC and MC. Therefore, in order to validate the on-line measurement accuracy of these soil properties, all the soil samples were kept in a fridge at a temperature of 4°C until analysis.



Figure 3-1: Shows the location of the four fields in England which were used in the study

3.1.2 On-line vis-NIR DRS and BD measurement

The on-line vis-NIR soil sensor available at Cranfield University was used to measure all four fields: this sensor was also used to measure soil BD (Mouazen et al., 2005). The on-line measurement kit consisted of a subsoiler, which is a 9

tonne capacity single-ended shear beam load cell (Griffith Elder & Company Ltd, Suffolk, UK) for the measurement of draught; a draw wire linear sensor (Penny + Giles Controls Ltd, Dorset, UK) which was connected to a wheel gauge for the measurement of subsoiler depth; a visible and near infrared (vis-NIR) sensor (tec5 Technology for Spectroscopy, AG, Oberursel, Germany) for the measurement of soil properties, namely, MC, OC, CC and PI. Soil BD can then be calculated as a function draught D (kN), depth d (m) and soil moisture content MC (kg kg^{-1}) based on the following function (Mouazen & Roman, 2006):

$$BD = \sqrt[3]{\frac{D+21.36MC-73.9313d^2}{1.6734}} \quad (3-1)$$

The on-line system is equipped with a DGPS (Trimble UK, Hook, UK) for recording the position of the sensor (Mouazen & Ramon, 2006). The data acquisition consisted of a tec5 analogue to digital data converter (tec5 AG, Oberursel, Germany) and Fylde FE-MM8 (Fylde Electronic Laboratories Ltd., Preston, UK) data acquisition hardware. AgroSpec (tec5 AG, Oberursel, Germany) and DASyLab (Version 8, measX GmbH & Co.KG, Germany) data logging software were employed as well. A semi-rugged laptop (Toughbook, Panasonic UK Ltd., Bracknell, UK) was used for running both data logging software programmes simultaneously with a measurement range of 305-2200 nm. Figure 3-3 illustrates the multi sensor platform for the on-line measurement of soil properties (Mouazen, 2006). All hardware, including the laptop, was enclosed in an IP-65 metal box during measurement so as to protect against dust and rain. The AgroSpec software logged DGPS and spectrophotometer reading set at 1 Hz. The DASyLab software logged draught force and subsoiler depth readings at 10 Hz. Both data streams were joined together using timestamps (Quraishi & Mouazen, 2012). A tractor battery was used to power the spectrometer system, laptop and DGPS.

However, each field was measured by covering different areas between 1.5 and 3 ha. The measurement was done with parallel lines with 10 m intervals between adjacent transects, as shown in (Figure 3-3).

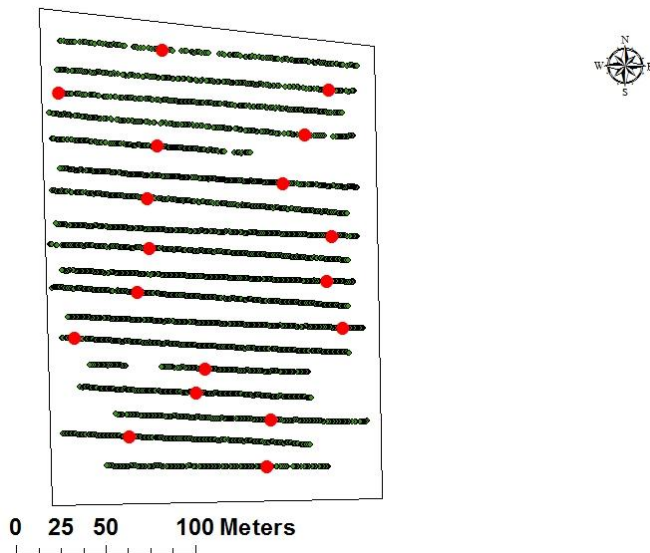


Figure 3-2: Shows the online measurement lines (black) and sampling points (red), shown for Vicarage field as an example

The tractor travel speed was around 2 km/h and the initial depth was set at 15 cm. About seven lines each were measured in three of the four study fields and 18 lines in the fourth, e.g. Vicarage field. It is worth mentioning that the on-line measurement was recorded after two days of heavy rain, which have a negative effect on vis-NIR prediction accuracy, a confirmed by Kuang and Mouazen (2013).

Table 3-1: The study fields, the on-line vis-NIR and EMI measurements took place

Field	Area, ha	Crop	Soil Texture
Vicarage Farm	3	Potatoes	Sandy Silt Loam
Marshall's Farm	4.5	Broccoli	Sandy Silt Loam
Wypemere Farm	8	Potatoes	Silty Clay
Thetford Farm	4	Potatoes	Clay Loam



Figure 3-3 : Illustrates the multi-sensor platform for on-line measurement of soil properties (Mouazen, 2006)

3.1.3 EMI instruments for measuring the electrical conductivity

A Dualem 1S instrument was used in all fields to measure ECa, with the sensor installed on a quad bike that was equipped with a GPS device. This was done in collaboration with Soyl precision farming (<http://www.soyl.co.uk/>). The sampling frequency was one reading every second at two depths (30 cm, shallow and 120 cm, deep), with the waves falling vertically on the surface. The ECa measurement was carried out in all fields about two weeks after the vis-NIR measurement.



Figure 3-4: Shows the Dualem 1S sensor with a quad bike during field measurement

3.1.4 Moisture content measurement

The measurements of the soil volumetric MC were carried out in all the fields using a Theta probe sensor type ML2X Delta-T Devices (Delta-T Devices Ltd, Cambridge, United Kingdom) to obtain an estimation of volumetric MC. Theta probe readings took place after two days of heavy rain. It was easy to use and made accurate soil moisture measurements (accuracy = $\pm 0.01 \text{ m}^3 \cdot \text{m}^{-3}$). The soil moisture probe was inserted into the soil, which in turn was connected to the data logger or readout unit. A current of 5-15V DC at 20mA was provided and within seconds the soil moisture was able to be data logged. The probes

can be easily installed deep into the soil by inserting them into holes. A theta probe ML2X is shown in Figure 3-5.



Figure 3-5: Shows the *Theta Probe ML2X* for the measurement of the moisture sensor

3.2 Laboratory Experiments

Overall, the 141 samples collected from the four fields (32 samples from Vicarage, 39 samples from Marshall's, 35 samples from Wypemere and 35 samples from Thetford) were analysed in the laboratory with relevant methods to measure MC, PI, OC and CC. The methods used for these measurements are described below.

3.2.1 Moisture Content (MC) analysis

The MC of the soil was determined by drying the soil samples in an oven at $105^{\circ}\text{C}\pm 5$ for a minimum of 24 hours (BS 7755, 1994). The moisture content measurement was deduced by calculating the difference between the mass of fresh samples and the samples after drying.

3.2.2 Organic Carbon (OC) analysis

After the sample has been dried in the oven at about 105°C for 24 hours, organic carbon can be measured using the Dumas combustion method (BS 7755, 1995). The dried soil samples were put into a small silver-foil capsule,

after which about 4 mol/L of hydrochloric acid was added until effervescence stopped (BS 7755 Section 3.8 (BSI, 1995)). A small amount of the soil samples -0.001 mg - was weighed with a TrusSpecCNS spectrometer (LECO Corporation, St. Joseph, MI, USA). The samples were returned to the oven and subjected to 90°C heat for about four hours, ± 15 minutes. After that, they were packed into a larger piece of aluminium foil and loaded into the carousel of the auto sampler. The sample mass was tested by entering the data on the instrument software of the sample named along with matrix-specific oxygen dosing.

3.2.3 Soil texture analysis

The soil texture was measured by the sieving and sedimentation method (BS 7755 Section 5.4 (BSI, 1998)), described as follows:

- a. **Organic matter removal:** Using a measuring cylinder, 30 ± 1 ml of demineralised water and 25 ml of 100 by volume of hydrogen peroxide from a dispenser were added to about 10 ml of air-dry soil <2 mm density for each of the samples using a specially made 10 ml brass scoop. These samples were placed in labelled polycarbonate bottles (4d.p.). They were mixed manually and put on a cold hotplate enclosed in a fume hood overnight to complete the decomposition. Afterwards, the temperature of the hotplate was raised to $100 \pm 2^\circ\text{C}$ for about 2 hours and the bottle was removed from the hotplate and allowed to cool.
- b. **Dispersal and wet sieving:** A measure of $200 \pm 1\text{g}$ of demineralised water was added to a bottle, which was vigorously shaken in a centrifuge at 2000 ± 100 rpm for at least 20 minutes and the supernatant sediment was discarded afterwards. Next, approximately 20 ± 2 ml of sodium hexametaphosphate buffer solution was added by dispenser and also 150 ± 2 ml of water was administered by a measuring cylinder. Later the bottles were capped tightly and shaken thoroughly overnight (18 hours) by an end-over-end shaker. After that, about 20 ± 2 ml sodium hexametaphosphate buffer solution was poured into a weighed bottle (to

4 d.p.), which had been dried in an oven at 105°C overnight. The bottle was reweighed after cooling in a desiccator. The contents of the bottles were washed gently through a 0.063 mm sieve into a 500 ml measuring cylinder with water and the residue was retained. The residue was then dried at 105±2°C for a minimum of 4 hours.

c. Dry-sieving the sand fraction: The contents of each beaker were taken from the oven and poured into a mechanical shaker made up of a nested column of sieves. The samples were shaken for about 15 minutes and then they were diluted with demineralised water until the mixture reached a volume of 500 ml for each cylinder respectively. Thereafter, each full sieve was recorded and transferred to the cylinder.

d. Determination of silt and clay fractions by pipette extraction: The cylinder was placed in a bath of water at 25 °C to equilibrate overnight. Aliquot parts of the mixture were put into two sets of glasses weighing 4 d.p. to receive the 0.002-0.063 mm range and <0.002 mm range of particles, respectively. After that, the cylinder was stirred gently for about 30 seconds and immediately 25 ml of aliquot parts were drawn from the 10 cm depth into the 0.002-0.063 mm set of glasses. After a period of 6 hours and 23 minutes had elapsed for the sedimentation for the < 0.002 mm range of particles, another 25 ml of aliquot parts was drawn from the 9 cm depth into the < 0.002 mm set of glasses. These were placed in an oven at 105 ±2°C for a minimum of 24 hours and after that they were allowed to cool in a desiccator and weighed. An average value can be obtained for all types of soil samples, such as sandy soil, clay and silt.

Looking at these equations, it can be deduced:

$$D = \frac{d}{20} \quad (3-2)$$

$$F = S + Z - D \times 20 \quad (3-3)$$

$$\%sand = \frac{\text{Mass of particle sand fraction}}{F} \times 100 \quad (3-4)$$

$$\%0.002 \text{ to } 0.063 \text{ mm} = \frac{(Z-C) \times 20}{F} \times 100 \quad (3-5)$$

$$\% < 0.002 \text{ mm} = \frac{(Z-D) \times 20}{F} \times 100 \quad (3-6)$$

Where, D = Dispersant factor

$$F \text{ factor} = \frac{(\text{mass of all sand sample}) + (\text{mass of all silt sample} - D) \times 20}{20}$$

d = oven dry mass of sodium hexametaphosphate buffer solution (g)

Z = mass of 0.002-0.063 mm pipetted sample (silt + clay) (g)

C = mass of <0.002 mm pipetted sample (clay) (g)

S = total mass of sand (g)

Using the United Kingdom soil textural classification scheme (Figure 3-6), the soil sample texture can be determined based on the percentage of sand, silt and clay.

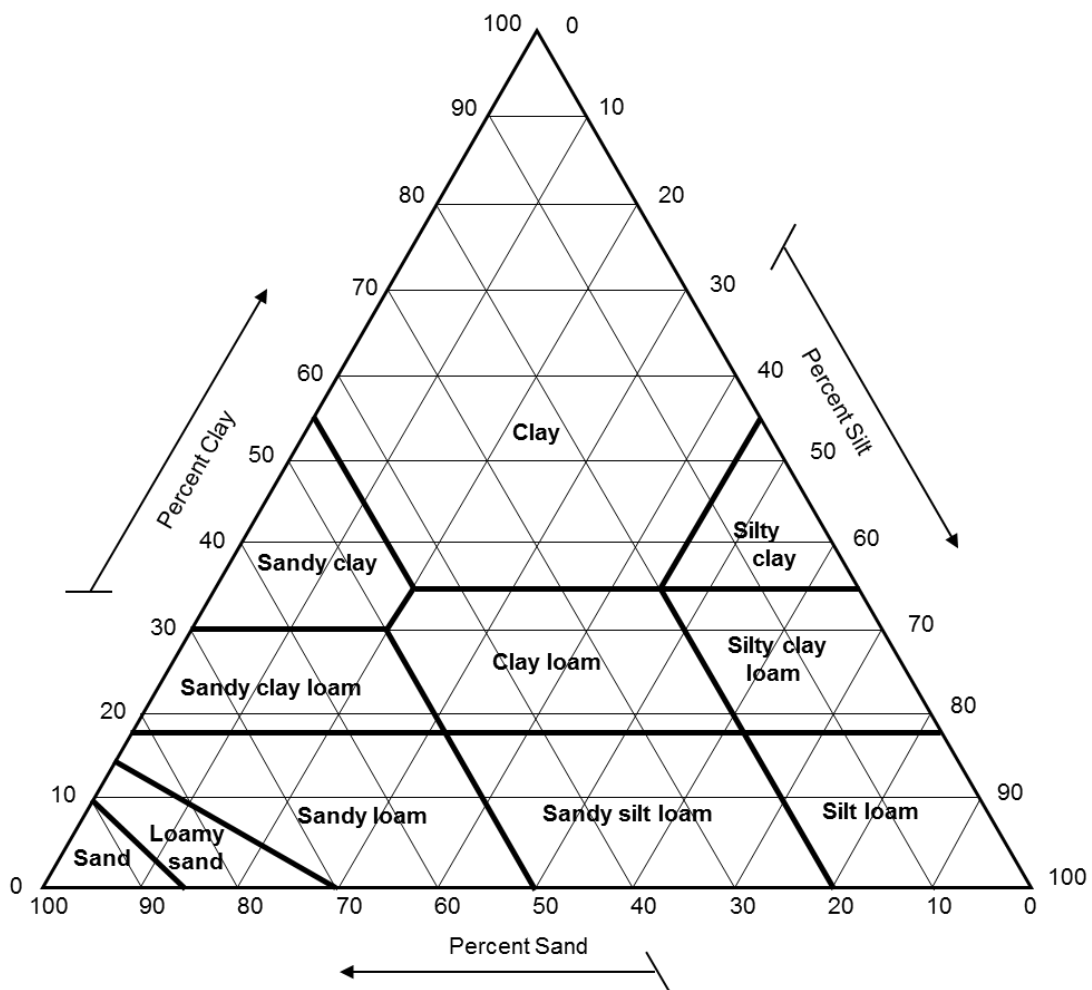


Figure 3-6: The United Kingdom soil classification scheme

3.2.4 Plasticity index analysis

The plasticity index of soil is evaluated by determining the plastic limit and the liquid limit BS 1377-2:1990:

- **Plastic limit (MC_p):** This is determined by taking a 20g portion of the fresh soil, moulding it into a ball between the fingers and rolling it. This sample is divided into two subsamples of about 10g. Using a glass rolling plate, a fine portion of the soil is moulded into a 3mm diameter thread, which retained its shape under pressure. These samples were then dried in the oven for 24 hours at a temperature of 105°C. The average MC is called the plasticity limit (MC_p).
- **Liquid limit (MCL):** This is determined using the cone penetrometer method. About 300g of fresh soil was mixed thoroughly with distilled water until it became a homogenous and coherent mass. Then, the brass cup was filled with the soil and it was kept in a container without trapped air pockets and left on a smooth surface. The cup was placed under the penetrometer (Figure 3-7) and the cone was lowered until it was just in contact with the soil surface. Next, the dial gauge was set to zero and the cone was released for 5±1 seconds. Thereafter, the dial gauge was lowered to the new position and the depth of penetration of the soil mass by the cone was reread and recorded. Afterwards, the cone was lifted out and cleaned and then the soil on the cup was moistened. A moist soil sample of 10g was taken from the area penetrated by the cone which determined the MC. The remaining soil was removed from the cup, moistened and mixed thoroughly with the original soil. This was repeated again for a minimum of four MC samples. The range of penetration should be between 15-25 mm. By using the linear graph of penetration values plotted against MC and read off MC that corresponds to a cone penetration of 20 mm to one decimal place the liquid limit (MCL) could be determined.

$$MC \% = \frac{(m_1 - m_2)}{(m_2 - m_o)} \times 100 \quad (3-7)$$

Where,

- MC = moisture content (%)
- m_o = is the mass of the dish (g)
- m_1 is the mass of the dish plus wet soil (g)
- m_2 is the mass of the dish plus oven-dried soil (g)

To calculate the Plasticity Index (PI), the following equation was used:

$$PI \% = MCL - MCP \quad (3-8)$$

Where,

- PI Plasticity index (%)
- MCL Liquid limit (%)
- MCP Plastic limit (%)



Figure 3-7: Shows the penetrometer and cone used to determine the liquid limit

3.2.5 Optical measurement

Altogether, 141 samples were collected and kept in a refrigerator at a temperature of about 4°C. After filtering out the noise, each soil sample was mixed thoroughly. Each sample was divided onto three Petri dishes, which were 2 cm deep and 2 cm in diameter. Before scanning with the AgroSpec mobile spectrophotometer with a wavelength range of 305 and 2200 nm (tec5 Technology for Spectroscopy, Germany), the surface of each sample was smoothed out by a spatula which ensured maximum light reflection and high signal-to-noise ratio (Mouazen et al., 2005) and was shaken gently. Employing the same vis-NIR on-line measurement used during the fields measurement, a 100% white reference was used before scanning, which had to be repeated every 30 min. Each sample was scanned 15 times from the three dishes and the average was used in one spectrum. The information from the derived average of the spectrum was used to build a model for CC, OC, MC and PI and to calibrate the result of online mobile measurements in the fields.

3.2.6 Pre-treatment of vis-NIR spectra

The Unscrambler® software Version 7.88 (Camo A/S, Oslo, Norway) was used for spectra pre-treatment and model development. The spectra pre-treatment aimed to remove the noisy part of the spectrum or eliminate some sources of variation not related to the measured value. After filtering out the noise, a wavelength range of 371-2150 was retained for further pre-treatment. Various data pre-processing options were used in this study to develop calibration models. A structured trial and error process was followed to determine the best pre-processing method, and the final selection of a pre-processing method was based on comparing the results of the different models. The successive steps of pre-processing the soil spectra are a) reducing the number of wavelengths by averaging three wavelengths in the visible and 15 wavelengths in the NIR range. A larger reduction factor was adopted in the NIR range, as larger noise existed in the NIR range as compared to the visible range. Based on optimisation of wavelength reduction versus measurement accuracy, the

selected reduction gave the best accuracy; *b*) maximum normalisation of data was then implemented which is typically done by placing all data on approximately the same scale and to obtain a more even distribution of the variances; *c*) Savitzky & Golay's 1st derivative (Savitzky & Golay, 1964) was followed to compute derivatives of the 1st order, based on a polynomial approximation of a portion of the curve. The 1st derivative was adopted using a second-order polynomial with a polynomial order of 2 fitted to the spectra. Yang et al., (2012) studied the effect of different pre-processing methods on the principal component analysis of soil classification. The results showed that 1st derivative tended to be the best option, and the 2nd derivative should be avoided due to the greater amount of noise introduced into the data; *d*) Smoothing was applied using a second-order polynomial with a polynomial order of three. The scatter effect in spectroscopy is caused by physical phenomena, such as particle size, rather than chemical properties. The 1st derivative and the smoothing with the Savitzky and Golay method that followed normalisation aimed to attenuate the effect of sharp peaks, which do not hold physical or chemical information.

3.2.7 Development of calibration models

A total of 262 samples used to develop calibration models for the CC (60 soil were from the four study fields before the on-line measurement, 107 samples collected from three fields in 2011 (Al-Dhumayri, 2012) and another 95 soil samples previously collected from five fields in the UK, four fields in Holland, two fields in Denmark, one field in Germany and one field in the Czech Republic (Kuang & Mouazen, 2011b)). Only, 167 samples were used to develop calibration model for MC and OC. Only 60 samples collected in this study were used for the development of the PI calibration model. It has used 60 samples from the study field to validate all soil properties of the vis-NIR on-line measurement.

Table 3-2: Comparison of sample statistics between the Calibration set and laboratory validation groups at all study fields

Fields		Calibration set				Validation set samples			
		OC	MC	PI	CC	OC	MC	PI	CC
Vicarage	NR	262	167	60	262	60	60	60	60
Farm	Min%	1.28	14.79	14.79	8.49	1.25	16.57	16.57	7.79
	Max%	1.66	22.61	22.61	16.08	1.69	22.49	23.20	13.84
	Mean%	1.42	19.50	19.43	12.33	1.41	20.21	20.40	10.95
	SD%	0.11	2.23	2.24	2.31	0.13	1.55	1.73	1.65
Wypemere	NR	167	167	60	262	60	60	60	60
Farm	Min%	6.49	30.09	17.18	22.82	5.91	32.57	16.16	37.94
	Max%	13.4	45.82	28.69	48.08	13.0	50.93	31.04	57.69
	Mean%	9.84	38.93	21.94	35.95	9.74	43.16	20.71	48.29
	SD%	1.93	5.19	3.16	6.54	2.02	5.59	4.11	6.04
Thetford	NR	167	167	60	262	60	60	60	60
Farm	Min%	1.20	18.38	11.61	14.69	1.11	17.44	12.69	20.18
	Max%	3.74	25.72	25.31	35.84	3.28	26.23	22.83	37.44
	Mean%	2.24	21.92	19.16	23.79	2.00	21.27	17.55	27.17
	SD%	0.69	2.27	3.89	5.87	0.55	2.58	3.09	5.75

The pre-treated spectra and the laboratory chemical measurement values were used to develop calibration models for OC, MC, CC and PI by means of the partial least squares (PLS) regression. The PLS is a bilinear modelling method where information in the original x data is projected onto a small number of underlying (“latent”) variables called PLS components. The y data are actively used in estimating the “latent” variables to ensure that the first components are those that are most relevant for predicting the y variables. Interpretation of the

relationship between x data and y data is then simplified as this relationship is concentrated on the smallest possible number of components. More detailed information about the PLS can be found in Martens and Naes (1989).

The calibration spectra were subjected to PLS regression with the leave-one-out cross validation using the Unscrambler 7.8 software (Camo Inc., Oslo, Norway). The number of latent variables for a model was determined by examining a plot of the leave-one-out cross-validation residual variance against the number of latent variables obtained from the PLSR. The latent variable of the first minimum value of residual variance was selected. Outliers were detected using the residual sample variance plot after PLSR. Samples located far from the zero line of residual variance were considered outliers and excluded from the cross-validation sample set (10%).

3.2.8 Statistical evaluation of PLS model performance

Root mean square error of calibration (RMSEC) and prediction (RMSEP) are measures of average differences between predicted and measured response values at calibration and validation stages, respectively (Yitagesu et al., 2009). For the evaluation of the model performance, RMSEP was used (Williams and Norris, 2001). The RMSEP can be expressed as follows:

$$\text{RMSEP} = \sqrt{\frac{1}{N} \sum_{i=1}^N (X_i - Y_i)^2} \quad (3-9)$$

where X_i is the predicted value and Y_i is the observed value.

RPD designated as rate of prediction deviation, which is the ratio of standard deviation (SD) of the measured values to RMSEP was used to compare between different models developed. The third parameter considered was the coefficients of determination (R^2). In fact, R^2 indicates the percentage of the

variance in the Y variable that is accounted for by the X variable. A value for R^2 between 0.50 and 0.65 indicates that more than 50% of the variance in Y is accounted for variance X, so that discrimination between high and low concentrations can be made. A value for R^2 between 0.66 and 0.81 indicates approximate quantitative predictions, whereas, a value for R^2 between 0.82 and 0.90 reveals good prediction. Calibration models having a value for R^2 above 0.91 are considered to be excellent (Williams, 2003). In the successful analysis of agricultural commodities, it is desirable to have $R^2 > 0.50$, RPD > 5 . Nevertheless, for samples of complex material, Williams and Norris (2001) classified values as follows: RPD < 1.0 indicates very poor model/predictions and their use is not recommended, RPD between 2.4 and 3.0 indicates poor model/predictions where only high and low values are distinguishable, RPD between 3.1 and 4.9 indicates fair model/predictions which may be used for assessment and correlation, RPD values between 5.0 and 6.4 indicates good model/predictions where quantitative predictions are possible, RPD between 6.5 and 8.0 indicates very good, quantitative model/predictions, and RPD $> 8.1+$ indicates excellent model/predictions. However, for complex agricultural material such as soil, another RPD standard was reported by researchers (Saeys et al., 2005; Viscarra Rossel et al., 2006). Viscarra Rossel et al. (2006) classified RPD values as follows: RPD < 1.0 indicates very poor model/predictions and their use is not recommended; RPD between 1.0 and 1.4 indicates poor model/predictions where only high and low values are distinguishable; RPD between 1.4 and 1.8 indicates fair model/predictions which may be used for assessment and correlation; RPD values between 1.8 and 2.0 indicates good model/predictions where quantitative predictions are possible; RPD between 2.0 and 2.5 indicates very good, quantitative model/predictions, and RPD > 2.5 indicates excellent model/predictions. The RPD values obtained in this study was classified according to the latter proposed limits, and were used to evaluate the accuracy of PLS models for the prediction of OC, MC and clay content.

3.2.9 Derivation of Water Holding Capacity index (WHC)

3.2.9.1 Multiple linear regression analysis

Key factors affecting the WHC are the OC, CC, PI and BD (see also the introduction). Therefore, WHC index can be derived if information about these soil properties is available. On-line measured values of OC, CC, PI and BD and ECa values measured with EMI are correlated against MC measured with the on-line sensor by means of a multiple linear regression analysis (MLR). The MLR analysis predicts values of dependant variable Y, when independent variables (x_1, x_2, \dots, x_p) are given. MC was considered as the dependent variable (Y), whereas OC, CC, PI and BD and ECa were considered as the independent variables. MLR was carried out using Microsoft Excel 2010. The values of constants of multi linear function were considered as the contribution weight of each property on WHC. When a strong correlation between a parameter and MC exists the contribution of that particular parameter to WHC was considered high and vice versa.

3.2.9.2 Artificial neural network

Neural networks are simplified biological version of human brain and consist of input, hidden and output layers (Günaydin, 2009). The hidden layer of a network consists of multiple numbers of neurons. The interconnected neurons have the capability to learn from data and can provide strong prediction of required output. The number of neurons is determined by training several models with different number of neurons and comparing the predictions with reference output (Miao et al., 2006, Khalilmoghadam et al., 2009). Having few numbers of hidden neurons may result in high training and testing errors, whereas, too many hidden neurons might give small training error but still perform poorly during testing due to over fitting and high variance (Sinha and Wang, 2008).

The model to predict WHC (or MC), as a function of OC, CC, PI, BD and ECa (independent variables) was developed with ANN, using STATISTICA 11 ANN

toolbox (StatSoft, Inc., Tulsa, USA). The network was a multilayer perceptron (MLP) ANN using the Broyden-Fletcher-Goldfarb-Shanno (BFGS) training algorithm and hyperbolic tangent (Tanh) as the hidden layer is nonlinear activations and output layer is linear activation function is as it produced the best results compared to other activation functions such as exponential and logarithmic functions.

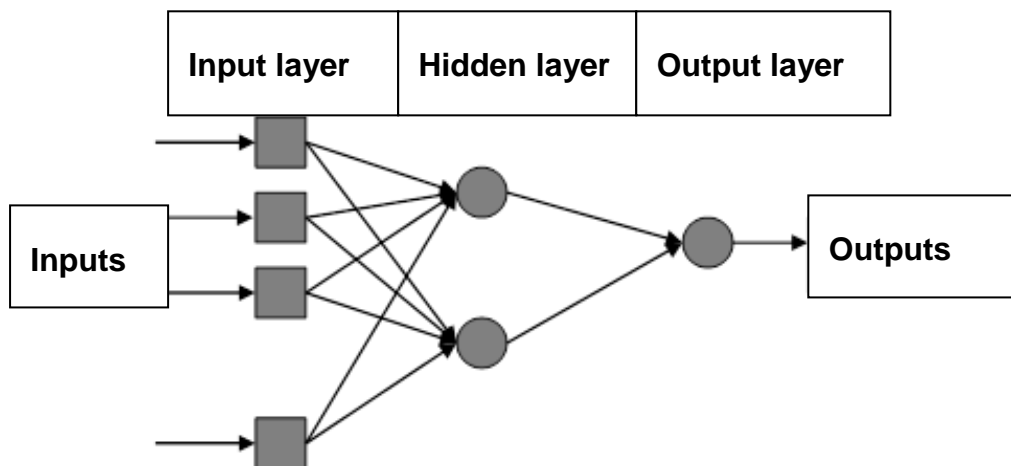


Figure 3-8: Four layer artificial neural network (ANN) used to model the WHC prediction

The network consisted of an input layer, a hidden layer and an output layer (Figure 3-8). The input layer includes four to five nodes depending on the number of input soil properties, whereas the output layer consisted of one node. The number of nodes in the hidden layer adjusted during the training and was anything from one to ten in order to achieve the optimised network structure with the lowest training error (Quraishi and Mouazen 2012). The data set was divided into a training set (80%), a validation set (10%) and a test set (10%). The training times were set to 1000.

MLR and ANN were both used to derive WHC index, for individual field and for the three fields together (Vicarage, Wypemere and Thetford). The field in

Marshall's Farm was excluded because it was with grass cover, and lead to unsuccessful on-line measurement. After WHC was calculated, values were normalised by means of maximum normalisation, by which values of WHC for all modelled cases were scaled between 0 and 1. The values of WHC were divided into four categories, namely, very high WHC (0.75-1), high (0.5-0.75), medium (0.25-0.5) and low WHC (0-0.25). This was to enable deriving management zones (e.g. for variable irrigation schemes) based on WHC maps.

3.2.10 Calculation of available water content (AWC)

AWC refers to the water content difference between the field capacity and the permanent wilting point. AWC in % was calculated using an empirical equation developed previously by Waive et al. (2000), as a function of clay and sand content:

$$AWC (\%) = 22.547 \ln(x) - 4.8811 x + 7.4356 \quad (3-10)$$

$$x = - 0.8981 (T_w)^2 + 3.8704 (T_w) + 1.9686 \quad (3-11)$$

$$T_w = 0.03 (CC) - 0.004 (\text{sand}) \quad (3-12)$$

Where x= fineness class,

T_w = texture weighing CC. Both T_w and sand content are in %.

By substituting on-line measured CC and laboratory measured sand content (as no good vis-NIR model was available to predict sand content), into Eqn (3.10 – 3.12) AWC was calculated.

3.2.11 Development of maps

Maps of soil properties including MC, OC, CC, PI, BD and ECa were developed for all three fields. Two types of maps were developed for each property, namely full-point and comparison maps. The full point maps consisted of all on-line predicted points of MC, OC, CC, PI, BD and ECa. The comparison maps compare between on-line predicted and laboratory measured properties based on the validation sets.

Semi-variograms analysis was carried out the full-point maps only using Vesper 1.63 software developed by the Australian Centre for Precision Agriculture (Minasny et al., 2005). An exponential model (Eqn. 3-13 and 3-14) was adopted to calculate semi-variance, since it resulted in the lowest root mean square error of prediction (RMSEP).

$$\gamma = C_0 + (C_1 X^{1-\rho}) \quad (3-13)$$

$$\rho = \exp \frac{-h}{A_1} \quad (3-14)$$

Where, γ is semi-variance, C_0 is the nugget value, C_1 is sill, h is the lag distance, and A is range.

Using the variogram data, full point maps of MC, OC, CC, PI, BD and ECa were developed using ArcGIS ArcMap (ESRI ArcGIS™ version 10, CA, USA). Ordinary kriging was performed using the semi-variogram data to map spatial variation accurately. For the comparison maps, since less than 100 points were available, the inverse distance weighing (IDW) method was used for both the measured and predicted maps of AWC and WHC. For full point maps, predicted OC, CC, MC, PI, and BD data was used to carry out kriging based on semi-variogram data provided in Table 4-8.

4 RESULTS AND DISCUSSION

4.1 Laboratory Results

4.1.1 Soil Particle Size Distribution (PSD)

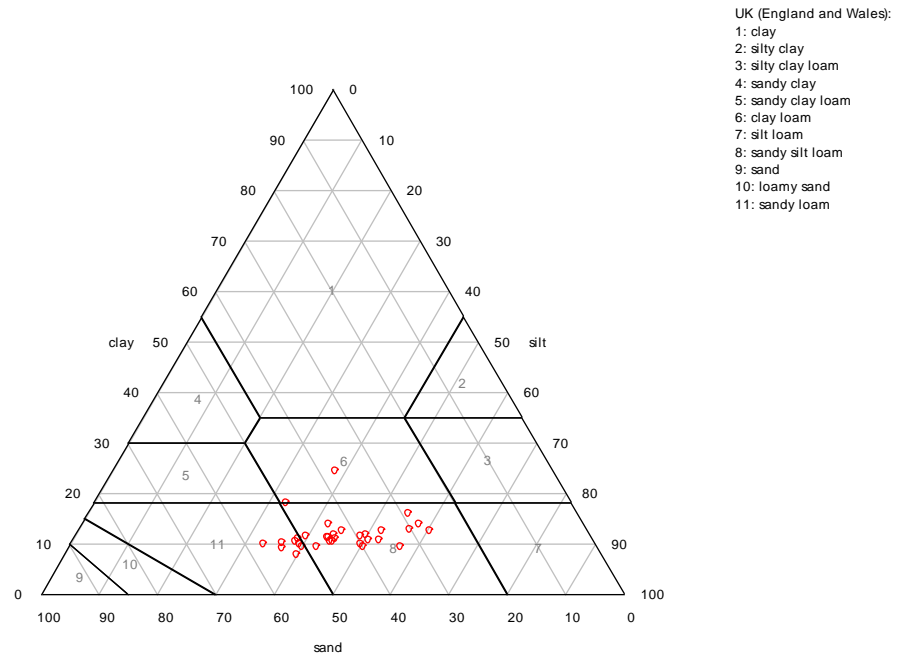
The results of PSD analysis in the four study fields are presented in Table 4-1 (for average field soil sample) and Figure 4-1a, b, c and d (for individual soil samples). The textures of the four fields are different, with sandy silt loam at Vicarage field, sandy silty loam at Marshall's field, silty clay at Wypemere field and clay loam at Thetford field. The variability in different textures was evenly distributed among these four fields within the samples set obtained, which for the essential to establish calibration model of vis-NIR spectroscopy. Throughout the process, the UK soil classification scheme was used.

Table 4-1: Average Soil Texture in the Four Study Fields

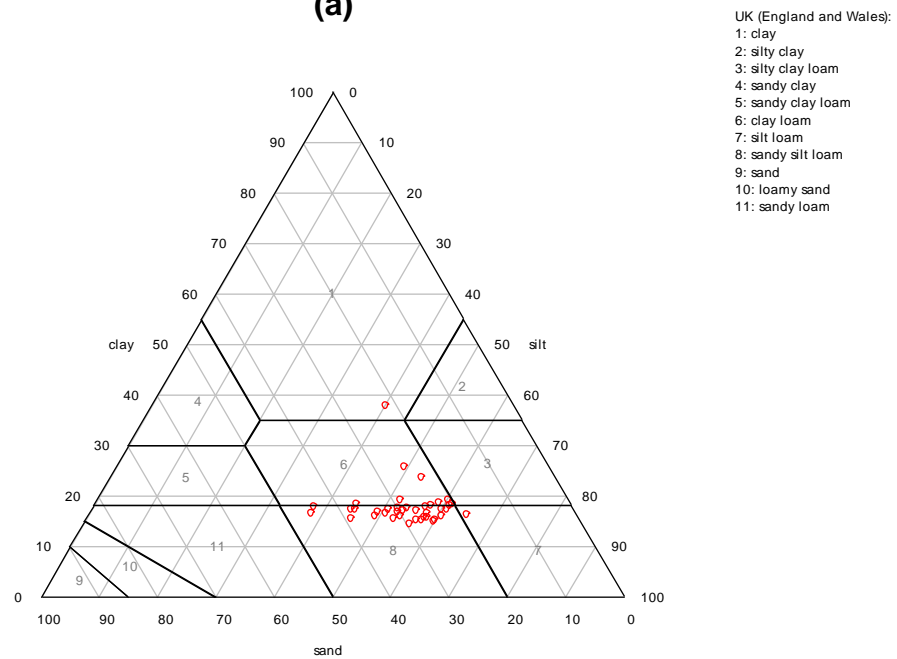
Site	No.of soil samples	Sand% (0.063-0.2 mm)	Silt% (0.002-0.063 mm)	Clay (<0.002 mm)	Texture type
Vicarage	32	42.847	45.464	11.689	Sandy silt loam
Marshall's	39	28.44	53.84	17.71	Sandy silt loam
Wypemere	35	5.076	45.279	49.645	Silty clay
Thetford	35	43.081	29.491	27.427	Clay loam

The passive influence of soil texture on vis-NIR models for the prediction of other soil properties has been highlighted in previous research (Mouazen et al., 2005b; Stenberg, 2010a; Stenberg et al., 2010b). The soils with higher clay contents were expected to result in a higher prediction accuracy compared to the soils with a higher content of sand fraction, which is attributed to the scatter

effect of sand particles (Mouazen et al., 2010; Kuang and Mouazen, 2013). Moreover, the effect was highly complicated, as both MC and texture have interactive effects, which need further evaluation, which is outside of the scope of the current study. However, the essential element to highlight at this stage is that the diverse samples in terms of soil texture have an impact on the accuracy of vis-NIR model performance.



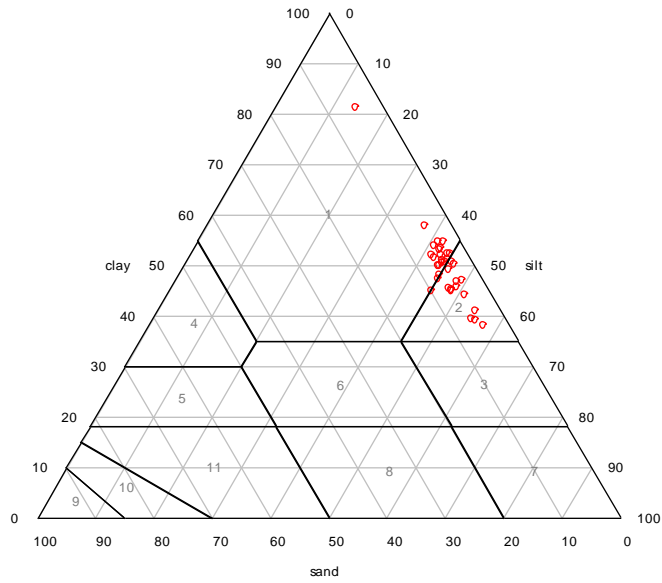
(a)



(b)

UK (England and Wales):

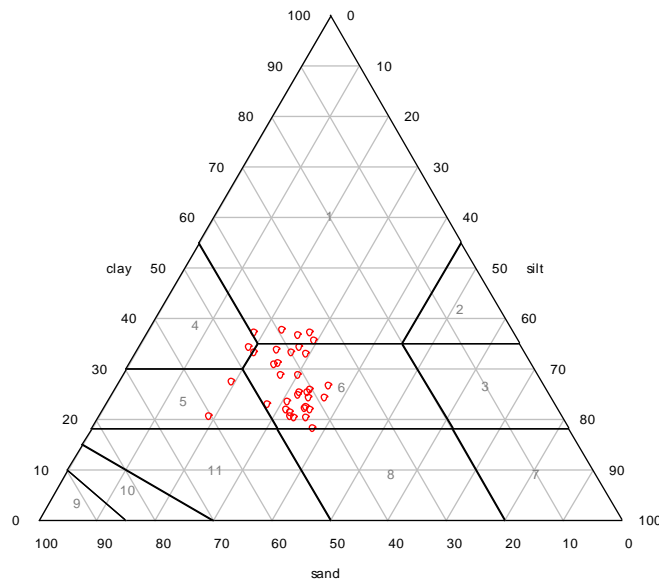
- 1: clay
- 2: silty clay
- 3: silty clay loam
- 4: sandy clay
- 5: sandy clay loam
- 6: clay loam
- 7: silt loam
- 8: sandy silt loam
- 9: sand
- 10: loamy sand
- 11: sandy loam



(c)

UK (England and Wales):

- 1: clay
- 2: silty clay
- 3: silty clay loam
- 4: sandy clay
- 5: sandy clay loam
- 6: clay loam
- 7: silt loam
- 8: sandy silt loam
- 9: sand
- 10: loamy sand
- 11: sandy loam



(d)

Figure 4-1: Texture of all samples collected from (a) Vicarage field, (b) Marshall's field, (c) Wypemere field and (d) Thetford field. The soil classification is set according to the UK Soil Classification Scheme

4.1.2 Organic Carbon (OC), Moisture Content (MC) and Plasticity Index (PI) results

Table 4-2 shows the results of the laboratory analysis of soil properties from the four study sites. The results clearly illustrate the differences among the four fields and the relationship between these properties. A high OC with a high MC and PI were measured at Wypemere field, whereas a low OC with a low MC and PI were shown at Vicarage field. However, Wypemere field showed very high values of OC and MC compared to the other three fields. High OC was found at Wypemere field compared with the other fields across the UK, while OC concentrations at Vicarage field, Marshall's field and Thetford field were found to be similar to most fields in the UK.

Table 4-2: Analyses of Organic Carbon (OC), Moisture Content (MC) and Plasticity Index (PI) for the Four Study Sites

Site	Property	Min (%)	Max (%)	Mean (%)	SD (%)	No. Samples
Vicarage	OC	1.227	4.527	1.571	0.754	32
	MC	15.51	23.20	18.69	2.19	32
	PI	2.190	12.60	5.774	2.198	32
Marshall's	OC	1.119	2.049	1.376	0.220	32
	MC	20.91	26.19	22.42	1.40	39
	PI	5.700	11.73	8.205	1.525	39
Wypemere	OC	1.500	17.85	9.472	3.416	35
	MC	26.87	52.81	40.24	6.54	35
	PI	14.58	31.04	20.11	4.065	35
Thetford	OC	1.068	7.107	2.213	1.265	35
	MC	14.53	26.23	19.57	3.09	35
	PI	9.200	22.83	15.92	3.848	35

SD = Standard deviation

Table 4-2 also indicates that variations in these soil properties between the four fields are considerable for example MC in Vicarage = 18.69, Marshall's = 22.42, Wypemere = 40.24 and in Thetford = 19.57. This must be taken into account when analysing the data using vis-NIR spectroscopy, as sample statistics including the range and SD highly affect the vis-NIR model performance (Kuang and Mouazen, 2011). These authors found that in a sample set with of a large SD and concentrations range, not only large RPD and R^2 values are expected, but also a large RMSEP.

4.2 Soil volumetric moisture content measured by Theta Probe

Table 4-3 shows the accuracy of the Theta probe for the measurement of average field volumetric MC. It is documented that the soil texture strongly affects the accuracy of Theta probe measurement of volumetric MC (Kaleta et al., 2005). Therefore, variable accuracy was recorded in different fields. For example, low accuracy was recorded at heavy soil texture (silt clay) in Wypemere field, whereas a better accuracy was recorded at light soils (sandy silt loam) in Vicarage field.

Table 4-3: Theta probe measurement of volumetric moisture content (MC) m^3 /m^3 from the four study sites

Site	No. samples	Mean (%)	Max (%)	Min (%)	SD (%)	RPD
Vicarage	18	19.19	30.4	5.8	8.2	1.08
Marshall's	21	25.2	31.8	12.8	4.07	0.86
Wypemere	21	25.95	36.10	15.7	6.42	0.34
Thetford	21	17.38	29.9	10.4	5.6	0.84

4.3 Soil apparent Electrical Conductivity (ECa)

Soil ECa values varied, depending on the soil texture and the soil MC. Table 4-4 shows the average apparent ECa (in mS/m) in the three study fields, as EMI measurement took place only in these three fields. The data highlights similar average ECa values measured at Vicarage field and Marshall's field, whereas high ECa value was measured at Wypemere Farm, which may be attributed to the high values of MC, OC and PI (Table 4-2). Indeed, the Wypemere field values are about 25% higher than the corresponding values of Marshall's field and Vicarage field. Moreover, it reflects the same trends in OC, MC and PI values in this field (Table 4-2). The variations in ECa values between fields and between zones within any specific field cannot be used for successful quantitative analyses of soil OC, CC, MC or PI, as EMI is simultaneously affected by various parameters including texture, compaction, salinity, MC and organic matter content (Sudduth et al., 2005; Hezarjaribi and Sourell, 2007; Kuang et al., 2011).

Table 4-4: Average ECa Measured at Two Different Depths (Shallow and Deep) in Three Fields

Site	Shallow ECa(mS/m)	Deep ECa (mS/m)
Vicarage	9.20	33.51
Marshall's	10.52	29.81
Wypemere	24.716	75.049

Maps of ECa illustrate clear spatial differences. Figure 4-2 indicates that ECa could be divided in a W-E direction into six clear zones, especially at the deep soil layer (0 cm to 120 cm).

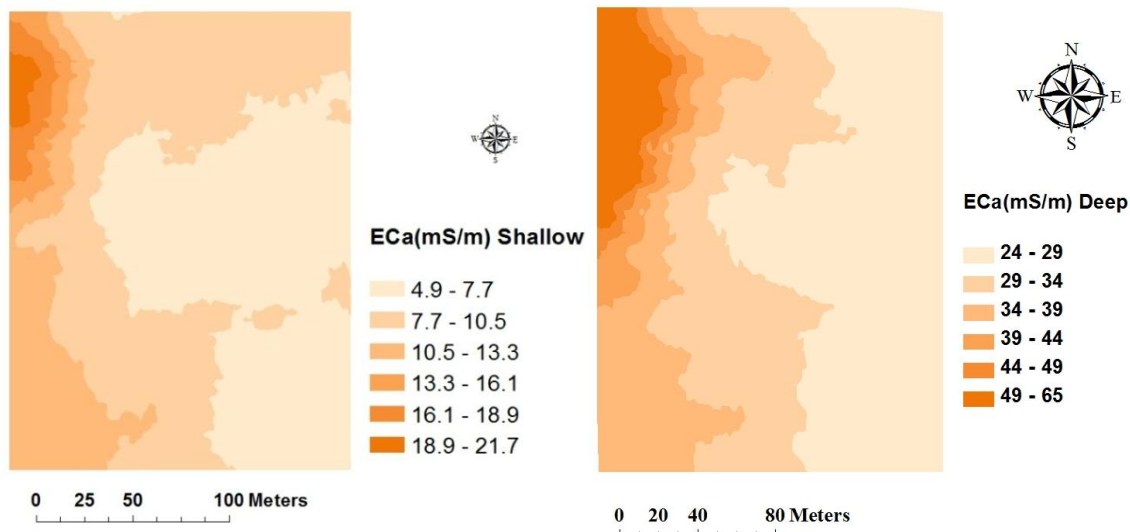


Figure 4-2: Spatial variation of apparent Electrical Conductivity (ECa) at two different depths: shallow (0 cm to 40 cm, left) and deep (0 cm to 120 cm, right) at Vicarage field

The ECa ranges measured in the current work were smaller than the values in previous studies (Aldhumayri, 2012). The smallest ECa values in two depths were shown in the middle variation of the ECa maps of Vicarage field and Marshall's field. Figure 4-3 shows that the ECa reading at Marshall's field, which is clearly of a lower range than that at Vicarage field. However, in the deep layer, higher ECa values are recorded than in the shallow layer.

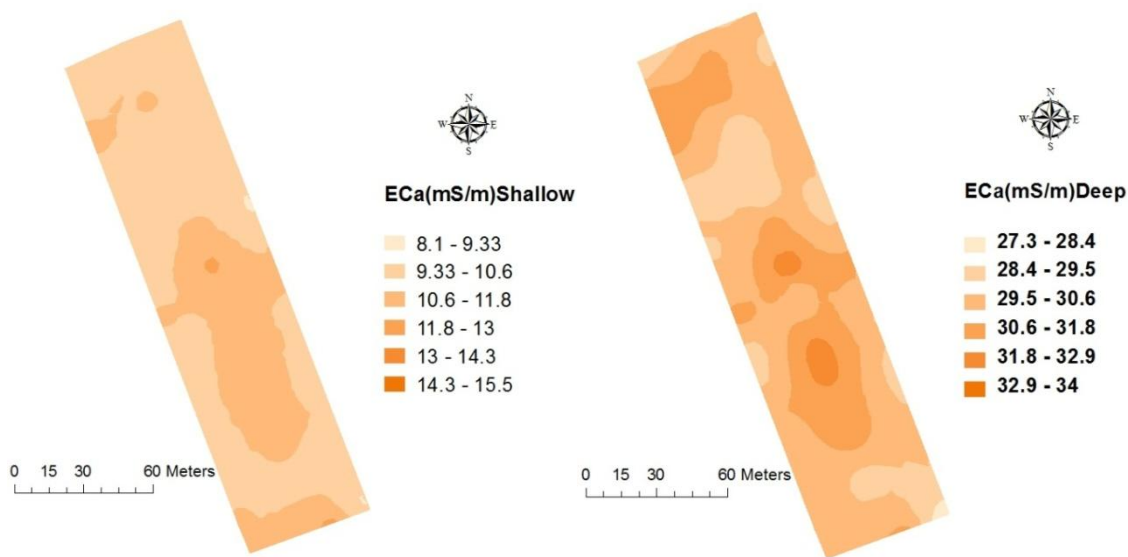


Figure 4-3: Spatial variation of apparent Electrical Conductivity (ECa) at two different depths: shallow (0 cm to 40 cm, left) and deep (0 cm to 120 cm, right) at Marshall's field

As illustrated at Wypemere field (Figure 4-4), much higher ECa ranges were recorded, which is in line with high levels of MC, OC and PI measured in this field. Also in Wypemere field the highest CC was measured (Table 4-1).

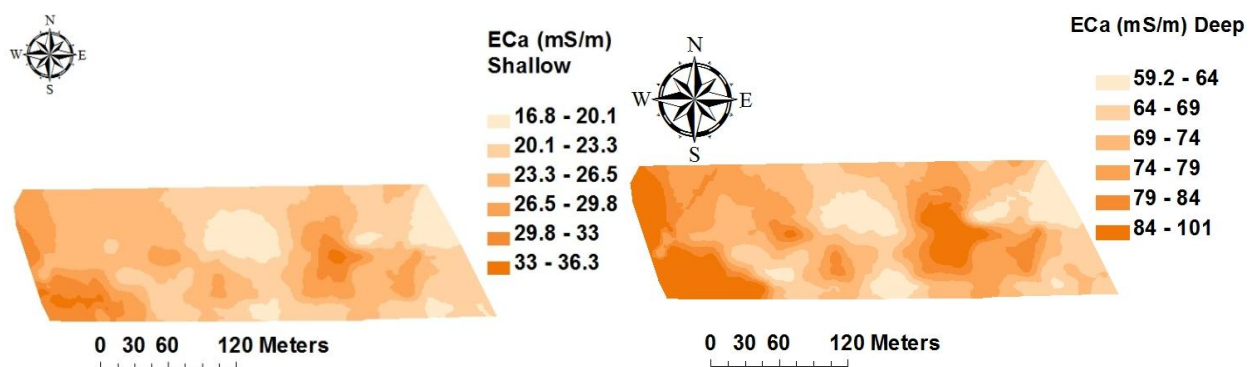


Figure 4-4: Spatial variation of apparent Electrical Conductivity (ECa) at two different depths: shallow (0 cm to 40 cm, left) and deep (0 cm to 120 cm, right) at Wypemere field

The large differences in ECa values measured at the three study fields suggest that ECa data should be used with caution. This is because the upper end of the ECa map at Vicarage field is almost equal to the lower end of the two depths measured at Wypemere field. The differences might be attributed to the different soil properties (see Table 4-2) or the different soil textures (see Table 4-1).

4.4 On-line Measurement

4.4.1 Bulk Density (BD) Measurement

The BD measurement was carried out in the study fields by using the on-line multi-sensor platform consisting of draught (measured with a load cell), depth (measured with a wheel gauge), and MC sensor based on vis-NIR spectroscopy. Equation (3-1) was used to calculate the BD. However, texture affects the values of BD derived with Eqn (3-1). Based on ANN, Quraishi and Mouazen (2012) enabled the correction of soil texture by developing correction factor (CF) for different soil texture classes. This CF was implemented in this study to correct for different textures measured in the study fields. Table 4-5 provides statistics of the corrected on-line measured BD in the study fields. The maximum BD of the loam soil measured at Marshall's field and Thetford field were almost of the same (1.677 and 1.691 Mg m⁻³, respectively). In Wypemere field, with silty clay soil type and high MC, a lower BD was measured. No data were recorded at Vicarage field, due to technical failure of the system that was discovered later during the data analysis.

Table 4-5: On-line measured bulk density (BD) in the three study sites

Site	CF	BD Mgm ⁻³			
		Min (%)	Max (%)	Mean (%)	SD (%)
Marshall's	0.016	0.887	1.677	1.267	0.117
Wypemere	0.27	0.500	1.355	0.884	0.145
Thetford	0.079	0.876	1.691	1.340	0.118

CF=Correction Factor

The BD maps developed with ordinary kriging based on exponential semivariograms are shown in Fig. (4-5). Table 4-6 provides the summary of semi-variance of full-point BD maps in the three study fields. The BD maps of Marshall's field shows two clear BD zones of high and low values. However, the BD distribution in Wypemere field is more complicated with much smaller values than that at Marshall's field. Three clear BD zones can be observed in Thetford field with different BD ranges.

Table 4-6: Summary of semi-variance properties of bulk density (BD) full-point maps in the three study fields

Site	Nugget (C ₀)	Sill (C ₁)	Range (A ₁)	Lag size (m)	RMSEP (%)
Marshall's	0.0042	0.0082	43.74	0.194	0.0041
Wypemere	0.0067	0.014	7.91	0.4	0.0011
Thetford	0.0057	0.0061	46.79	0.333	0.0008

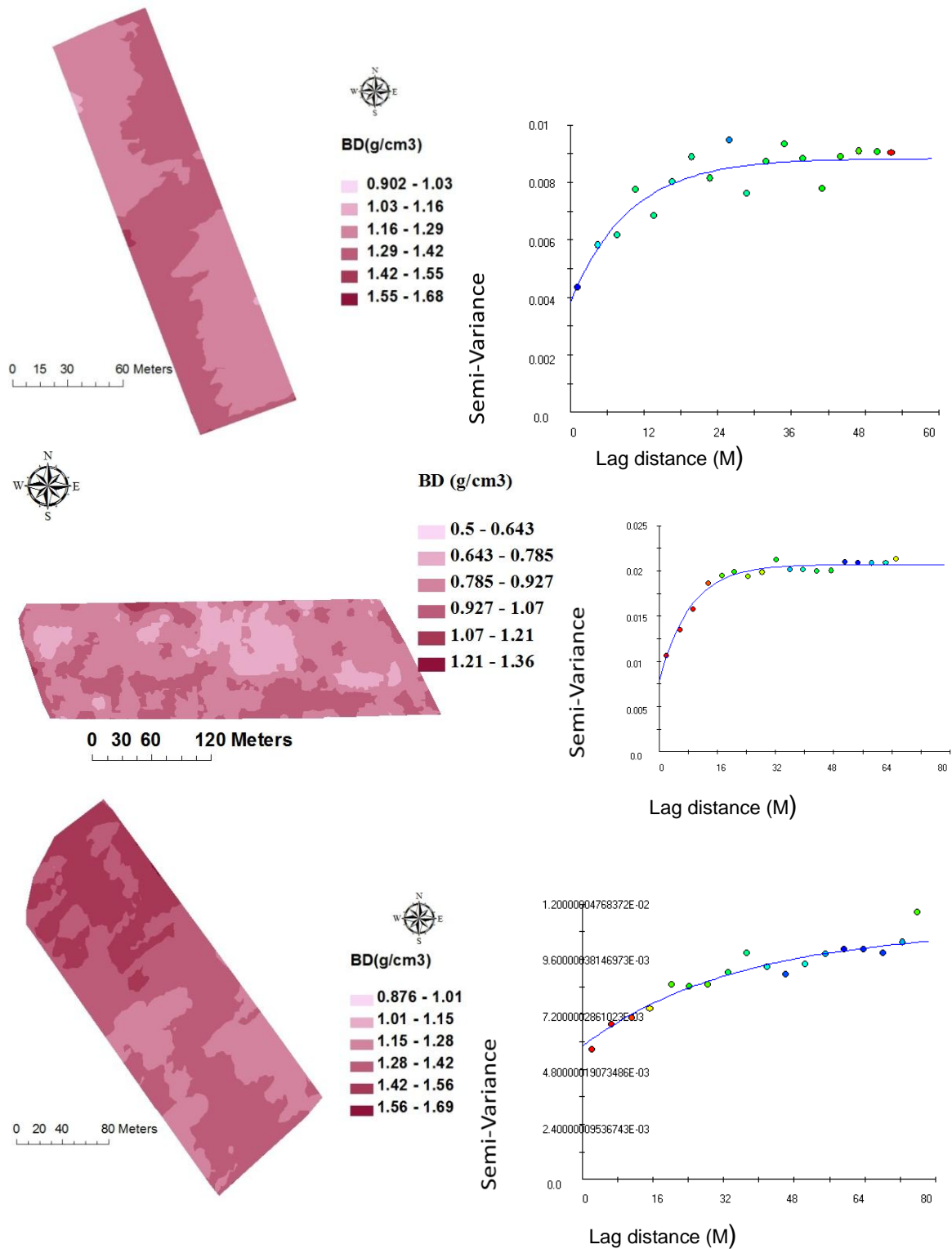


Figure 4-5: Full-point bulk density (BD) maps based on exponential variograms shown for Marshall's field (top), Wypemere field (middle) and Thetford field (bottom)

4.4.2 On-line soil spectra

The on-line vis-NIR spectra were collected at Wypemere field, with the spectra noisy parts between 305 to 370 and 2150 to 2200 nm removed from two edges of the spectra during spectra pre-treatment, as shown in Figure 4-6. This figure shows typical soil spectra collected at Wypemere field with low reflectance (indicating the high absorption of the soil). The high absorption at Wypemere field was explained by either the dark soil colour (Mouazen et al., 2006) or high MC (Mouazen et al., 2005) of the soil. Wypemere field has high MC, OC and PI content which explains the darker soil colour and also the high absorption and low reflection (Figure 4-6).

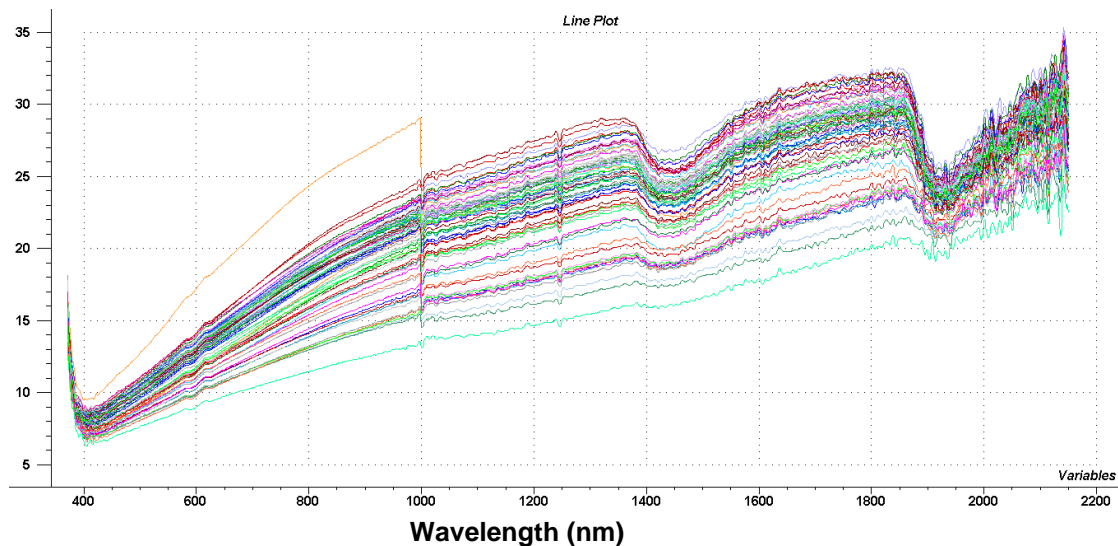


Figure 4-6: On-line soil spectra collected at Wypemere field

4.4.3 Accuracy of on-line vis-NIR measurement of soil properties

Figure 4-7 explains the different steps performed during this study from data collection to validation and mapping. Approximately 1500 to 2000 points per ha were collected (at a rate of 2 points per metre) by the multi-sensor platform, which depended on the measurement speed.

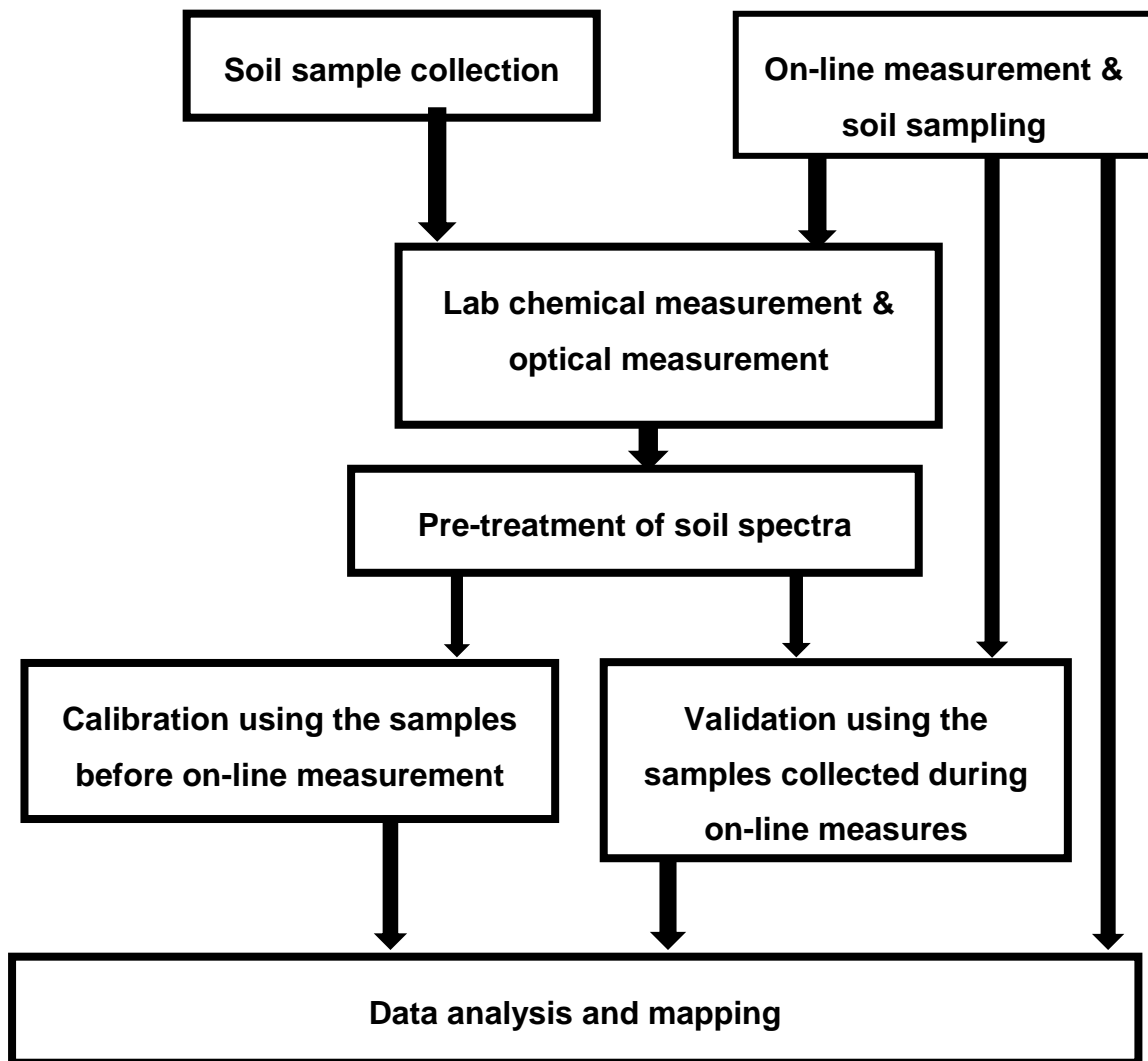


Figure 4-7: Schematic illustration of different steps towards online measurement and mapping of soil properties

To validate the accuracy of the vis-NIR sensor with laboratory analysis, values of the manually collected samples were compared with the on-line vis-NIR predicted concentrations at the same positions (Table 4-7). By validating the PLS models for the prediction of OC and MC based on 167 samples collected in the UK (60 samples collected in the current study), similar accuracy indicators (Table 4-7) were obtained as compared to those of previous studies (Mouazen et al., 2006; Mouazen et al., 2005; Aldhumayri, 2012). RPD values

were above 2 for OC and MC on all fields, except for the MC at Thetford field (RPD = 1.94) where prediction performance was classified as good (Viscarra Rossel et al., 2006). At Wypemere field, the OC value was larger than 2.5, indicating excellent prediction performance (Viscarra Rossel et al., 2006), whereas the RPD in the remaining fields were between 2.0 and 2.5, indicating very good quantitative model predictions (Viscarra Rossel et al., 2006). Based on the above discussion, it can be confirmed that the accuracy of on-line vis-NIR in these fields with vegetable crop prediction by measuring the OC and MC. This accuracy is also comparable with achieved for fields with arable crops (Kuang and Mouazen, 2013).

Table 4-7 shows the validation results of clay model developed based on 167 samples collected from seven sites in the UK and 95 samples from European soil (Kuang and Mouazen, 2011b). A lower accuracy for CC (RPD = 1.41 to 1.77) was obtained, compared to MC and OC. The prediction accuracy for CC can be classified as fair to moderate. Even smaller accuracy was achieved for the PI (RPD = 1.25 to 1.45), which can be classified as fair predictions (Viscarra Rossel et al., 2006). The lowest accuracy for PI prediction can be attributed to the low number of samples (60) used to develop the PI calibration model (Kuang and Mouazen, 2012). This necessitates in the future the need to consider a larger number of samples, which was not possible to be completed under the limited time and resources of the current work. Scatter plots of measured versus on-line predicted soil properties are shown in the Figure_Apx-2.

Table 4-7: Summary of the on-line vis-NIR Measurement accuracy of organic carbon (OC), moisture content (MC), clay content (CC) and plasticity index (PI) in three Fields at Vicarage, Wypemere and Thetford

Site		R2	RMSEP (%)	RPD	SD (%)
OC	Vicarage	0.71	0.06	2.00	0.12
	Wypemere	0.83	0.72	2.57	1.85
	Thetford	0.83	0.25	2.44	0.61
MC	Vicarage	0.82	0.97	2.06	2
	Wypemere	0.85	2.49	2.10	5.23
	Thetford	0.75	1.2	1.94	2.33
CC	Vicarage	0.64	1.4	1.41	1.98
	Wypemere	0.65	3.94	1.46	5.75
	Thetford	0.69	3.1	1.77	5.5
PI	Vicarage	0.55	2.6	1.25	2
	Wypemere	0.66	2.43	1.48	3.6
	Thetford	0.6	2.77	1.28	3.55

4.4.4. Mapping

4.4.4.1. Comparison maps

Figures 4-8, 4-9, 4-10 and 4-11 show comparison maps of measured versus on-line predicted MC, OC, CC and PI, respectively. Large spatial similarity between measured and predicted soil properties can be observed particularly for OC and MC, which confirms the robustness and accuracy of the on-line vis-NIR sensor for the measurement of MC and OC, which is in line with results achieved in a previous work for vegetable crop fields (Al-Dhumayri, 2012). Similarly, the on-line sensor provided reasonably similar spatial distribution for CC to laboratory measured maps, in two fields (Vicarage and Thetford) out of three. Probably the high MC (Table 4-3) recorded in Wypemere field is the reason for the low accuracy, as high MC levels in heavy soils seem to worsen the situation where the largest deterioration in the prediction accuracy of the vis-NIR spectroscopy was recorded (Kuang and Mouazen, 2013). Although the statistical evaluation of the on-line prediction of PI shows this property to be the worst property to be evaluated with the vis-NIR spectroscopy (Table 4-7), comparison maps shows reasonable similarities in all three study fields

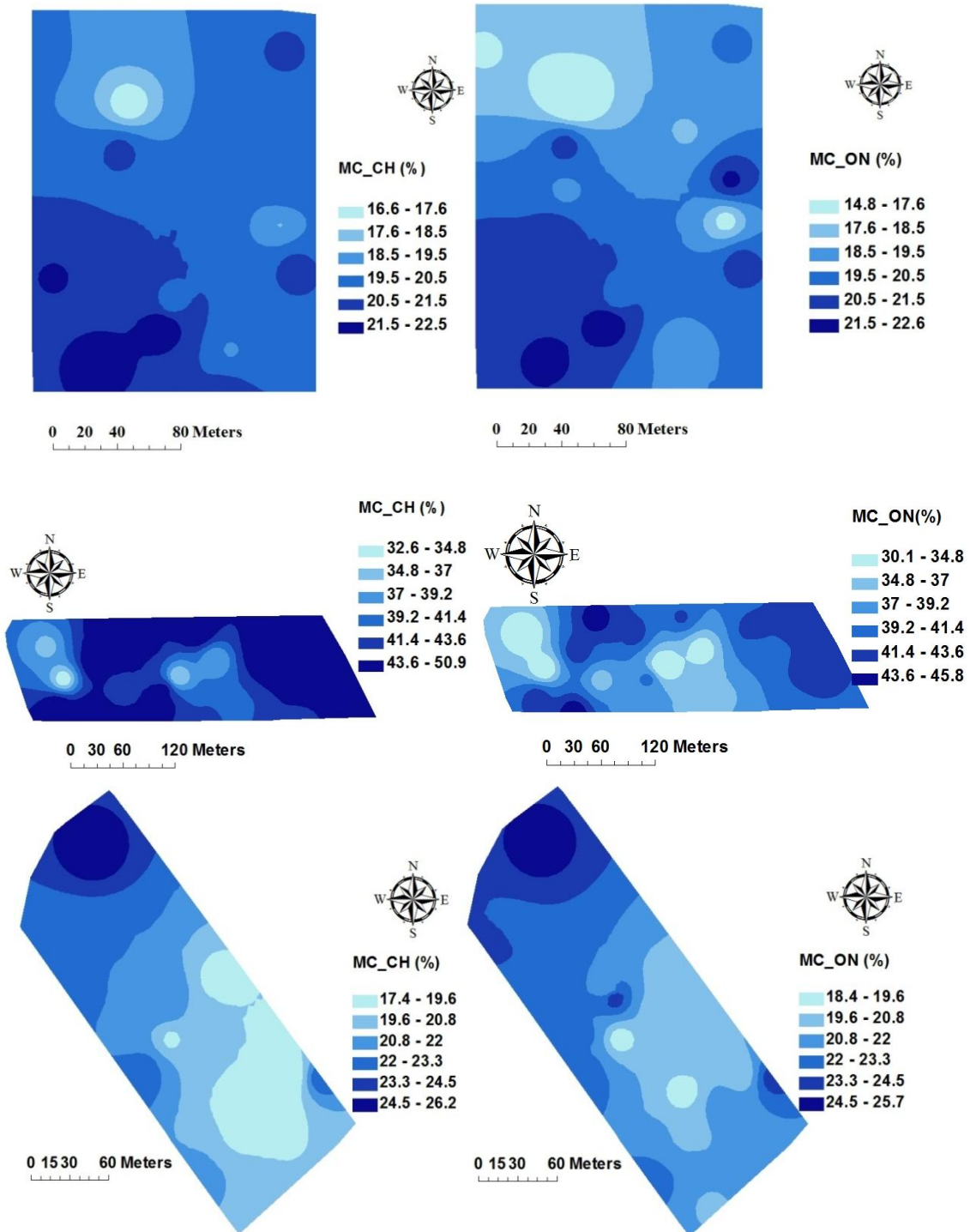


Figure 4-8: Comparison maps between laboratory- (left) and online-predicted (right) measured soil moisture content (MC) at Vicarage (top), Wypemere (middle) and Thetford Fields (bottom)

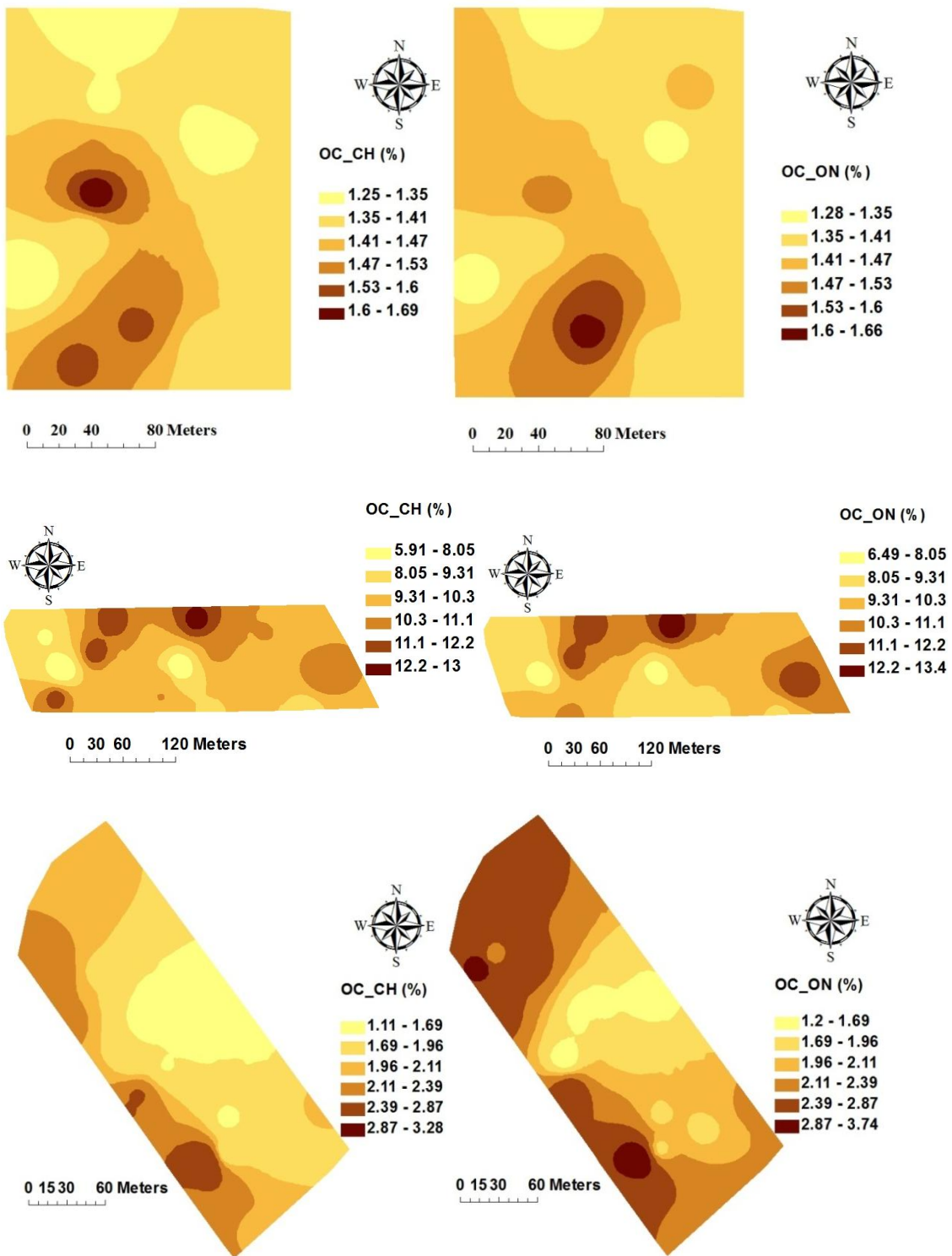


Figure 4-9: Comparison maps between laboratory (left) and on-line (right) measured soil organic carbon (OC), at Vicarage (top), Wypemere (middle) and Thetford fields (bottom)

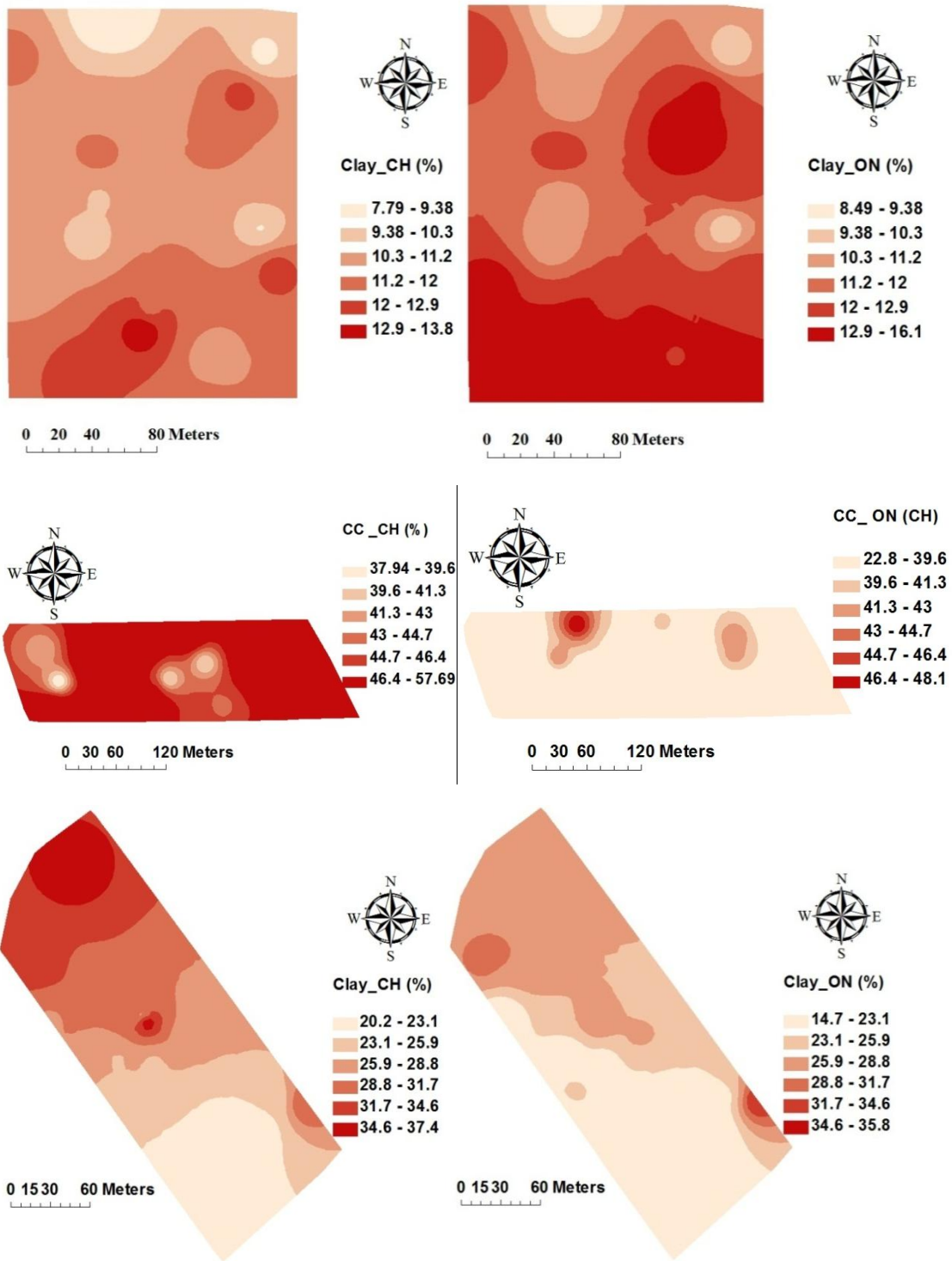


Figure 4-10: Comparison maps between laboratory (left) and on-line (right) measured soil clay content (CC) at Vicarage (top), Wypemere (middle) and Thetford fields (bottom)

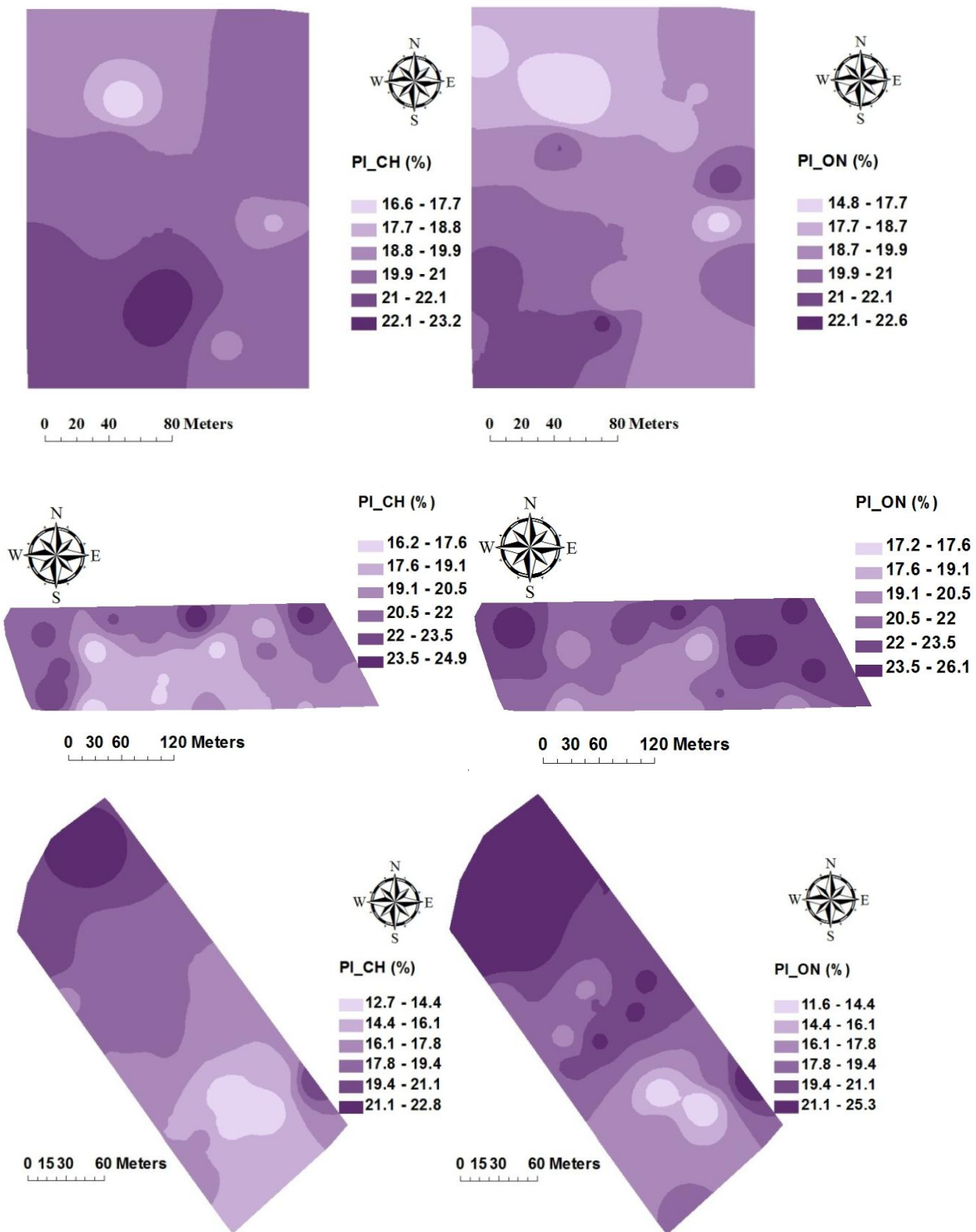


Figure 4-11: Comparison maps between laboratory (left) and on-line (right) measured soil plasticity index (PI) at Vicarage (top), Wypemere (middle) and Thetford fields (bottom)

4.4.4.2. Full-point maps

All data points collected with on-line vis-NIR sensor were used to develop maps to illustrate the spatial variation in OC, MC, CC and PI in the three study farms. Before kriging, exponential semivariograms were developed using VESPER 1.6 software. Table 4-8 shows the semi-variance parameters for the studied soil properties. ArcGIS 10.0 was utilised to develop the final maps for MC, OC, CC and PI, shown for soil MC (Figure 4-12), OC (Figure 4-13), CC (Figure 4-14) and PI (Figure 4-15). Strong spatial similarities observable in the three fields between CC, PI and MC reflects the strong correlation between these properties. This is in line with other reports on the strong correlation between these properties (Nelson and Miller, 1992). In fact, the higher the CC and the PI, the higher is the soil water holding capacity, hence, MC. Although reports suggest OC to be associated with high MC, as OC increases soil absorption of water, this seems to be correct in Wypemere Field only, according to the full-point maps (Figures 4-12 and 4-13).

Table 4-8: Summary of Semi-variance data of OC, MC, CC and PI in all sites with Exponential Model Variograms

Site	Prop	(C ₀)	(C ₁)	(A ₁)	Lag size (m)	RMSEP (%)
Vicarage	CC	11.43	20.51	25.85	0.371	1.966
	MC	9.58	15.15	6.133	0.371	2.400
	OC	0.0035	0.016	49.27	0.371	0.0022
	PI	8.805	19.81	7.246	0.371	3.346
Wypemere	CC	9.13	24.09	25.46	0.4	2.654
	MC	13.36	19.55	14.43	0.4	2.377
	OC	1.011	3.611	24.58	0.4	0.3928
	PI	7.412	22.47	0.56	0.4	1.738
Thetford	CC	24.21	44.27	27.44	0.344	2.055
	MC	32.33	55.07	20.36	0.344	3.178
	OC	1.839	1.912	18.15	0.344	0.277
	PI	11.56	44.79	0.676	0.344	3.964

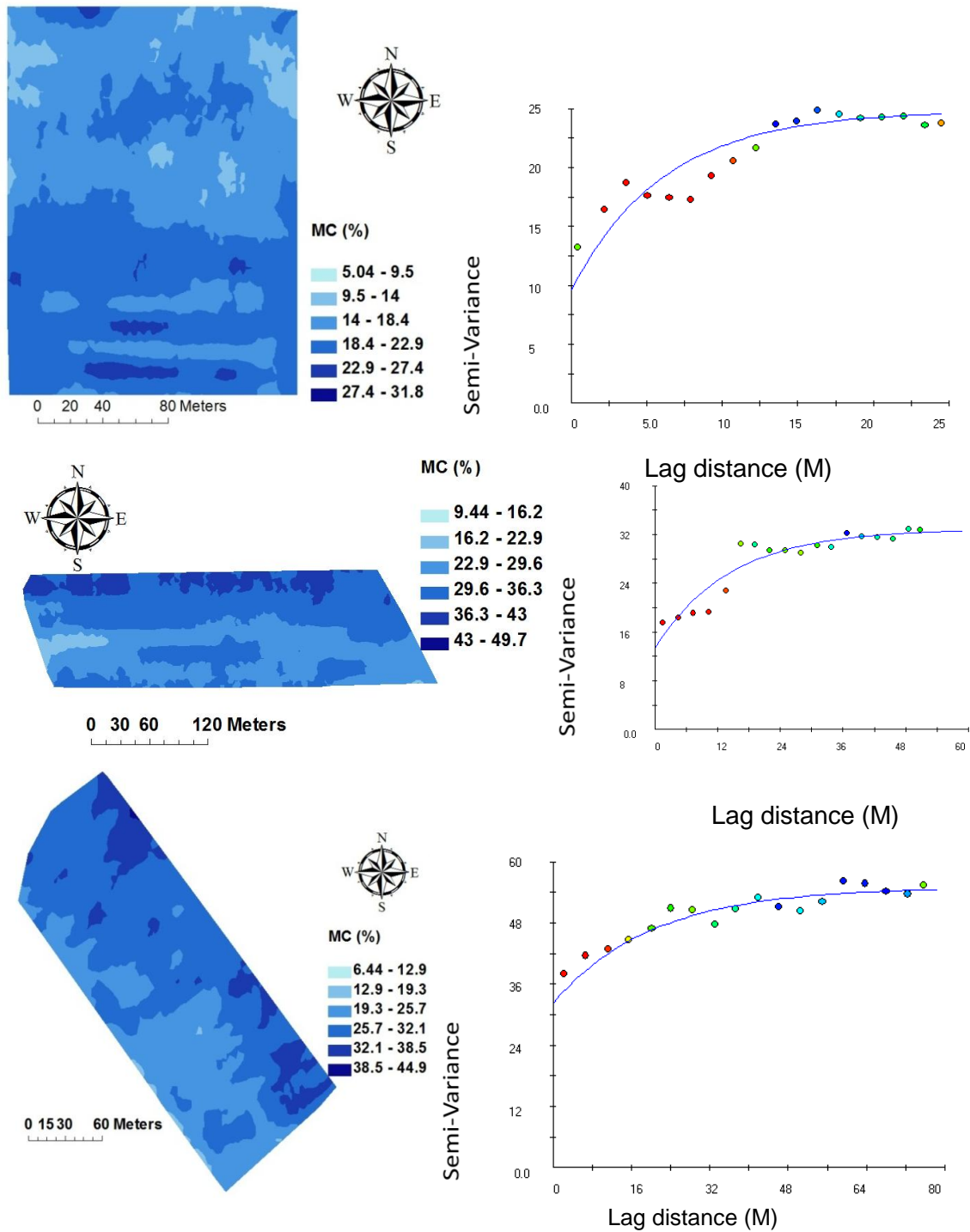


Figure 4-12: Developed maps of moisture content (MC) of Vicarage (top), Wypemere (middle) and Thetford fields (bottom) based on an exponential variogram of all online-measured points

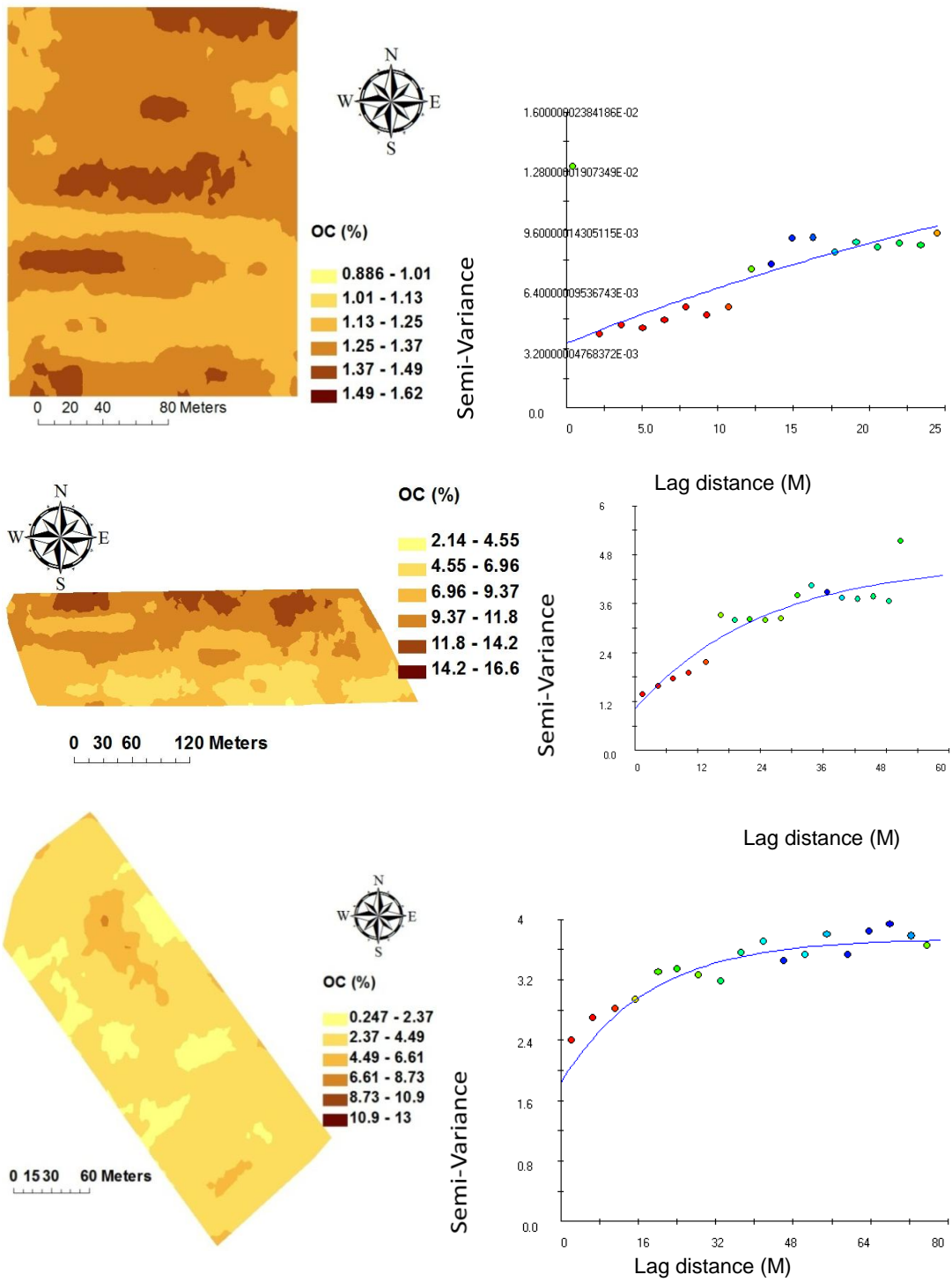


Figure 4-13: Full-point maps of organic carbon (OC) of Vicarage (top), Wypemere (middle) and Thetford fields (bottom) based on an exponential variogram of all on-line measured points

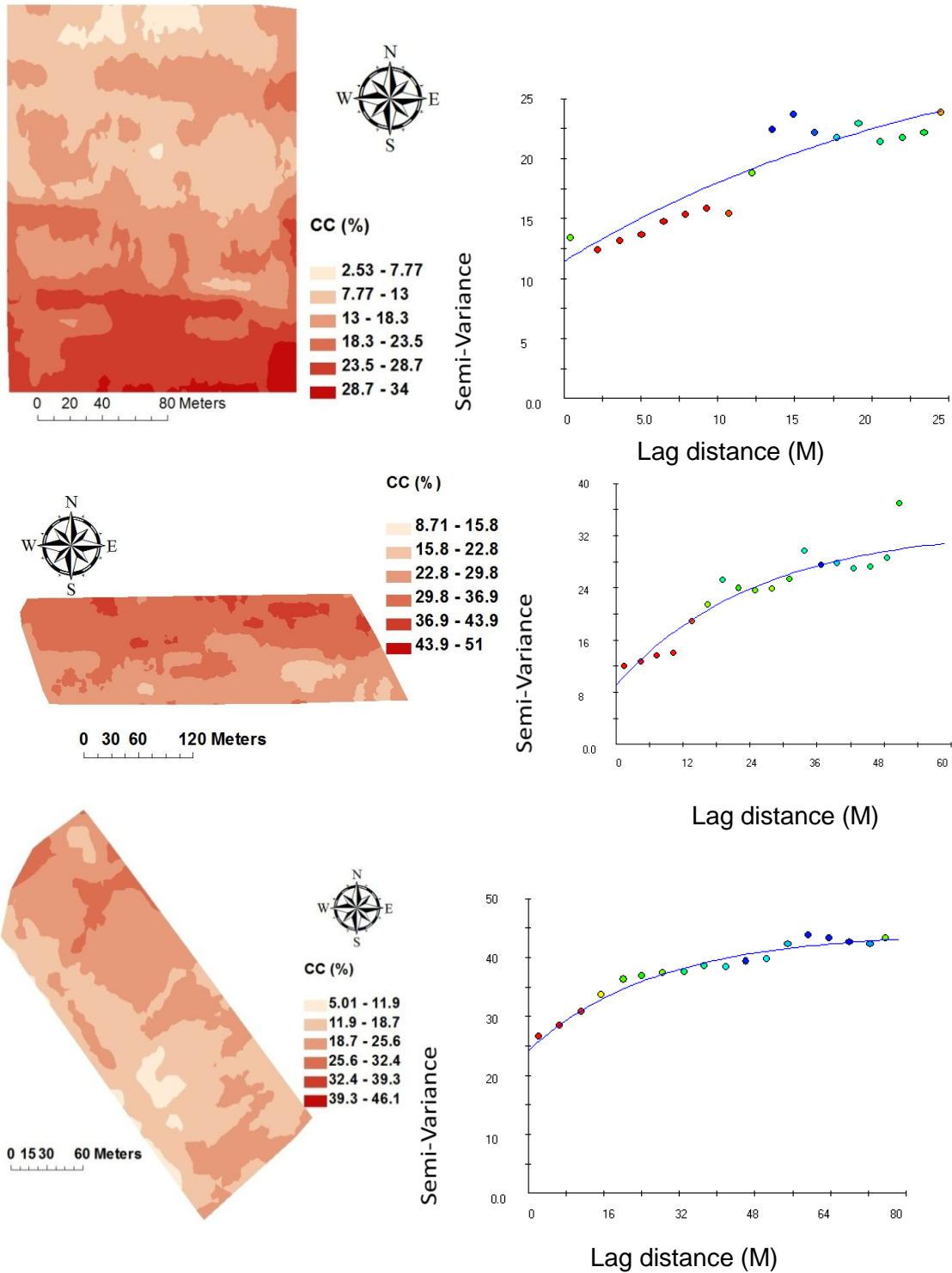


Figure 4-14: Full-point maps of clay content (CC) of Vicarage (top), Wypemere (middle) and Thetford fields (bottom) based on an exponential variogram of all on-line measured points

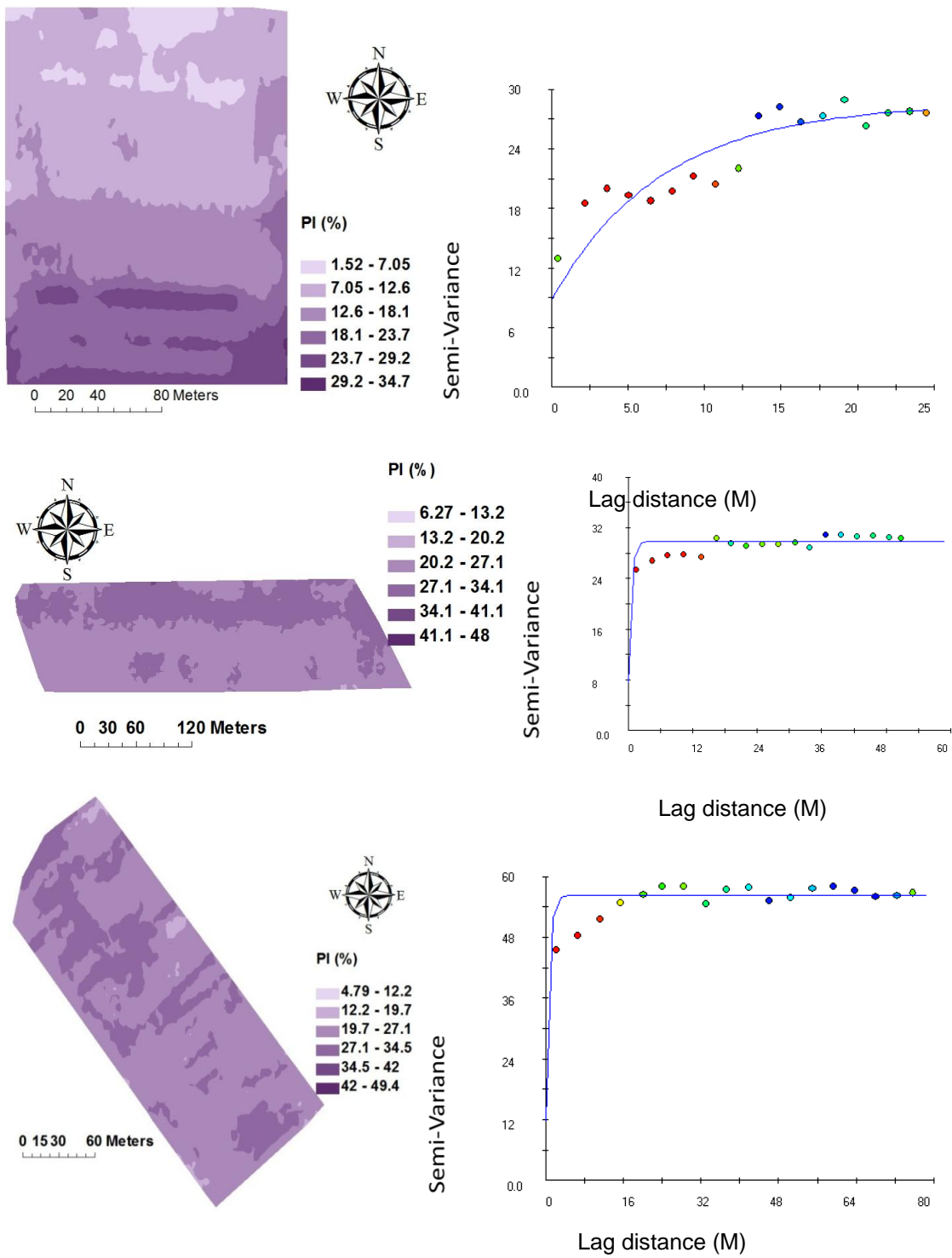


Figure 4-15: Full-point maps of plasticity index (PI) of Vicarage (top), Wypemere (middle) and Thetford fields (bottom) based on an exponential variogram of all on-line measured points

By comparing the maps of the soil properties measured with the on-line vis-NIR sensor (Figures 4-5, 4-11, 4-12, 4-13, 4-14 and 4-15) with the corresponding ECa maps measured with the EMI (Figures 4-2 and 4-4), visual (partial) spatial similarity between MC and ECa can be observed in Wypemere Field. Zones with high ECa associated with low MC and vice versa. In fact, the strongest spatial similarity of all properties under consideration including BD exists in Wypemere field. One explanation might be the high MC of the field, which is led by the high OC, CC and PI. At Vicarage Farm, no correlation was evident between ECa and the other soil properties measured with the vis-NIR sensor. At Wypemere field, both the ECa and vis-NIR maps show a clear division of the field into similar zones. The similarity between vis-NIR and EMI maps in Wypemere field encouraged the inclusion of ECa data for further analyses, whereas ECa was excluded for the other two fields, as weak spatial similarity between EMI and vis-NIR maps was observed.

4.4.5 Water-Holding Capacity (WHC) Index

The development of the WHC index may contribute to the improvement of placing soil moisture sensor and irrigation scheduling including automated variable rate irrigation system. The on-line measured OC, CC, PI, BD and ECa were used to determine the WHC in the study sites, as explained in Chapter 3. The MLR derived and normalised values of WHC (0-1) were divided into four equal classes, namely, low (0 - 0.25), medium (0.26 - 0.5), high (0.51 - 0.75) and very high (0.76 - 1). The constant values calculated by MLR are shown in Table 4-9 for individual fields and for all three fields data pooled together. This Table illustrates that the strongest impact (largest positive constant value) is for PI (0.76), BD (1.22) and OC (2.34) in Vicarage, Wypemere and Thetford field, respectively. However, in Vicarage field a strong negative impact of OC on MC (-0.91) was observed, which is in line with full-point maps shown in Figures 4-15 and 4-16. Examining the MLR constant values calculated for all three field data confirms BD to have the largest negative correlation with MC (constant

value = -4.97). This data also shows OC to have the largest correlation with MC (1.41). It is worth noting that ECa has in most occasions the smallest correlation with MC, confirming the previous discussion that ECa is simultaneously affected by several factors (CC, BD, salinity, etc.).

The smallest constant value in Vicarage Field was for CC (0.09), whereas a moderate constant value was calculated for PI. However, negative constants were found for OC and ECa, whereas the constant value for BD equals 0. At Wypemere Field with a heavy soil texture (silty clay), weak correlation between MC with OC and ECa was observed. After BD CC was found to be the second influencing factor on MC. A negligible negative influence was that of PI. A very high constant was calculated for OC in Thetford field. A weak correlation between MC with CC and PI and a negative correlation with BD is observed in this field with clay loam soil. It can be concluded that differences in soil texture in the 3 different fields are affecting the values of MLR constants. By comparing the constant values of the individual fields with the values from all sites (Table 4-9) differences should be expected in output maps created using either individual or combined (all sites) MLR constants.

Table 4-9: Constant values of multiple linear regression (MLR) analysis in the three fields

	Vicarage	Wypemere	Thetford	All Sites
MC	1	1	1	1
OC	-0.91	0.57	2.43	1.41
CC	0.09	0.81	0.25	0.41
PI	0.76	-0.03	0.14	-0.03
BD	0	1.22	-1.62	-4.97
ECa	-0.03	0.13	0	-0.01

Figure 4-16 shows WHC maps calculated based on constant values of MLR calculated constants for each individual field and for the three sites. A clear increase in WHC towards the southern part of the field is shown by both methods of WHC calculation. Both WHC maps are similar to corresponding MC, CC and PI maps (Figures 4-12, 4-14 and 4-15). High WHC zones correspond to high PI, CC and MC, which indicates that the direction followed to calculate the WHC in the current work is correct. Thus, the spatial variation of WHC is in line with the corresponding variations in MC, CC and PI, which was explained by the positive relationships of these properties with WHC (Nelson and Miller, 1992). However, as indicated before when compared to CC, MC and PI maps, OC map show opposite spatial distribution as compared to WHC map. At Wypemere field, some points were with high WHC values at the northern east part of the field. A similar tendency was found using both methods. Both maps, confirms that the spatial variation in WHC is similar to that of CC, OC, MC and PI (Figures 4-12 to 4-15). Zones with high WHC values associate with

corresponding zones with high values of MC, CC, PI and OC. Although partial similarity can be observed between WHC maps (Figure 4-16) on one side and ECa (Figures 4-2 and 4-4) on the other hand, zones with high ECa (correspond to zones with low WHC and vice versa. The WHC maps in Thetford Field show three classes only, because only few points in the high WHC range of 0.75 – 1 can be observed. Soil OC was reported to have an influence on WHC (Nelson and Miller, 1992). However, this is only particularly clear in Thetford and Wypemere fields (Figures 4-13). Similarity between WHC (Figure 4-16) and BD (Figure 4-5) maps can only be seen in Thetford and Wypemere fields. Zones with high WHC in Thetford field in particular, correspond to zones with low BD and vice versa.

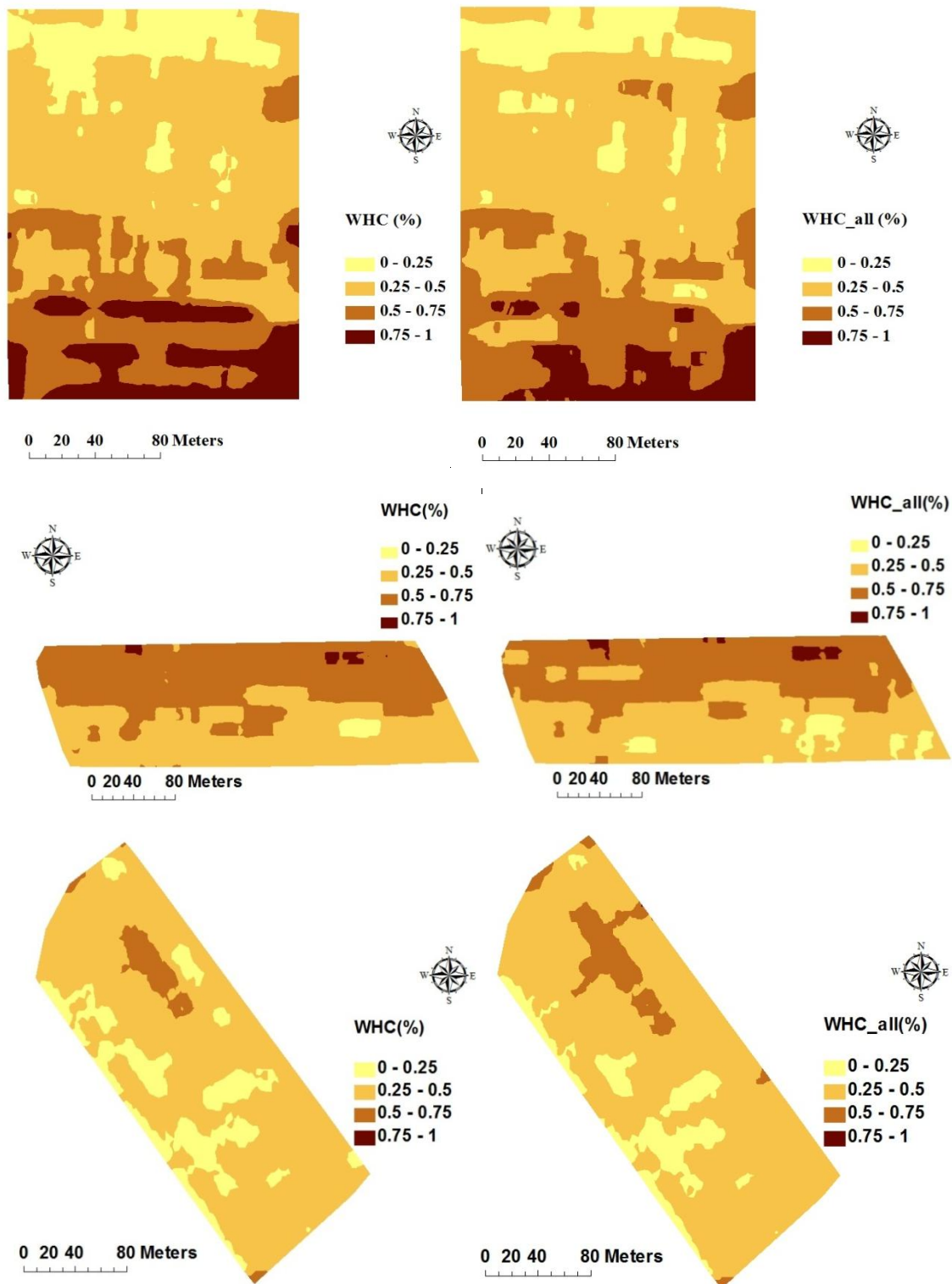


Figure 4-16: Water-holding capacity (WHC) maps with four classes: low, medium, high and very high WHC calculated based on constants of multiple linear regression analysis (MLR) of individual field data (left) and all three fields data (right)

The ANN analysis with similar input data provided, in general, similar WHC maps to those calculated with MLR analysis. However, more detailed variation within a WHC category was obtained with MLR as compared to ANN. Figure 4-17 shows the WHC maps based on the ANN tools for individual field and data from all three study fields. Similar spatial variations to that obtained with MLR (Figure 4-16) can be observed for all fields.

Table 4-10 shows the average WHC calculated for all sites with ANN and MLR analyses. Except for Wypemere field, average WHC calculated with ANN analysis were considerably different than the corresponding ones calculated with MLR, with the highest differences occurred in the silty clay field at Vicarage field.

Table 4-10: Average water holding capacity (WHC) calculated for the three study fields using the artificial neural network (ANN) and multiple linear regressions (MLR) analysis

Site	WHC (MLR for each site)	WHC (MLR for all sites)	WHC (ANN for each site)	WHC (ANN for all sites)
Vicarage	31.72	22.67	19.45	18.84
Wypemere	28.24	33.91	28.89	38.18
Thetford	23.39	19.31	22.12	25.49

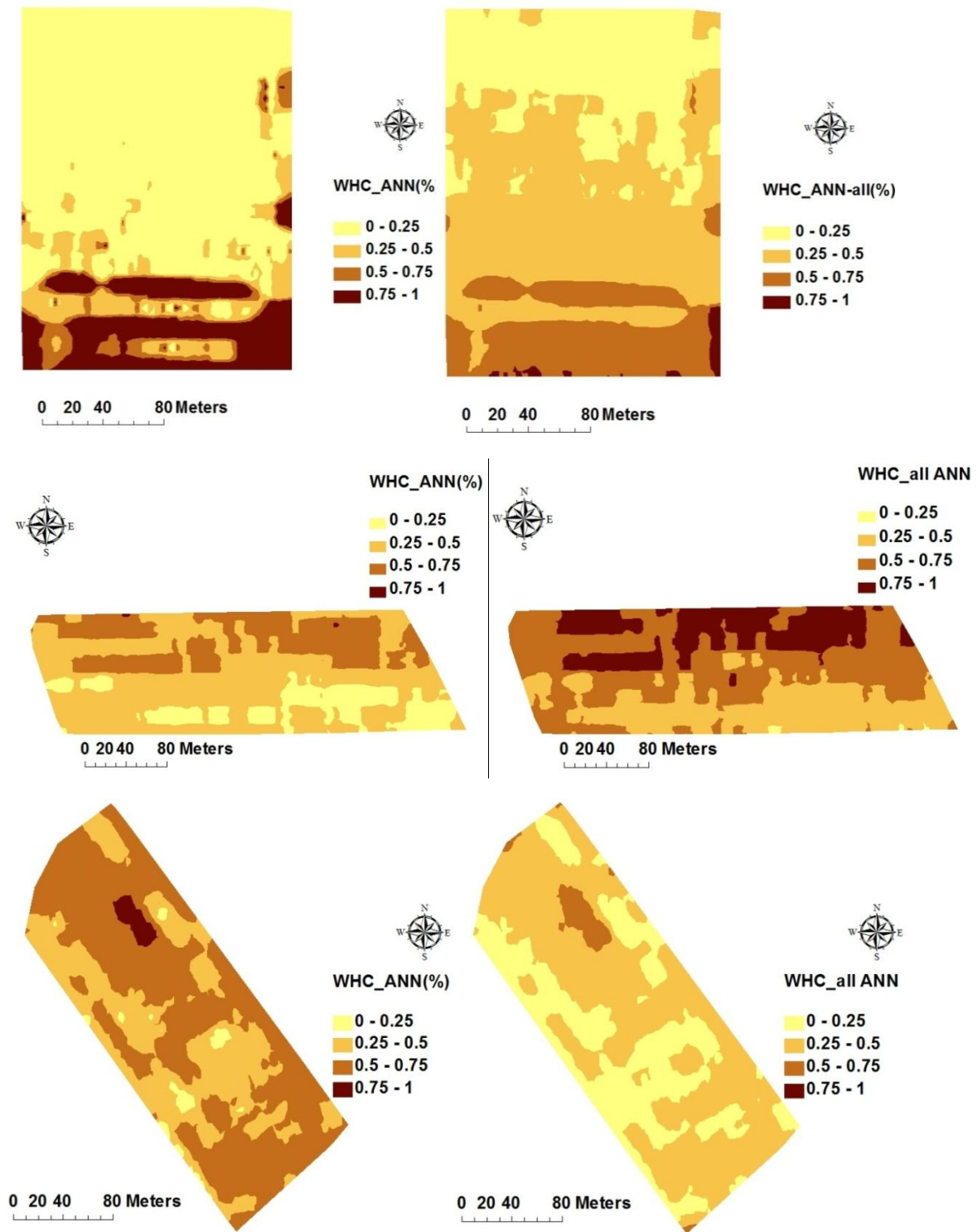


Figure 4-17: Water-holding capacity (WHC) maps with four classes: low, medium, high and very high WHC calculated based on artificial neural network (ANN) of individual field data (left) and all three fields data (right)

Regardless of method used to drive the WHC values, zones with high WHC will suffer of less fluctuation of MC throughout the cropping season, as compared to zones with lower WHC. High WHC zones will need smaller number of soil moisture sensors, as compared to those with low WHC. For instance, it can be proposed that 4 sensor per unit area (e.g. one ha) will be sufficient for category 1 (0 - 0.25), 3 sensors for category 2 (0.25 – 0.50), 2 for category 2 (0.50 – 0.75) and 1 for category 4 (0.75 – 1).

4.4.6 Available Water Content (AWC)

AWC refers to the water content difference between the field capacity and the permanent wilting point, which is very important range for plant growth (Hedley et al., 2010). These authors attributed variation in MC to the difference in topography and to the water stored in the soil profile. The best practice, precision and irrigation scheduling decisions were made by them by utilising water stored in the soil profile. This accounted for the high-resolution spatial and temporal differences in soil water status. Many methods can be used to calculate AWC; one way is represented by Equation (3-8) (Waine et al., 2000). Table 4-11 shows the average calculated AWC for all study sites based on on-line measured CC and laboratory measured sand content. The table indicates a small difference among different fields, with the largest value of AWC found in the fine heavy soil texture in Wypemere field. Also high MC, was accompanied with high values of AWC and WHC; the opposite was also true (i.e., low MC was accompanied with low AWC and WHC).

Table 4-11: Average AWC of the study fields calculated based on on-line measured clay content (CC) and laboratory measured sand content

Site	Fineness Class	MC, %	AWC, %
Vicarage	3.2	17.73	17.3
Wypemere	4.7	30.98	19.3
Thetford	3.6	27.28	18.4

Figure 4-18 shows the AWC maps for the three study fields. The largest AWC calculated for all fields was around 19 %. However, the range of variation differs among different fields with the biggest range occurred in Vicarage field and the smallest occurred in Wypemere field. Partial spatial similarities can be observed between the AWC and WHC maps (Figures 4-17 and 4-18), explaining the positive correlation between AWC and WHC, which is only partially captured by Eqn (3-8), as only clay and sand fractions were used to calculate AWC. The availability of quantitative estimation of AWC will enable the calculation of water to be used variably for irrigation in different zones in the three fields. But, the calculation of AWC should also be based on other soil properties such as OC, BD, MC, PI and ECa, which can be done with the on-line multi-sensor platform. However, this requires the development of an empirical equation to calculate AWC based on on-line measured soil properties, which is recommended for future work.

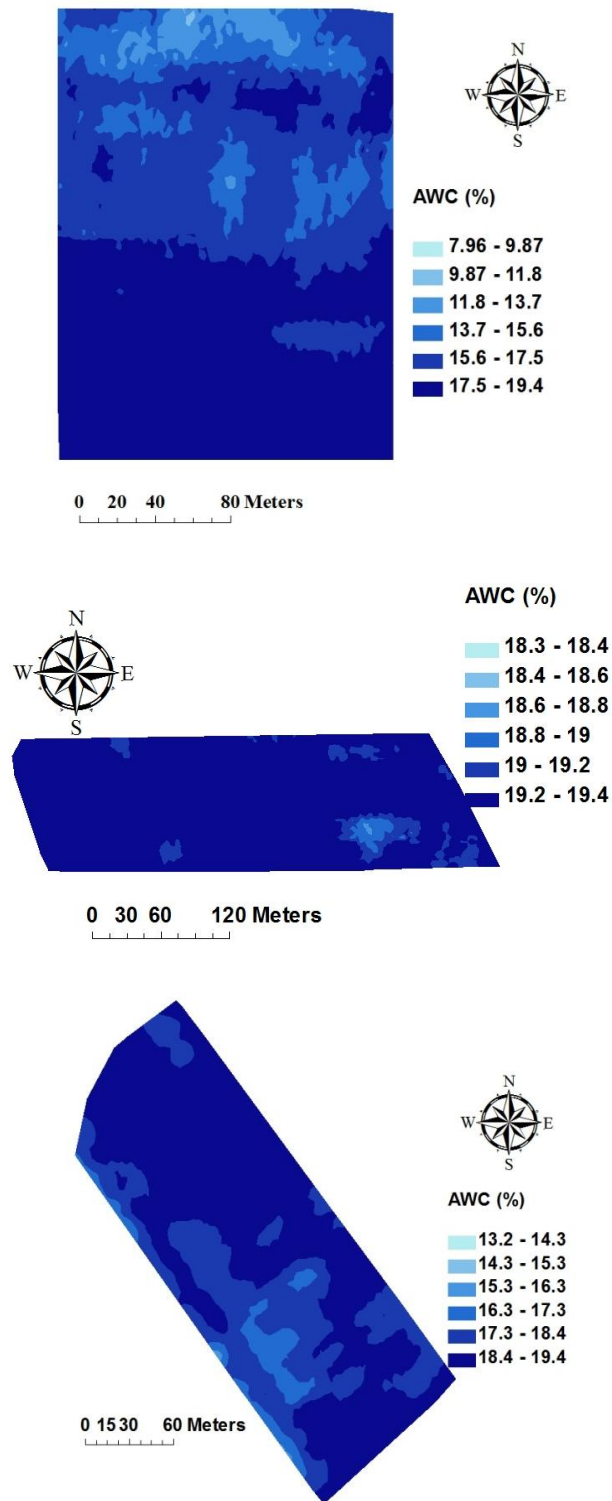


Figure 4-18: Available water content (AWC) in Vicarage (top), Wypemere (middle) and Thetford fields (bottom), calculated as a function of on-line measured CC and laboratory measured sand content

To compare between AWC calculated based on average clay and sand content measured with laboratory reference, the PSD analysis method was used for each of the four WHC categories (both MLR and ANN) (0 – 0.25; 0.25 – 0.5; 0.5 – 0.75; 0.75 – 1) with corresponding values of AWC calculated with Eqn (3-8), based on on-line measured CC for all points and laboratory measured sand content for multiple points. The AWC in the three fields with different WHC zones was determined for ANN and MLR analysis shown in table_Apx-1.

The accuracy of the vis-NIR prediction of AWC as compared to laboratory measured AWC based on WHC-category measured clay content (CC) and sand content with the PSD test shown in table_Apx-2.

The accuracy of AWC was the largest in Vicarage field and the lowest in Thetford field (Table_Apx-2). The predicted AWC in Vicarage field was in a close agreement with laboratory measured values for individual ($R^2 = 0.01$ and $RMSE = 2.08$) and multi-field MLR ($R^2 = 0.99$ and $RMSE = 2.16$) analyses. A reasonably good accuracy was also achieved with ANN for multi-field ANN analysis in the same field ($R^2 = 0.76$ and $RMSE = 2.23$). The reason for the lower accuracy of predicting AWC in Wypemere and Thetford field, as compared to the high accuracy of predicting in Vicarage field is attributed to the low CC in this field. This also necessitates the need to develop a more complicated model to calculate AWC as a function not only of CC and sand content (Eqn 3-8), but also OC, PI, BD and ECa. When this is completed a more accurate prediction of AWC will be possible, based on on-line measured soil properties. In addition, a new vis-NIR model to predict sand content will be needed in the future, in addition to the improvement needed to PI model developed in this study with 60 soil samples only.

5 CONCLUSIONS

In this thesis on-line measured bulk density (BD), clay content (CC), moisture content (MC), organic carbon (OC), and plasticity index (PI) measured with a multi-sensor platform, and apparent electrical conductivity (ECa) measured with an electromagnetic induction (EMI) sensor were for the first time fused using MLR analysis and ANN to derive a new index designated as WHC. This aimed to optimise the position and number of soil sensors to be used to provide input data for variable rate irrigation. The available water content (AWC) was calculated using an empirical equation, as a function of on-line measured CC and laboratory measured sand content. This was considered to enable calculating the amount of water used for variable rate irrigation in the vegetable crop production fields. The results achieved allowed for the following conclusions to be drawn:

1- The use of the on-line visible and near infrared (vis-NIR) sensor enabled the measurement of moisture content (MC) and organic carbon (OC) successfully, with good to excellent accuracy (RPD = 1.94 – 2.54). Less accurate measurement of CC and PI was recorded (RPD = 1.25 – 1.77); the latter was attributed to the small number of soil samples (60). The prediction accuracies of CC and PI were classified as moderate to fair model performance. More data are required in order to develop a robust vis-NIR calibration model particularly for the PI.

2- Examining the on-line vis-NIR measurement output revealed that strong correlations exist between MC, CC and PI, which is in line with previous reports available in the literature. Although OC was reported to have a strong correlation with MC, this was true in two out of three fields in the current study.

3- The apparent electrical conductivity (ECa) readings measured with Dualem 1S EMI sensor showed only minor correlation with MC and other soil properties during the MLR analysis.

4- MLR and ANN analyses enabled the calculation of the WHC successfully. The WHC maps were developed based on four normalised classes of low (0 - 0.25), medium (0.25 - 0.5), high (0.5 - 0.75) and very high (0.75 - 1). These maps illustrated spatial similarity particularly with CC, PI and MC maps, although appreciable similarity with OC map was observed. Since ECa has only minor correlation with MC, ECa was found to have a weak effect on WHC values derived with MLR and ANN analyses. Spatial similarity between WHC and BD map was only recorded in one out of three fields.

5- The AWC maps derived with empirical model as a function of CC and sand content indicated low AWC at zones where low WHC was calculated and vice versa.

Therefore, the use of multi-sensor and data fusion approach was a useful concept for guiding the positions and density of the moisture sensor and optimising the amount of water used for irrigation.

Future Work

The research question chosen in this study is highly complicated and needs further investigation to evaluate the agronomic, environmental and economic consequences of adopting the multi-sensor and data fusion approach to derive values of WHC and AWC. Given the time frame of the current MSc project, it was not feasible to carry out further developments. Therefore, further work is needed to establish robust calibration models of the vis-NIR sensor for the measurement of CC and PI by accounting for more fields with vegetable crop production. The AWC values were derived in the current work using an empirical equation as a function of CC and sand content. A more accurate calculation of AWC might be achievable by establishing a new AWC model as a function not only of CC and sand content, but OC, PI, ECa and BD.

REFERENCES

- Abdu, H., Robinson, D.A., Jones, S. B. (2007). "Comparing bulk soil electrical conductivity determination using the DUALEM-1S and EM38-DD electromagnetic induction instruments". *Soil Science Society of America Journal*, 71 (1), pp.189–196.
- Aldhumayri, M. H. (2012). "Optimizing Position of Moisture Sensors by Mapping of Clay Content, Moisture Content and Organic Carbon". MSc by Research Thesis, Cranfield University, Cranfield, the UK, pp. 84.
- Al-Kheer, a. A., Kharmanda, M. G., Hami, a. El, & Mouazen, a. M. (2011). "Estimating the variability of tillage forces on a chisel plough shank by modelling the variability of tillage system parameters". *Computers and Electronics in Agriculture*, 78(1), pp.61–70.
- Anthonis, J., Mouazen, a. M., Saeys, W., & Ramon, H. (2004). "An Automatic Depth Control System for Online Measurement of Spatial Variation in Soil Compaction, Part 3: Design of Depth Control System. *Biosystems Engineering*", 89(1), pp.59–67.
- Asgarzadeh, H., Mosaddeghi, M. R., Mahboubi, A. A., Nosrati, A., & Dexter, A. R. (2010). "Soil water availability for plants as quantified by conventional available water, least limiting water range and integral water capacity". *Plant and Soil*, 335(1-2), pp.229–244.
- Bacci, L. and Checcacci, E. (2004). "Il pilotaggio dell'irrigazione nelle colture florovivaistiche (In Italian)", In: Pardossi, A., Incrocci, L., Marzioletti, P. (Eds), *Uso Razionale delle Risorse nel Florovivaismo*, L'Acqua, ARSIA Firenze, Italy, 5, pp.147–156.
- Bacci, L., Battista, P., Rapi, B., Sabatini, F. and Checcacci, E. (2003). "Irrigation control of container crops by means of tensiometers". *Acta Hort, (ISHS)*, 609, pp.467–474.

- Balendonck, J. and Hilhorst, M. A. (2001). "WET Sensor application note". IMAG Report, Wageningen, the Netherlands.
- Barthès, B. G., Brunet, D., Hien, E., Enjalric, F., Conche, S., Freschet, G. T., d'Annunzio, R., et al. (2008). "Determining the distributions of soil carbon and nitrogen in particle size fractions using near-infrared reflectance spectrum of bulk soil samples". *Soil Biology and Biochemistry*, 40(6), pp.1533–1537.
- Ben-Dor, E., Banin, A. (1995). "Near-infrared analysis as a rapid method to simultaneously evaluate several soil properties". *Soil Science Society of America Journal*, 59 (2), pp.364–372.
- Bogrekci, I., Lee, W. S. (2004). "Soil particle size effect on absorbance spectra of sandy soils in UV-VIS-NIR regions". *ASAE Annual International Meeting 2004*, pp.4347–4356.
- Braun, S. M., Hinds, P., Malzer, G. L., Bell, J., Mulla, D. and Rebert, P. C. (1999). "Terrain attributes and soil nitrogen: spatial effects on corn yield responses to nitrogen fertilization for a northern, glaciated landscape. In: P. C. Robert, R. H. Rust, and W. E. Larson (eds.)", *Proceedings of the 4th International on Precision Agricult. Madison, WI, USA.*, pp.195–202.
- British Standard Institute (BSI) (1990), "British Standard BS 1377 Section 2:1990 Methods of test for Soils for civil engineering purposes". BSI 389 Chiswick High Road, London W4 4AL, UK.
- British Standard Institute (BSI) (1994), "British Standard BS 7755:1994, Determination of dry matter and water content on a mass basis by a gravimetric method". BSI 389 Chiswick High Road, London W4 4AL, UK.
- British Standard Institute (BSI) (1995), "British Standard BS 7755 Section 3.8: 1995, Determination of dry organic and total carbon after dry combustion (elementary analysis)". BSI 389 Chiswick High Road, London W4 4AL, UK.

- British Standard Institute (BSI) (1998), "British Standard BS 7755 Section 5.4:1998, Determination of particle size distribution in mineral soil material-Method by sieving and sedimentation". BSI 389 Chiswick High Road, London W4 4AL, UK.
- Brunet, D., Barthès, B. G., Chotte, J.-L., & Feller, C. (2007). "Determination of carbon and nitrogen contents in Alfisols, Oxisols and Ultisols from Africa and Brazil using NIRS analysis: Effects of sample grinding and set heterogeneity". *Geoderma*, 139(1-2), pp.106–117.
- Cañasveras, J. C., Barrón, V., Del Campillo, M. C., Torrent, J., & Gómez, J. a. (2010). "Estimation of aggregate stability indices in Mediterranean soils by diffuse reflectance spectroscopy". *Geoderma*, 158(1-2), pp.78–84.
- Cardenas-Lailhacar, B., & Dukes, M. D. (2010). "Precision of soil moisture sensor irrigation controllers under field conditions". *Agricultural Water Management*, 97(5), pp.666–672.
- Chang, C. W., Laird, D.A., Hurburgh Jr., C. R. (2005). "Influence of soil moisture on near-infrared reflectance spectroscopic measurement of soil properties". *Soil Science*, 170(4), pp.244–255.
- Chang, C.-W., Laird, D.A., Mausbach, M.J., Hurburgh C.R., J. (2001). "Near-infrared reflectance spectroscopy - Principal components regression analyses of soil properties". *Soil Science Society of America Journal*, 65(2), pp.480–490.
- Corwin, D. L., & Lesch, S. M. (2005). "Apparent soil electrical conductivity measurements in agriculture". *Computers and Electronics in Agriculture*, 46(1-3), pp.11–43.
- Cozzolino, D., & Morón, a. (2006). "Potential of near-infrared reflectance spectroscopy and chemometrics to predict soil organic carbon fractions". *Soil and Tillage Research*, 85(1-2), pp.78–85.

- Fambro, R., Golson, K. F., Tsegaye, T. D., Coleman, T. L., Metzl, R., Tadess, W., & Clendenon, D. (2003). "Evaluation of soil property variability within the Alabama Mesonet", pp. 7929–7931.
- Forbes, J. C., Waston, R. D. (1992). "Plants in Agriculture", Cambridge University Press, Cambridge, UK.
- Friedman, S. P. (2005). "Soil properties influencing apparent electrical conductivity: a review". *Computers and Electronics in Agriculture*, 46(1-3), pp.45–70.
- García-Garizábal, I., Causapé, J., & Abrahao, R. (2011). "Application of the Irrigation Land Environmental Evaluation Tool for flood irrigation management and evaluation of water use". *Catena*, 87(2), pp.260–267.
- Gomez, C., Viscarra Rossel, R. a., & McBratney, A. B. (2008). "Soil organic carbon prediction by hyperspectral remote sensing and field vis-NIR spectroscopy: An Australian case study". *Geoderma*, 146(3-4), pp.403–411.
- Guerrero, C., Zornoza, R., Gómez, I., & Mataix-Beneyto, J. (2010). "Spiking of NIR regional models using samples from target sites: Effect of model size on prediction accuracy". *Geoderma*, 158(1-2), pp.66–77.
- Gunaydin, O., 2009. Estimation of soil compaction parameters by using statistical analyses and artificial neural networks. *Environmental Geology* 57, 203–215.
- Hall, D. G. M., Reeves, M. J., Thomason, A. J. and Wright, V. F. (1977). "Water retention porosity and density of field soil survey technical monograph". Soil Survey, No. 9.
- Han, W., Wu, P., yang, Q., Feng, H. (2005). "Advances and comparisons of uniformity evaluation index of sprinkle irrigation". *Transaction of Chinese Society of Agricultural Engineering*, pp.172–175.

- Hedley, C.B., Yule, I.J., Eastwood, C.R., Shepherd, T.G., Arnold, G. (2004). "Rapid identification of soil textural and management zones using electromagnetic induction sensing of soils". *Australian Journal of Soil Research*, 42 (4), pp.389–400.
- Hedley, C. B.; Yule, I. J.; Tuohy, M. P., and Kusuma, B. H. (2010). "Proximal Sensing Methods for Mapping Soil Water Status in an Irrigated Maize Field". pp. 375–385.
- Hussain, K., Majeed, A., Nawaz, K., Afghan, S., Ali, K., Lin, F., Zafar, Z., Raza, G. (2010). "Comparative study of subsurface drip irrigation and flood irrigation systems for quality and yield of sugarcane". *African Journal of Agricultural Research*, pp.3026–3034
- James, I. T., Waine, T. W., Bradley, R. I. and Taylor, J. C. (2000). "A comparison between traditional methods and EMI scanning for determining soil textural boundaries". *Paper Number 00-PA-014, Presented at the AgEng/EurAgEng 2000, Warwick, UK.*
- James, I. ., Waine, T. ., Bradley, R. ., Taylor, J. ., & Godwin, R. . (2003). "Determination of Soil Type Boundaries using Electromagnetic Induction Scanning Techniques". *Biosystems Engineering*, 86(4), pp.421–430.
- Kaleita, A.L., Heitman, J.L., Logsdon, S.D. , (2005). "Field calibration of the Theta Probe for Des Moines lobe soils". *Applied Engineering in Agriculture* 21 (5) , pp. 865-870.
- Keller, T., Trautner, a, & Arvidsson, J. (2002). "Stress distribution and soil displacement under a rubber-tracked and a wheeled tractor during ploughing, both on-land and within furrows". *Soil and Tillage Research*, 68(1), pp.39–47.
- Khalilmoghadam, B., Afyuni, M., Abbaspour, K.C., Jalalian, A., Dehghani, A.A., Schulin,R., 2009. Estimation of surface shear strength in Zagros region of

- Iran – a comparison of artificial neural networks and multiple-linear regression models. *Geoderma* 153, 29–36.
- Keller, T., Trautner, a, & Arvidsson, J. (2002). “Stress distribution and soil displacement under a rubber-tracked and a wheeled tractor during ploughing, both on-land and within furrows”. *Soil and Tillage Research*, 68(1), pp.39–47.
- Kuang, B. and Mouazen, A. M. (2013). “Effect of spiking strategy and ratio on calibration of on-line visible and near infrared soil sensor for measurement in European farms”. *Soil and Tillage Research*, in press.
- Kuang, B., & Mouazen, a. M. (2011). “Calibration of visible and near infrared spectroscopy for soil analysis at the field scale on three European farms”. *European Journal of Soil Science*, 62(4), pp.629–636.
- Kuang, B., & Mouazen, a. M. (2012). “Influence of the number of samples on prediction error of visible and near infrared spectroscopy of selected soil properties at the farm scale”. *European Journal of Soil Science*, 63(3), 421–429.
- Kuang, B., Mahmood, H. S., Quraishi, Z., Hoogmoed, W. B., Mouazen, A. M. and Van Henten, E. J. (2011). “Sensing soil properties in the laboratory, in situ and on-line - a review”. *Advances in Agronomy*, pp.155– 224.
- Kuang, B.; Mouazen, A.M., (2013). “Non-biased prediction of soil organic carbon and total nitrogen with vis-NIR spectroscopy, as affected by soil moisture content and texture”. *Biosystems Engineering*. (in print).
- Kvaerner, S. H., Haugen, L. E., & Borresen, T. (2007). “Variability in topsoil texture and carbon content within soil map units and its implications in predicting soil water content for optimum workability”. *Soil and Tillage Research*, 95(1-2), 332–347.
- Kvaerner, S. H., Haugen, L. E., Borresen, T., Schulz, H., Glaser, B., Forbes, J. C., Waston, R. D., Peets, S., et al. (2007). “Expansive soils problem and

- practice in foundation and pavement engineering". *Soil and Tillage Research*, 95(1), 419.
- Li, Z., Wang, N., Hong, T., Franzen, A., & Li, J. (2010). "Closed-loop drip irrigation control using a hybrid wireless sensor and actuator network". *Science China Information Sciences*, 54(3), pp.577–588.
- Lu, M., & Ma, G. (2011). "Impact study of regional climate change on agricultural irrigation water". 2011 International Symposium on Water Resource and Environmental Protection, pp. 2172–2175.
- Maleki, M. R., Van Holm, L., Ramon, H., Merckx, R., De Baerdemaeker, J., & Mouazen, a. M. (2006). "Phosphorus Sensing for Fresh Soils using Visible and Near Infrared Spectroscopy". *Biosystems Engineering*, 95(3), pp.425–436.
- Maleki, M. R., Mouazen, a. M., De Ketelaere, B., Ramon, H., & De Baerdemaeker, J. (2008). "On-the-go variable-rate phosphorus fertilisation based on a visible and near-infrared soil sensor". *Biosystems Engineering*, 99(1), pp.35–46.
- Maleki, M. R., Mouazen, a. M., Ramon, H., & De Baerdemaeker, J. (2007). "Optimisation of soil VIS–NIR sensor-based variable rate application system of soil phosphorus". *Soil and Tillage Research*, 94(1), pp.239–250.
- Martens, H. and Naes, T. (1989). *Multivariate calibration*. 2nd ed. John Wiley & sons, Chichester, UK.
- Miao, Y., Mulla, D.J., Robert, P.C. (2006). "Identifying important factors influencing corn yield and grain quality variability using artificial networks. *Precision Agriculture* 7, 117-135.
- Minasny, B., McBratney, A.B. and Whelan, B.M., (2005), *Vesper 1.62 Spatial prediction software for precision agriculture*. 1.62nd ed. Australian Centre for

Precision Agriculture, McMillan Building A05, The University of Sydney, NSW 2006.

McNeill, J. D. (1980). "Electrical conductivity of soil and rocks". *Technical Note, TN-5. Geonics Ltd., Mississauga, Ontario, Canada.*

Mouazen, A. (2003). "Two-dimensional prediction of spatial variation in topsoil compaction of a sandy loam field-based on measured horizontal force of compaction sensor, cutting depth and moisture content". *Soil and Tillage Research, 74(1), 91–102.*

Mouazen, A. M. a. M. M., Ramon, H., Al-Kheer, a. A., Kharmanda, M. G., Hami, a. El, Kuang, B., Parsons, L. R., et al. (2007)." Expansive soils problem and practice in foundation and pavement engineering". *Soil and Tillage Research, 95(1), pp.419.*

Mouazen, A. M., 2006. Soil Survey Device. International publication published under the patent cooperation treaty (PCT). World Intellectual Property Organization, International Bureau. International Publication Number: WO2006/015463; PCT/BE2005/000129; IPC: G01N21/00; G01N21/00.

Mouazen, A. M., & Ramon, H. (2006). "Development of on-line measurement system of bulk density based on on-line measured draught, depth and soil moisture content". *Soil and Tillage Research, 86(2), pp.218–229.*

Mouazen, A. M., & Ramon, H. (2009a). "Expanding implementation of an on-line measurement system of topsoil compaction in loamy sand, loam, silt loam and silt soils". *Soil and Tillage Research, 103(1), pp.98–104.*

Mouazen, a. M., Anthonis, J., & Ramon, H. (2005). "An Automatic Depth Control System for Online Measurement of Spatial Variation in Soil Compaction, Part 4: Improvement of Compaction Maps by using a Proportional Integrative Derivative Depth Controller". *Biosystems Engineering", 90(4), pp.409–418.*

- Mouazen, A. M., De Baerdemaeker, J., & Ramon, H. (2005a). "Towards development of on-line soil moisture content sensor using a fibre-type NIR spectrophotometer". *Soil and Tillage Research*, 80(1-2), pp.171–183.
- Mouazen, A. M., Karoui, R., Deckers, J., De Baerdemaeker, J. and Roman, H. (2006). "Characterization of soil water content using measured visible and near infrared spectra". *Soil Science Society of America Journal*, 70, pp.1295–1302.
- Mouazen, a. M., Karoui, R., Deckers, J., De Baerdemaeker, J., & Ramon, H. (2007). "Potential of visible and near-infrared spectroscopy to derive colour groups utilising the Munsell soil colour charts". *Biosystems Engineering*, 97(2), pp.131–143.
- Mouazen, a. M., Kuang, B., De Baerdemaeker, J., & Ramon, H. (2010). "Comparison among principal component, partial least squares and back propagation neural network analyses for accuracy of measurement of selected soil properties with visible and near infrared spectroscopy". *Geoderma*, 158(1-2), pp.23–31.
- Mouazen, A.M., Anthonis, J., Saeys, W., & Ramon, H. (2004). "An Automatic Depth Control System for Online Measurement of Spatial Variation in Soil Compaction, Part 1: Sensor Design for Measurement of Frame Height Variation from Soil Surface". *Biosystems Engineering*, 89(2), pp.139–150.
- Mouazen, Abdul Mounem. (2003)."Modelling Compaction from On-line Measurement of Soil Properties and Sensor Draught", pp.203–212.
- Nelson, J. D. and Miller, D. J. (1992). "Expansive soils problem and practice in foundation and pavement engineering". John Wiley, New York, 259.
- Okparanma, R. N., and Mouazen, A. M. (2011). "Techniques for screening and risk-based assessment of petroleum hydrocarbon-contaminated soils: a

review of conventional and emerging methods". *Environmental Science and Technology*.

Padhi, J., & Misra, R. K. (2011). "Sensitivity of EM38 in determining soil water distribution in an irrigated wheat field". *Soil and Tillage Research*, 117, pp. 93–102.

Pardossi, A., Incrocci, L., Incrocci, G., Malorgio, F., Battista, P., Bacci, L., Rapi, B., et al. (2009). "Root zone sensors for irrigation management in intensive agriculture. *Sensors*" (Basel, Switzerland), 9(4), pp.2809.

Parsons, L. R., & Bandaranayake, W. M. (2009). "Performance of a New Capacitance Soil Moisture Probe in a Sandy Soil". *Soil Science Society of America Journal*, 73(4), pp. 1378.

Peets, S., Mouazen, A. M., Blackburn, K., Kuang, B., & Wiebensohn, J. (2012). "Methods and procedures for automatic collection and management of data acquired from on-the-go sensors with application to on-the-go soil sensors". *Computers and Electronics in Agriculture*, 81, pp.104–112.

Phene, C. J. (2010). "Drip irrigation can reduce California's water application by 2.4×10⁶ ac-ft. per year without yield reduction". *5th National Decennial Irrigation Conference 2010*, pp.834–860.

Quraishi, M. Z., & Mouazen, A. M. (2013). *Soil & Tillage Research Development of a methodology for in situ assessment of topsoil dry bulk density*, 126, pp.229–237. In press.

Quraishi, M. Z., & Mouazen, A. M. (2013). "Calibration of an on-line sensor for measurement of topsoil bulk density in all soil textures". *Soil Tillage Research* 126, pp. 219–228. In press.

Reedy, R. C., & Scanlon, B. R. (2003). "Soil Water Content Monitoring Using Electromagnetic Induction, (November)", pp.1028–1040.

- Reeves, J. B., III, McCarty, G. W. & Meisinger, J. J. (1999). "Near infrared reflectance spectroscopy for the analysis of agricultural soils". *J. Near Infrared Spectrosc*, 7, pp.179–193.
- Saeys, W., Mouazen, a. M., Anthonis, J., & Ramon, H. (2004). "An Automatic Depth Control System for Online Measurement of Spatial Variation in Soil Compaction, Part 2: Modelling of the Depth Control System". *Biosystems Engineering*, 89(3), pp.267–280.
- Sammis, T., Sharma, P., Shukla, M. K., Wang, J., & Miller, D. (2012). "A water-balance drip-irrigation scheduling model". *Agricultural Water Management*, 113, pp.30–37.
- Schulz, H., & Glaser, B. (2012). "Effects of biochar compared to organic and inorganic fertilizers on soil quality and plant growth in a greenhouse experiment". *Journal of Plant Nutrition and Soil Science*, 175(3), pp.410–422.
- Shibusawa, S.; Anom, W. S. I. M.; Sato, H.; Sasao, A.; Hirako, S.; Otomo, A.; Blackmore, S. (2000). "On-line real-time soil spectrophotometer". *Proceedings of the 5th International Conference on Precision Agriculture, Bloomington, Minnesota, USA, 16-19 July, 2000*. pp.1–13.
- Sinha, S.K., Wang, M.C., 2008. Artificial neural network prediction models for soil compaction and permeability. *Geotechnical and Geological Engineering* 26, pp.47–64
- (2000). "On-line real-time soil spectrophotometer". *Proceedings of the 5th International Conference on Precision Agriculture, Bloomington, Minnesota, USA, 16-19 July, 2000*. pp.1–13.
- Stenberg, B., Jonsson, A. and Borjesson, T. (2002). "Near infrared technology for soil analysis with implications for precision agriculture". *In: A Davies and R Cho (Eds.) Near Infrared Spectroscopy: Proceedings of the 10th International Conference, NIR Publications, Chichester, UK*, pp. 279–284.

- Stenberg, B. (2010). "Effects of soil sample pretreatments and standardised rewetting as interacted with sand classes on Vis-NIR predictions of clay and soil organic carbon". *Geoderma*, 158(1-2), pp.15–22.
- Stenberg, B., Viscarra Rossel, R.A., Mouazen, A.M., Wetterlind, J. (2010). "Visible and Near Infrared Spectroscopy in Soil Science", pp. 163–215).
- Sudduth, K. a., Kitchen, N. R., Wiebold, W. J., Batchelor, W. D., Bollero, G. a., Bullock, D. G., Clay, D. E., et al. (2005). "Relating apparent electrical conductivity to soil properties across the north-central USA". *Computers and Electronics in Agriculture*, 46(1-3), 263–283.
- Sudduth, K.A., Hummel, J. W. (1993). "Soil organic matter, CEC, and moisture sensing with a portable NIR spectrophotometer". *Transactions - American Society of Agricultural Engineers*, 36 (6), pp.1571–1582.
- Terhoeven-Urselmans, T., Schmidt, H., Georg Joergensen, R., & Ludwig, B. (2008). "Usefulness of near-infrared spectroscopy to determine biological and chemical soil properties: Importance of sample pre-treatment". *Soil Biology and Biochemistry*, 40(5), pp.1178–1188.
- Triantafyllis, J., Odeh, I.O.A., Jarman, A.L., Short, M.G., Kokkoris, E. (2004). "Estimating and mapping deep drainage risk at the district level in the lower Gwydir and Macquarie valleys, Australia". *Australian Journal of Experimental Agriculture*, 44 (9), pp.893–912.
- Urdanoz, V., & Aragüés, R. (2012). "Comparison of Geonics EM38 and Dualem 1S electromagnetic induction sensors for the measurement of salinity and other soil properties". *Soil Use and Management*, 28(1), pp.108–112.
- USDA. (1998). "Soil quality resource concerns: available water capacity", *Soil Quality information Sheet, USDA Natural Resources Conservation Service. (Online) Available: <http://soils.usda.gov> (assessed 16 November 2011).*

- Viscarra Rossel, R. a., Cattle, S. R., Ortega, a., & Fouad, Y. (2009). "In situ measurements of soil colour, mineral composition and clay content by vis-NIR spectroscopy". *Geoderma*, 150(3-4), pp.253–266.
- Viscarra Rossel, R. a., McGlynn, R. N., & McBratney, a. B. (2006a). "Determining the composition of mineral-organic mixes using UV-vis-NIR diffuse reflectance spectroscopy". *Geoderma*, 146, pp.403-411.
- Viscarra Rossel, R. a., Walvoort, D. J. J., McBratney, a. B., Janik, L. J., & Skjemstad, J. O. (2006b). "Visible, near infrared, mid infrared or combined diffuse reflectance spectroscopy for simultaneous assessment of various soil properties". *Geoderma*, 131(1-2), pp.59–75.
- Viscarra Rossel, R.A., and Behrens, T. (2010). "Using data mining to model and interpret soil diffuse reflectance spectra". *Geoderma*, 158, pp.46–54.
- Vohland, M., & Emmerling, C. (2011). "Determination of total soil organic C and hot water-extractable C from VIS-NIR soil reflectance with partial least squares regression and spectral feature selection techniques". *European Journal of Soil Science*, 62(4), pp.598–606.
- Vrindts, E., Mouazen, a. M., Reyniers, M., Maertens, K., Maleki, M. R., Ramon, H., & De Baerdemaeker, J. (2005). "Management Zones based on Correlation between Soil Compaction, Yield and Crop Data". *Biosystems Engineering*, 92(4), pp.419–428.
- Waine, T. W., Blackmore, B. S., and Godwin, R. J. (2000). "Mapping available water content and estimating soil textural classes using electro-magnetic induction", paper presented at the AgEng/EurAgEng 2000, Warwick, UK, Nr. 00-SW-044.
- Waiser, T. H., Morgan, C. L. S., Brown, D. J. and Hallmark, C. T. (2007). "In-situ characterization of soil clay content with visible near-infrared diffuse

reflectance spectroscopy". *Soil Science Society of America Journal* 71, pp. 389–396.

Wetterlind, J., Stenberg, B., & Söderström, M. (2010). Increased sample point density in farm soil mapping by local calibration of visible and near infrared prediction models. *Geoderma*, 156(3-4), pp.152–160.

Yang, H., Kuang, B., Mouazen, A. M. (2011a). "In situ determination of growing stages and harvest time of tomato (*lycopersicon esculentum*) fruits using fiber-optic visible-near-infrared (Vis-NIR) spectroscopy". *Applied Spectroscopy*, 65 (8), pp.931–938.

Yang, H., Kuang, B., Mouazen, A. M. (2011b). "Selection of spectral preprocessing methods for soil texture classification". *Advanced Materials Research*, 181-182, pp.416–421.

Yang, H., Kuang, B., & Mouazen, a. M. (2012). "Quantitative analysis of soil nitrogen and carbon at a farm scale using visible and near infrared spectroscopy coupled with wavelength reduction". *European Journal of Soil Science* 63, pp.410–420.

Zhang, D., Zhou, Z., Zhang, B., Du, S., & Liu, G. (2012). "The effects of agricultural management on selected soil properties of the arable soils in Tibet", China. *Catena Journal* (93), pp.1-8.

Zhu, Q., Lin, H., Doolittle, J. (2010). "Repeated electromagnetic induction surveys for improved soil mapping in an agricultural landscape". *Soil Science Society of America Journal*, 74 (5), pp.1763–1774.

Appendix

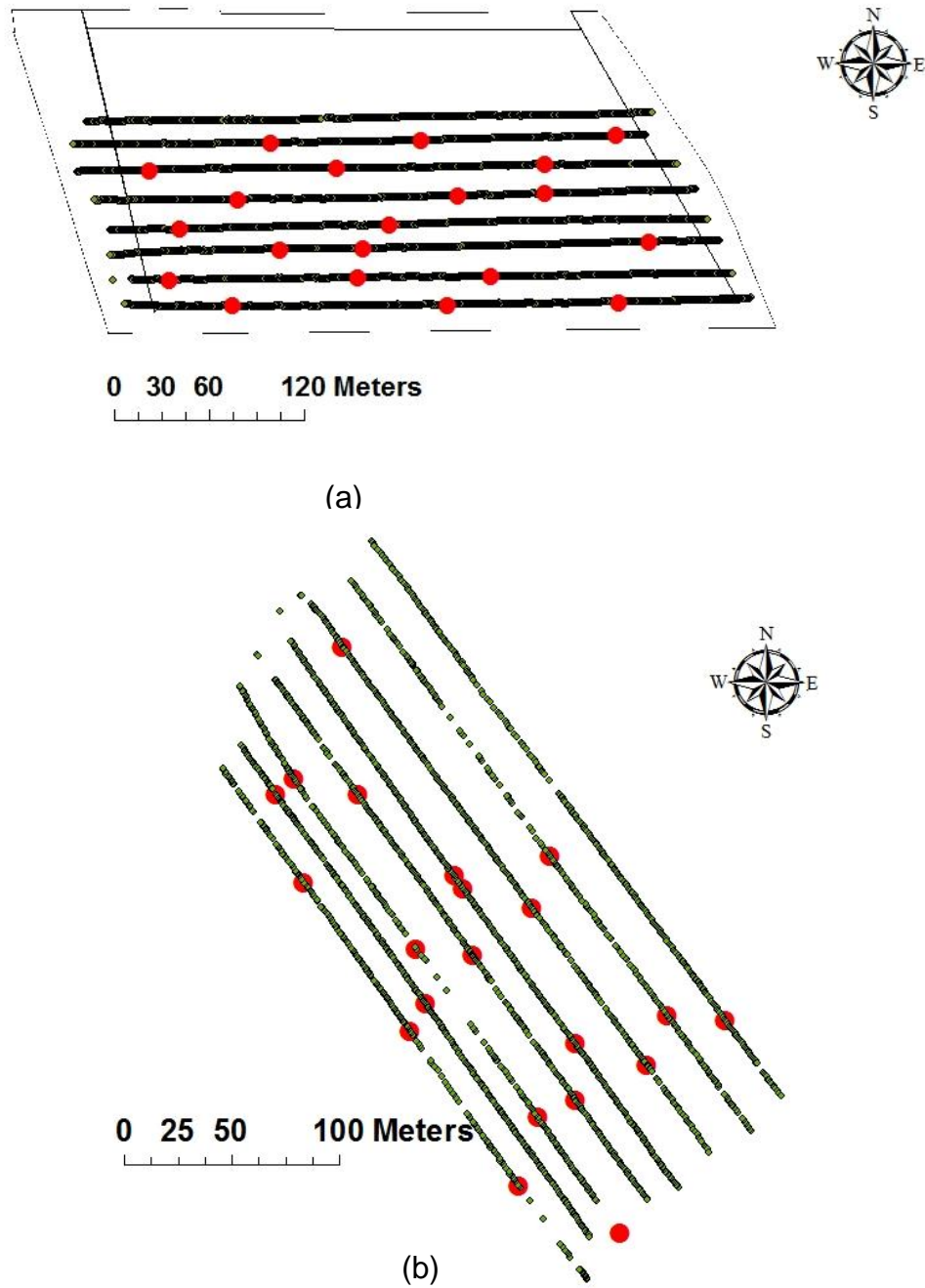
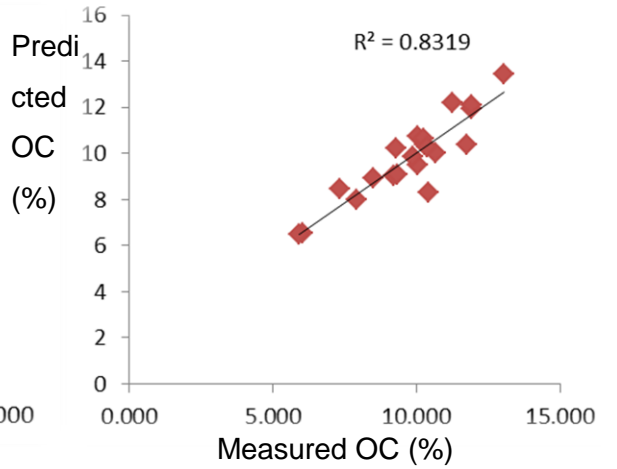
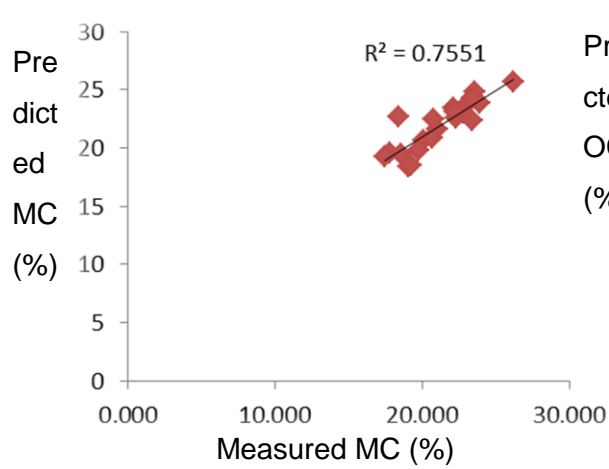
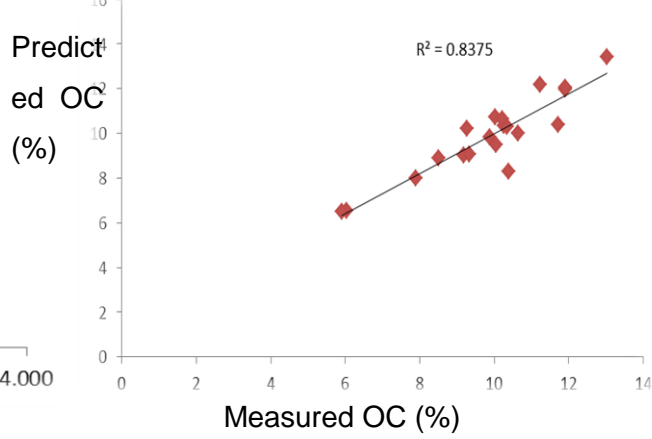
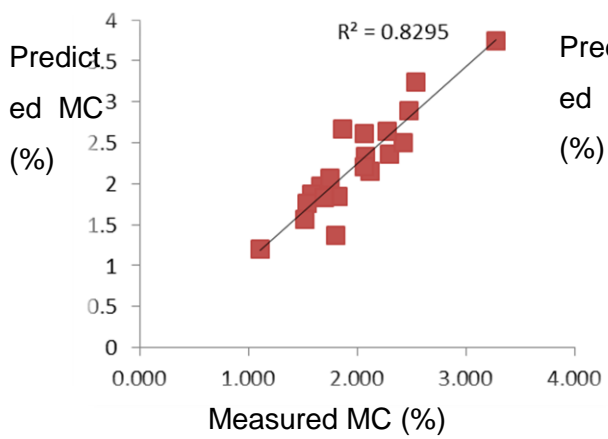
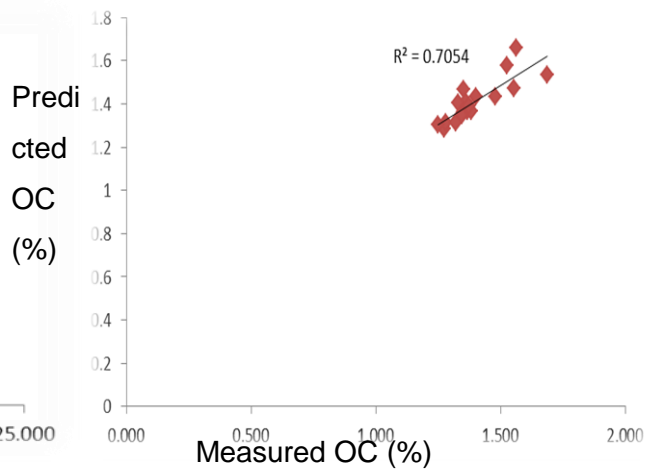
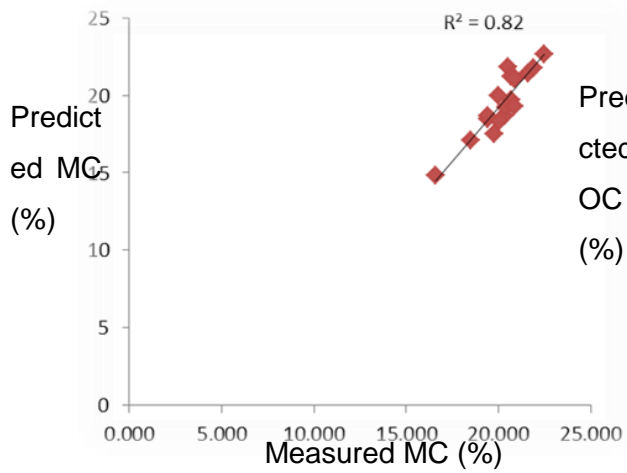
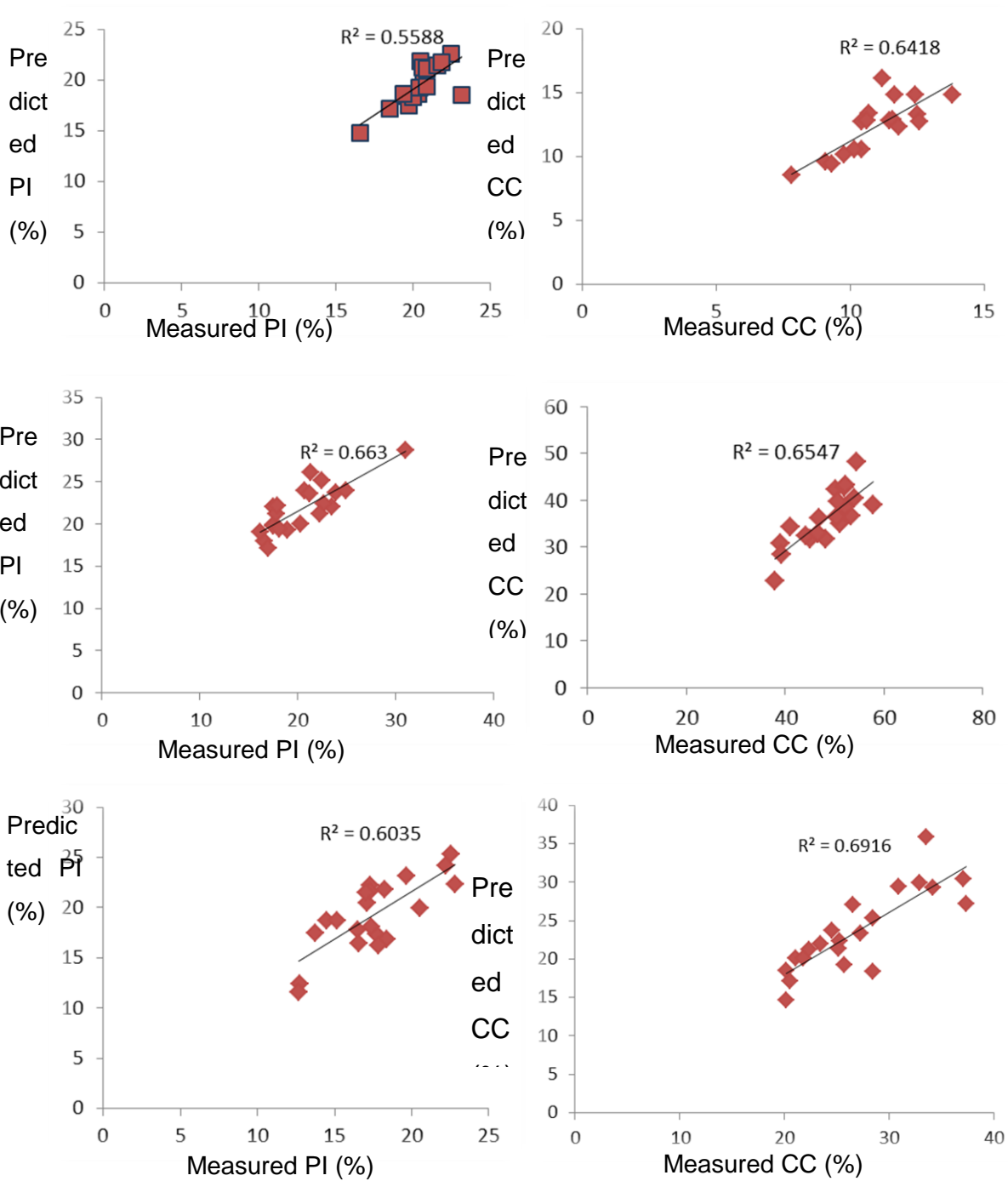


Figure _Apx-1: Shows the online measurement lines (black) and sampling points (red), shown in Wypemere field (a) and Thetford field (b)





Figure_Apx-2: Scatter plots of the on-line predicted versus laboratory measured moisture content (MC) (a), organic carbon (OC) (b), clay content CC (c) and plasticity index (d) at Vicarage Farm (top), Wypemere Farm (middle) and Thetford Farm (bottom)

Table_APX-1: Comparison between the available water content (AWC) calculated by Eqn. (3-8) using on-line predicted clay content (CC) and laboratory measured sand content with corresponding AWC values calculated based on average laboratory measured CC and sand content of water holding capacity (WHC) zones.

Method	WHC	Vicarage Farm		Wypemere Farm		Thetford Farm	
		AWC (%)		AWC (%)		AWC (%)	
		On-line	Lab	On-line	Lab	On-line	Lab
MLR	0-0.25	14.54	14.87	18.83	18.74	16.89	19.09
	0.25-0	17.53	16.18	19.37	18.94	18.52	19.22
	0.5-0.7	18.92	16.09	19.33	18.89	19.23	19.36
	0.75-1	19.36	16.64	19.07	18.74	19.39	17.89
All Fields	0-0.25	13.75	14.84	19.13	18.88	16.47	18.91
MLR	0.25-0	17.47	15.93	19.38	19.01	18.43	19.17
	0.5-0.7	19.04	16.30	19.33	18.84	19.22	19.36
	0.75-1	19.38	16.62	19.14	18.71	19.39	16.19
ANN	0-0.25	17.29	15.44	19.20	18.94	16.26	19.25
	0.25-0	18.90	15.38	19.39	18.97	17.39	19.20
	0.5-0.7	18.68	17.00	19.26	18.75	18.60	19.20

	0.75-1	19.22	16.64	19.03	18.81	18.93	19.24
All Fields	0-0.25	16.18	15.47	19.20	18.90	17.28	19.03
ANN	0.25-0	18.06	15.66	19.35	19.01	18.65	19.28
	0.5-0.7	19.25	16.92	19.38	18.75	19.23	19.39
	0.75-1	19.37	16.50	19.27	18.82	19.39	16.19

Table_APX-2: Accuracy of the vis-NIR prediction of AWC with Eqn (3-8) as compared to laboratory measured AWC based on WHC-category average clay content (CC) and sand content measured with PSD test. Comparison is made for AWC calculated with artificial neural network and multiple linear regression. (MLR) analysis

Method	Vicarage Farm				Wypemere Farm				Thetford Farm			
	R ²	RPD	RMSEP (%)	SD (%)	R ²	RPD	RMSEP (%)	SD (%)	R ²	RPD	RMSEP (%)	SD (%)
MLR	0.90	1.05	2.08	2.18	0.83	0.71	0.35	0.25	0.14	0.83	1.38	1.14
All-MLR	0.99	1.19	2.16	2.58	0.47	0.33	0.40	0.13	0.16	0.65	2.05	1.34
ANN	0.25	0.34	2.52	0.85	0.22	0.40	0.37	0.15	0.13	0.68	1.78	1.22
All-ANN	0.76	0.66	2.23	1.48	0.04	0.19	0.45	0.08	0.19	0.52	1.85	0.96